Master's thesis

NTNU
Norwegian University of Science and Technology
Faculty of Economics and Management
Dept. of Industrial Economics and Technology Management

Andreas Lien

Using Branch and Price to Optimize the Production of Salmon Under the Risk of Gender Maturation

Master's thesis in Industrial Economy and Technological Management
Supervisor: Peter Schütz
June 2022

Photo credit: Andrey Armyagov

NTNU
Kunnskap for en bedre verden

Andreas Lien

Using Branch and Price to Optimize the Production of Salmon Under the Risk of Gender Maturation

Master's thesis in Industrial Economy and Technological Management
Supervisor: Peter Schütz
June 2022

Norwegian University of Science and Technology
Faculty of Economics and Management
Dept. of Industrial Economics and Technology Management

NTNU
Norwegian University of
Science and Technology

Preface

This master thesis is written during the spring of 2022, as a part of the subject TIØ4905 Managerial Economics and Operations Research, Master's Thesis.

I would like to express gratitude towards Eidsfjord Sjøfarm AS and Aquagen AS as industrial partners throughout the project. Their data, knowledge and support has contributed significantly to the thesis.

Above all, I would like to thank my supervisor Peter Schütz. He has provided me with key discussions and feedback. Furthermore, the feedback has been thorough and honest, which has in turn greatly improved my final delivery. It has always been a priority for Peter to supervise and do it properly. Thank you so much!

Abstract

In this thesis we examine how production planning in industrial salmon production is affected by the risk of gender maturation and the inclusion of gender-partioned smolt types. We model a two-stage stochastic mixed-integer program for the tactical planning problem salmon farmers face in the sea stage of salmon farming. We develop two objective functions, the expected value and CVaR of the value of harvests, to incorporate risk-neutral and risk-averse attitudes in the model. The model determines the timing, location and size of deployments and harvests, as well as the smolt type of deployments.

We develop a solution method to reduce the running time of the problem. Firstly, we perform a Dantzig-Wolfe decomposition and use column generation to exploit the structure of the problem. Thereafter, we propose and apply a branch and price algorithm with several extensions to find solutions that comply with the integrality conditions. The branch and price algorithm performs better than Gurobi's MIP solver by slightly improving the lower bound and substantially improving the upper bound of the problem.

When analyzing the production plan, we discover that the expected value and CVaR of the value of harvests increase with the inclusion of gender-partitioned smolt types. Independent of the objective function deployments of regular smolt rarely occur. Determining the preferred smolt type is a trade-off between increasing the growth of salmon and decreasing the risk of gender maturation. Moreover, the preferred smolt type for a deployment largely depends upon the objective function and the relative value of gender matured salmon. The majority of deployed smolt is male when the decision maker is risk-neutral and the relative value of salmon that have experienced gender maturation is high. However, female smolt is preferred when the decision maker is risk-averse and the relative value of salmon that have experienced gender maturation is low.

Sammendrag

I denne oppgaven undersøker vi hvordan produksjonsplanlegging i industriell lakseproduksjon påvirkes av risikoen for kjønnsmodning og inkludering av kjønnsfordelte smolttyper. Vi modellerer et to-trinns stokastisk blandet heltallsprogram for det taktiske planleggingsproblemet lakseoppdrettere står overfor i sjøstadiet av lakseoppdrett. Vi utvikler to objektiv funksjoner, forventet verdi og CVaR av verdien av høstinger, for å inarbeide risikonøytrale og risikoaverse holdninger i modellen. Modellen bestemmer tidspunkt, plassering og størrelse på utsett og høsting, samt smolttype av utsett.

Vi utvikler en løsningsmetode for å redusere kjøretiden til problemet. Vi begynner med å utføre Dantzig-Wolfe dekomponering og bruker kolonnegenerering til å utnytte strukturen til problemet. Deretter foreslår og anvender vi en branch and price algoritme med flere utvidelser for å finne løsninger som innfrir heltallskravene. Branch and price algoritmen gir bedre resultater enn Gurobi sin MIP-løser når vi løser problemet, ved at branch and price algoritmen forbedrer den nedre grensen noe og den øvre grensen vesentlig.

Ved å analysere produksjonsplanen, oppdager vi at forventet verdi og CVaR av verdien av høstinger øker med inkluderingen av kjønnsfordelte smolttyper. Uavhengig av objektiv funksjonen forekommer utsett av regulær smolt svært sjeldent. Valg av smolttype er en avveining mellom å øke veksten av laks og redusere risikoen for kjønnsmodning. Dessuten avhenger den foretrukne smolttypen for utsett i stor grad av objektiv funksjonen og den relative verdien til kjønnsmodnet laks. Mesteparten av utsatt smolt er hannfisk når beslutningstakeren er risikonøytral og den relative verdien av laks som har opplevd kjønnsmodning er høy. Hunnsmolt foretrekkes imidlertid når beslutningstakeren er risikoavers og den relative verdien av laks som har opplevd kjønnsmodning er lav.

Contents

List of Figures

List of Tables

Chapter 1

Introduction

There is an increasing need for a higher production of food as the world population is projected to reach peak population, with 11.2 billion people, in 2100 (United Nations, 2017). Since seafood production can be sustainable, it can play an important part in meeting the increasing demand for food. Moreover, seafood production is greener than land-based meat production. In fact, a kilogram of pork or beef, respectively, has a CO_2 equivalent (a unit used to compare CO_2 emissions) of 30 and 5.9, while salmon has a CO_2 equivalent of 2.5 (Norwegian Seafood Council, 2016a).

Seafood production is projected to double by 2050 (DNV, 2021). Moreover, seafood production consists of production at capture fisheries and aquaculture. The global production at capture fisheries has stagnated in recent years, while aquaculture still looks like a promising alternative for the future. In the period from 1995 to 2015, the aquaculture production increased from 28 million tonnes to over 106 million tonnes (Ritchie and Roser, 2019).

In 2019 aquaculture production accounted for 77 % of all fish production in Norway (OECD, 2020), where 95 % was salmon production. Also, Norway is the largest national producer of farmed salmon in the world, having produced 50.4 % of global production in 2020 (Mowi, 2021). An overview of Norwegian salmon production from 1980 to 2018 is shown in Figure 1.1. Maintaining the growth, experienced before 2010 is impossible. The average annual growth rate of Norwegian salmon production is decreasing, with the rate expected to fall to 4 % in 2024 (Mowi, 2021).

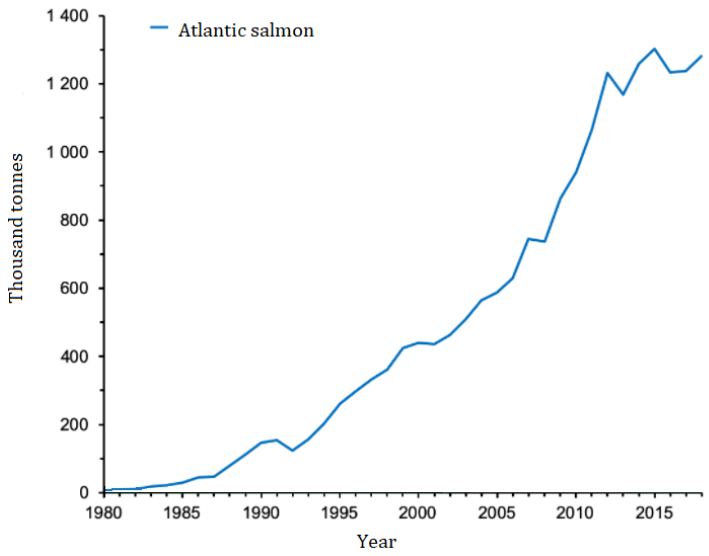

Figure 1.1: An overview of the production of salmon in Norway form 1980 to 2018. Retrieved from Grefsrud et al. (2019).

Since the first successful farming of salmon in Norway, many developments have been made within the industry (Misund, 2021). These include biological and technological advancements, along with production planning improvements (Global Farming Initiative, 2022). As a result, the production at existing locations has increased and more locations have been opened for production. Examples of biological advancements are breeding and the addition of new smolt types (Nofima, 2022). Technological advancements include light manipulation, which increases growth, and new equipment (Stefansson et al., 2005). Improvements made within production planning contribute to higher production at different locations, while ensuring that companies comply with restrictions. Many of these advancements have made salmon grow faster and enable earlier harvests (Aquagen, 2022).

Due to production restrictions, Norwegian farming companies primarily have two alternatives to increase their revenues and production. One option is to move into the relatively unexplored industry of offshore salmon production (The Fish Site, 2022). On one hand, the company will be able to increase their production drastically, due to fewer restrictions in offshore farming. On the other hand, the rough weather at offshore installations necessitates higher start-up, production and maintenance costs. The other option is to make the

production system more efficient nearshore (Guttormsen, 2008). To achieve this, restrictions must be utilized to a greater extent. This can be achieved with the introduction of gender-partioned smolt types. Here it is possible to increase production and reduce the risk of lost production value. Increasing the efficiency nearshore will be the focus for the remainder of the thesis.

Even though a more efficient production system will maximize the profits, it is important that it is done given a risk level that salmon farmers are comfortable with. The reason for this is that they are moderately risk-averse. Bergfjord (2009) presents the biggest sources of risk as diseases, the sales price of salmon and institutional risks. There are several reasons why salmon experience a drop in their sales price, such as gender maturation (Iversen et al., 2016). Moreover, in this thesis we focus upon price drops caused by gender maturation. It is of interest to avoid gender maturation since it is unpredictable, decreases the sales price of salmon and increases the risk of lost production value.

This thesis builds upon the work presented in Lien (2021). We will study how the inclusion gender-partioned smolt types affect the production plan for a salmon farming company. By deploying different smolt types we can increase the growth of salmon or reduce the risk of gender maturation. Also, we will examine the risk of lost production value caused by gender maturation. Both the expected value and the risk measure CVaR will be used as objectives in the thesis. Unlike Lien (2021), this thesis will use a different solution method to solve more scenarios. We will use Dantzig-Wolfe decomposition and column generation to exploit the structure of the problem. Then, we use a branch and price algorithm with extensions to find integer feasible solutions. By increasing the number of scenarios, the results will represent the real world better.

The chapters in the thesis are organized in the following way. We begin by introducing relevant concepts and information in Chapter 2, such as the industrial value cycle of a salmon, the regulatory framework and risk-averse optimization. Next, we present the literature review in Chapter 3. We continue in Chapter 4 by describing the planning problem which will be the focus of the thesis. We present the modeling approaches in Chapter 5. In Chapter 6 we describe the mathematical model of the problem. Then, we present the method used to solve the problem in Chapter 7. In Chapter 8 we examine the case study which forms the basis for the data used in the problem. Thereafter, we present the computational results in Chapter 9. We discuss areas for further research in Chapter 10. Lastly, in Chapter 11 final remarks are presented.

Chapter 2

Background

In this chapter we introduce relevant aspects of risk-averse production planning within Norwegian salmon farming. We begin by presenting the stages of the industrial salmon life cycle to gain a better understanding of the different types of decisions salmon farming companies need to make. We continue with presenting a classification of different planning problems that salmon farming companies face, with a focus on tactical planning. Then, we present the governmental regulatory requirements and restrictions that limit and steer production in Norway. Thereafter, we continue by discussing the biological risks of salmon farming, with a focus on gender maturation, that effect production planning within salmon farming. Next, we introduce and compare the characteristics of the three smolt types we use in this thesis. Then, we describe different methods of performing risk-averse optimization in the planning process of industrial salmon farming. Lastly, we present the area of study for the remainder of the thesis.

2.1 Industrial Salmon Life Cycle

The salmon life cycle begins in freshwater before moving to seawater due to salmon being an anadromous species (Mowi, 2021). Figure 2.1 shows the different stages within the life cycle of a salmon.

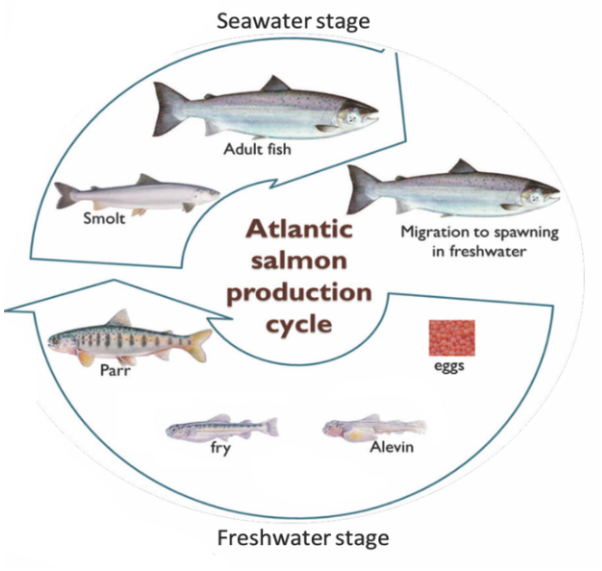

Figure 2.1: The salmon life cycle. Retrieved from Munang'andu et al. (2016).

2.1.1 Freshwater Stage

The freshwater stage consists of four development stages, which are eggs, alevins, fries and parrs. The freshwater stage takes place in closed facilities on land with a duration between 10 and 16 months (Norwegian Seafood Council, 2022). To get salmon with desirable characteristics breeding companies analyze a broodstock's reproductive cells. Then, the breeding company picks eggs that have the best characteristics, regarding biomass and disease resistance (Aquagen, 2022). Thereafter, the eggs are put into incubators for approximately 50 to 60 days, with a temperature that lies between 8 $°C$ and 10 $°C$ (Salmar, 2022). The hatching of the alevins marks the beginning of the next stage. Alevins cannot swim and get nutrition through their own yolk sac.

The alevins become fries when they are able to swim (National Park Service, 2019). Unlike alevins, fries get nutrition not only from their yolk sac but also from their habitat (National Park Service, 2019). Even though fries have high mortality rates in nature, the use of developed techniques and technologies in industrial farming have almost eliminated fatalities at this development stage. When fries begin to develop camouflage patterns, such as vertical stripes and spots, they become parrs (Marine Institute, 2020). During the transition to

the next stage, parrs experience the smoltification process, where they become smolt. At this stage, they are able to survive in seawater (Marine Institute, 2020). Furthermore, their chances of survival in seawater increase with their increased weight. In industrial production the smoltification process can occur during all seasons, while it only takes place during the fall in nature.

2.1.2 Seawater Stage

The seawater stage consists of three different stages, which are smolt, pre-gender maturation salmon and post-gender maturation salmon. In industrial farming the salmon are placed in pens and nets in the seawater for a duration between 12 and 18 months (Aquagen, 2022). A cohort is made up of all of the smolt that are deployed in the same pen simultaneously. Unlike the industrial freshwater stage, the industrial seawater stage occurs in an open facility where the salmon are exposed to parasites and diseases (Barentswatch, 2021b). Even though the stage of post gender maturation is a natural stage of the seawater development, it is of great interest to avoid it. The main reason for this is that gender maturation downgrades the value of salmon.

To ensure high quality of meat and avoid lower growth rates, it is important to minimize the stress that salmon experience (Deependra, 2011). Furthermore, the salmon are not fed during the week prior to harvest to empty the intestines (Jakobsen, 2020). Thereafter, the salmon are anesthetized and harvested (Norwegian Seafood Council, 2016b). After harvest, the salmon are prepared, before being sold to distributors.

2.2 Planning within industrial salmon farming

The complexity that follows industrial salmon farming makes it beneficial to focus on planning to optimize production. Furthermore, industrial salmon farming covers several smaller planning and decision problems. To categorize these problems and create structure, we will use the framework proposed in Anthony (1965). Here all planning problems can be classified as operational, tactical or strategic problems. The problems vary by size, time duration and involvement from upper management. Moreover, the different types of planning problems are subject to different types of uncertainty. We have a

larger focus on tactical planning, since we want to solve a tactical planning problem of salmon farming in this thesis.

2.2.1 Operational

Operational planning problems are characterized by having little involvement from the upper management as well as typically having a time duration of up to three months. Many operational problems involve evaluation, control and execution at different facilities. Having a focus on operational planning is important to maintain a company's relationship with workers, suppliers and customers. Typical operational planning is made up of short-term decision making at individual locations. Due to uncertainties like demand for salmon and timing of deliveries from suppliers, these problems have a high need for continuous replanning. Examples of operational problems within fish farming include the use of equipment, daily tasks at a facility and feeding schedules.

2.2.2 Tactical

Tactical planning problems are characterized by having a medium length duration with a focus on resource utilization. Moreover, tactical planning largely depends upon the availability and stock of different resources. Tactical planning applies in fish farming by companies having to abide by requirements and biomass restrictions with finite capacities, while maximizing profits.

Making a production plan is an important part of tactical planning in fish farming. A tactical production plan consists of many different decisions. Here we will present some of the decisions that must be made. The company must decide upon the timing and number of salmon deployed and harvested at all locations. Moreover, the company must determine which smolt type and deployment weight they wish to deploy, according to their different characteristics. Companies also have to decide when to fallow locations. Fallowing is the process of cleaning and disinfecting the location and equipment between deployment and harvest.

In tactical planning a farming company is exposed to uncertainty through biological risks, such as gender maturation. By focusing on tactical production planning, companies can increase profits and reduce the risk of gender

maturation. This will be the focus for the remainder of the thesis.

2.2.3 Strategic

Strategic planning problems are characterized by high involvement of upper management, little replanning and having a planning horizon with a time duration between five and 10 years. Planning problems that typically fall within this level are resource acquisition and management of change. Having a strong strategic plan is very important for companies, as it steers the entire company in a good direction. Within salmon farming, strategic decisions include acquiring production licenses at new locations, the merging of companies and investments in offshore fish farming. Uncertainty in strategic planning can appear through the long-term sales price of salmon and governmental regulations, which in turn can affect whether a strategic decision is profitable.

2.3 Regulatory framework

The tactical planning problem we want to solve is restricted by the regulations imposed by the Norwegian government. Requirements and restrictions, concerning the facility, location, environment, cleanliness and more are specified. They form the basis for the maximum allowable biomass (MAB) that can be employed at the same time. The presentation of the regulatory framework is primarily taken from the Aquaculture Act.

2.3.1 Biomass restrictions and requirements

In 2017 the Ministry of Trade, Industry and Fisheries divided the Norwegian coast into 13 distinct production zones. The division of the production zones is shown in Figure 2.2.

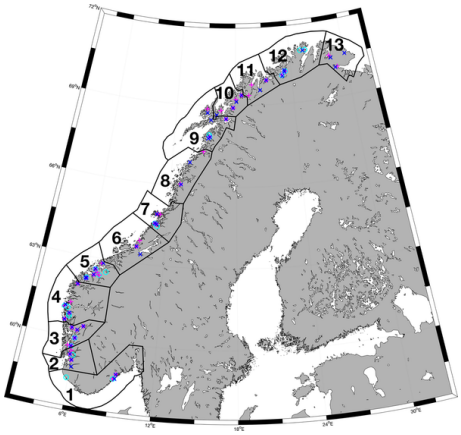

Figure 2.2: The production zones that constitute the Norwegian coast.

For a company to carry out industrial farming production in a production zone, it must have a production license issued by the Norwegian government. The location, regional and company-wide MAB are regulated in the production license. The regional MAB is all production that occurs in a single production zone. In most cases, production licenses are limited to one production zone. As a result, all companies that operate in the same production zone must abide by the same MAB restrictions (Mowi, 2021). Nevertheless, companies can apply for permission to combine their MAB across separate production zones. The MAB of a production license varies greatly and is dependent on the facility and location (Mowi, 2021). However, in a standard production license the MAB is 780 tonnes for most production zones. In the northernmost production zones, Troms and Finnmark, the MAB of a standard production license is 945 tonnes (Fiskeridirektoratet, 2022).

2.3.2 Operational restrictions and requirements

The Aquaculture Act specifies operational requirements and restrictions in industrial salmon farming due to the potential ramifications it can have on the ecosystem. The location, time and size of the deployments and harvests for the next two years must be a part of a yearly operational plan.

A company risks losing their production license if a location remains empty for 24 months. Furthermore, the duration of fallowing at a location must at least

be two months. If a company breaks restrictions, it risks fines and possibly losing production licenses. Moreover, companies have to limit deployments to two deployment periods each year.

2.4 Biological risks

Even though the regulatory framework is in place to keep industrial salmon farming sustainable, biological risks still have a notable impact on production. Furthermore, the typical salmon farmer's risk averse attitudes makes it a priority to minimize biological risks (Bergfjord, 2009). There is a divide between risk factors that degrade the value of the salmon and lower biomass production. Moreover, some risk factors fall into both categories. In this section we present some of the biggest biological risks that affect the tactical production planning problem of salmon farming.

2.4.1 Growth

In salmon farming, the main value driver for salmon farmers is the harvested biomass (Eidsfjord, 2021). The value of the harvested biomass is largely dependent on the length of a rearing period for a cohort due to farmers being able to deploy more salmon if the rearing periods are shorter. Furthermore, shorter production cycles reduce the risk of gender maturation, lice and other diseases in salmon production. Hence, there is a trade-off between increasing growth and decreasing the risk of gender maturation, lice and other diseases.

The growth rate of a salmon is determined by its genetic profile and external factors (Aquagen, 2021). The size and frequency of feedings largely impact the growth, with most salmon farmers feeding when there is an appetite for it. External factors that affect the growth rate include salinity, seawater temperature, oxygen levels, stocking density, disease treatments and light conditions (Føre et al., 2016). Production facilities are placed at locations with a favorable seawater temperature and salinity levels. Moreover, facilities can to a large extent pick the stocking density and manipulate lighting with floodlights (Eidsfjord, 2021). The occurrence and treatment of lice and other diseases decrease the growth rates by lowering natural growth conditions and through the use of necessary treatments (Eidsfjord, 2021).

The growth of salmon is also influenced by the age and gender maturation (Aquagen, 2021). In general, the growth rate of a salmon increases after deployment at sea, until it decreases as it nears the end of its life cycle (Aunsmo et al., 2014). Moreover, gender maturation decreases the growth rates.

2.4.2 Gender maturation

Gender maturation is a natural biological process that gives salmon the ability to reproduce. This transformation demands a large portion of energy, which has adverse consequences within industrial salmon farming (Aquagen, 2021). Distinctive skin coloration appears on the salmon and the meat quality is lowered during gender maturation (Deependra, 2011). As a result, there is a reduction in the market value of the salmon (Eidsfjord Sjøfarm et al., 2017). The reduction is dependent upon the market and can vary between 5 and 95 % (Aquagen, 2021). Bergfjord (2009) lists the price risk as one of the main risks within industrial salmon farming. Therefore, salmon farming companies want to minimize the percentage of a cohort that experiences gender maturation to reduce the risk of lost production value. However, this can be challenging due to salmon experiencing gender maturation at different points in time.

Aquagen AS have carried out studies which show that the percentage of a cohort that has experienced gender maturation at harvest, also known as the gender maturation percentage, varies between 0 and 35 %. Most cases of gender maturation occur during the second late-summer and autumn that the salmon are employed in seawater. Nonetheless, gender maturation can, in some rare cases, occur as early as the freshwater stage (Fjelldal et al., 2020).

Studies show that gender maturation is a result of a combination of biological and environmental factors (Eidsfjord Sjøfarm et al., 2017). The biological factors consist of the weight, age, gender and fitness factor of an individual salmon (Eidsfjord Sjøfarm et al., 2017). Environmental factors consist of the temperature of the seawater, light and the salinity of the seawater. To minimize the cases of gender maturation, farming companies use light manipulation (Pino Martinez et al., 2021).

The gender maturation percentages reported from farming companies in Norway are increasing (Aquagen, 2021). Even though, there is little research on the causes of this, it is suspected that higher deployment weights and increasing sea temperatures during the summer are contributing factors (Eidsfjord Sjøfarm et al., 2017). When farming companies study salmon, they get an indication of what percentage of the cohort has gone through gender maturation. However, the actual percentage of salmon that have experienced gender maturation may vary greatly from this indication (Aquagen, 2021). Thus, the company needs to determine if they should let the cohort keep growing or harvest it. By postponing harvest, more salmon in the cohort might go through gender maturation, while the quality of the meat will keep declining. However, salmon in the cohort that have not experienced gender maturation may still have a large potential for further growth and higher market value.

2.4.3 Mortality

Salmon farmers expect a cumulative mortality rate of salmon between 10 and 15 % before harvest in a normal production cycle (Bang Jensen et al., 2020). Most of the fatalities are caused by lice and other diseases. They are considered the biggest financial and biological risks within the industry. Law enforced restrictions are in place and good practices are in wide use to ensure sustainability and good health conditions for salmon. Furthermore, lice and other diseases easily spread between facilities or onto wild salmon.

Salmon lice live on salmon as a parasite in nature, without doing much harm to the salmon. However, in salmon farming large amounts of salmon live in a limited space. Such high concentrations of salmon, do not occur in nature. As a result, lice are able to reach volumes that cause physical damage to salmon, even leading to fatalities in some cases (Barentswatch, 2021b).

To minimize the occurrence and severity of lice and other diseases, farming companies have reactive and preventive measures. Vaccination is used efficiently to mitigate the number of cases of some diseases (Mowi, 2021). Moreover, the risk of other diseases has been reduced through improved environmental conditions, management and treatments. In the time period where the wild salmon migrate, stricter restrictions are in place to avoid the spreading of lice and diseases (Nodland, 2016). To ensure that salmon do

not build resistance towards any type of treatments, farming companies rotate between different types of treatments (Barentswatch, 2021b). Furthermore, as an extreme measure to avoid transmission of disease to other farming locations, it might be necessary to slaughter the entire salmon population at a location.

2.5 Smolt types

Different smolt types are to varying degrees susceptible to different biological risks. Smolt type characteristics are important aspects of minimizing salmon fatalities and the number of gender maturation cases, while maximizing growth. This can contribute to an increased value of harvests or a decreased risk of lost production value for salmon farmers. In this thesis we focus on three smolt types, to examine which smolt types should be used in the production planning problem of salmon farming. They are regular, female and male smolt. Female and male smolt are regular smolt partitioned by gender. Table 2.1 shows a ranking of how the different smolt types perform when it comes to the different biological risks. Details concerning the ranking of the smolt types is explained in the upcoming sections. The presentation of the different smolt types is retrieved from Eidsfjord Sjøfarm et al. (2017) and Aquagen (2021).

Smolt type	**Growth rates**	**Mortality rates**	**Gender maturation percentage**
Regular	Medium	High	Medium
Female	Low	Low	Low
Male	High	Medium	High

Table 2.1: Ranking of the smolt types when it comes to different biological risks. Green, yellow and red respectively indicate whether the smolt type performs the best, neutral or worst.

2.5.1 Regular smolt

Most of the smolt that are deployed in Norway are regular smolt. Moreovoer, it is is a non-gender sorted smolt, with approximately an equal amount of female

and male smolt. Many of the other smolt types are still at a level of research, but it is expected that this will change in the coming years (Aquagen, 2021). Breeding companies sell different types of regular smolt, with small variations in the biological characteristics. In this thesis all references to regular smolt are to the version of regular smolt that Aquagen AS provide.

Studies show that male and female smolt have different optimal feeding schedules due to having different biological characteristics (Aquagen, 2021). As a result, mixing female and male smolt in a cohort removes the possibility of optimizing the feeding schedules based upon the gender. Instead, the feeding schedule becomes a compromise between the two genders. Therefore, the expected weight development of regular smolt is much closer to the weight development of female salmon compared to male salmon.

2.5.2 Female smolt

Female smolt have lower growth rates than regular smolt. Therefore, they are the smolt type that requires the most time to reach harvestable sizes. Their feeding schedules necessitate less feeding than other types of smolt. However, female smolt have the lowest risk of gender maturation, with the percentages being close to zero (Aquagen, 2021). This makes it easier to predict the value of the salmon before harvest. Lastly, female smolt have the lower mortality rates than regular smolt.

2.5.3 Male smolt

Male smolt have the highest growth rates of all three smolt types. As a result, they can be harvested earlier than the other smolt types. This necessitates a feeding schedule with larger or more frequent feedings. The risk of salmon experiencing gender maturation before harvest is higher than regular and female smolt. Therefore, a larger percentage of male smolt experience a price drop during their rearing period, which makes it more challenging to predict the value of male salmon before harvest compared to female salmon. Finally, male smolt have higher mortality rates than regular smolt and lower mortality rates than female smolt.

2.6 Risk-averse optimization

Biological risks, like gender maturation, give rise to the risk of lost production value in salmon farming, which leads to risk-averse decision makers. For this reason it is necessary to capture risk-averse attitudes when modeling the tactical problem of production planning in salmon farming. This can be achieved through the use of risk-averse optimization (Ruszczyński and Shapiro, 2009). Moreover, there is a broad selection of risk measures to choose from. They have different applications and there is still dispute on which is better to use in optimization (Roman et al., 2007).

In this section, we report a set of desirable properties that we use to determine which risk measure to use for the remainder of the thesis. Further, we present three widely used risk measures: standard deviation, value at risk and conditional value at risk, and we select one for further use based upon the desirable properties.

2.6.1 Desirable properties

Artzner et al. (1999) presents four mathematical properties to decide the quality of a risk measure. If a risk measure satisfies all four it is known as a coherent risk measure. Coherence has become the most widely accepted set of properties for a risk measure (Tsanakas, 2004). Moreover, the properties are sub-additivity, monotonicity, positive homogeneity and translation invariance.

Sub-additivity applies when the combined risk of two portfolios is no higher than the individual risk of one of the portfolios. Moreover, monotonicity implies that a portfolio has a lower risk of loss when the return in every scenario is higher. Positive homogeneity applies when the value of the portfolio and the amount of risk are proportional. Lastly, translational invariance implies that the risk of a portfolio decreases with the amount of risk neutral assets that is supplied to the portfolio.

Risk can be divided into downside and upside risk (Fisher and D'Alessandro, 2021). Downside risk is the risk of obtaining less than the expected value, while upside risk is the risk of obtaining more than the expected value (Fisher and D'Alessandro, 2021). Furthermore, for our optimization problem, we want the risk measure to only include downside risk, as upside risk is rarely of interest

in risk-averse optimization (Grootveld and Hallerbach, 1999). This is due to downside risk not meeting expectations, while upside risk exceeding them.

2.6.2 Standard deviation

Standard deviation is the most widely used risk measure. It measures how spread the dataset is in relation to the mean (Hayes, 2021). The applications of the risk measure are endless and it has been the dominating risk measure in many industries such as portfolio selection (Segal, 2022). Standard deviation satisfies all of the desirable properties of a coherent risk measure (Cirillo, 2022). However, standard deviation measures upside risk and downside risk. Therefore, since we want to focus on downside risk, other risk measures can be more appealing.

2.6.3 Value at risk

Value at risk (VaR) became a popular risk measure in portfolio selection in the 1990's (Adamko et al., 2015). It is a measure of the upper quantile of the potential deviation from the expected return (Roman et al., 2007). However, using VaR as the risk measure in risk-averse optimization is challenging. Tasche (2002) shows that VaR can give rise to aggregation problems, since it lacks the property of sub-additivity. Moreover, this discourages diversification and increases the risk of the portfolio (Danielsson et al., 2005).

2.6.4 Conditional value at risk

The risk measure conditional value at risk (CVaR) has become a well-known risk measure (Artzner et al., 1999). It measures the expected value of the losses that lie below the VaR. CVaR is sub-additive and leads to a convex problem (Artzner et al., 1999). Moreover, CVaR is a coherent risk measure that only measures the downside risk. Therefore, it is typically a better fit for optimization and will be the risk measure we use in this thesis.

2.7 Area of further study

For the remainder of the thesis we study and model the tactical production planning problem of salmon farming. The source of uncertainty will be gender maturation which forms the basis for the risk of lost production value. We produce a production plan that determines the optimal choice of smolt type as well as the optimal timing, size and location of deployments and harvests of salmon. Moreover, the production plan must comply with the regulatory framework. We maximize the expected value and CVaR to respectively capture the risk-neutral and risk-averse attitudes of salmon farmers.

Chapter 3

Literature review

In this chapter we study literature relevant to risk-averse tactical salmon production planning. We begin by studying production planning within aquaculture. Thereafter, due to the limited existing literature on risk-averse production planning within aquaculture, we review risk-averse production planning problems within other industries.

3.1 Production planning within aquaculture

The modeling of production planning within aquaculture has developed since it was introduced in 1986. To begin with, it was modeled as an optimal rotation problem. Thereafter, it became more common to model it as a linear optimization problem. More recently, authors have incorporated different types of uncertainties within the aquaculture industry in their model.

3.1.1 Early models

Karp et al. (1986) apply the optimal rotation problem within aquaculture production planning to determine the size and timing of deployments, harvests and restockings. Initially, the optimal rotation problem was used to estimate the length of a growth period of timber to maximize the present value of the income stream (Faustmann, 1849). Similar to Karp et al. (1986), Bjørndal

(1988) studies the optimal timing of harvests within fish farming by applying the optimal rotation problem to aquaculture. Bjørndal creates a bioeconomical model where the objective is to maximize profits. Hence, his main focus is to study the relationship between costs and timing of harvests. He comes to the conclusion that selective harvesting based upon weight categorization can be beneficial due to smolt experiencing different growth rates in the same cohort.

Other authors, like Arnason and Hean, build upon the model presented by Bjørndal. Arnason (1992) looks at the relationship between the feeding schedule of fish and timing of harvests. He discovers that the two aspects are largely connected. Later, Hean (1994) introduces a model that finds the optimal management strategy of fish production. Unlike previous models, it includes release costs, which lets the decision maker determine the optimal size of deployments. Heaps (1995) studies whether it is beneficial to perform culling of cohorts before harvest, given that the growth rates are dependent upon density. Culling is performed to remove undesirable characteristics in the fish population, which in this case is small fish with low growth rates.

Pascoe et al. (2002) develop a bioeconomical model and study how existing models that apply optimal rotation within aquaculture do not represent actual aquaculture. Their primary reason for this is that most of the existing models exclude risk. Furthermore, they present a comparison of actual aquaculture production planning and their model. The comparison demonstrates several weaknesses of the optimal rotation problem. Moreover, they conclude that the optimal rotation length is an understatement of the actual rearing period. Their reasoning is that their rotation problem does not include all critical aspects of fish farming. They believe that other modeling approaches are more appropriate for studying production planning within aquaculture, such as models utilizing dynamic programming.

3.1.2 Linear and dynamic programming

Forsberg (1996) presents a linear programming model that determines the optimal size of deployment and harvest at an individual facility. Moreover, the model aims at maximizing profits while abiding by the MAB constraints of the facility. Each salmon within the cohort is placed into a discrete weight class. Furthermore, a Markov process is used to estimate the transition probabilities between the different weight classes. As a result, all of the

salmon belonging to the same weight classification have equal probabilities of transition. Weight-dependent prices are also included in the model. Like Bjørndal (1988), Forsberg (1999) studies different harvesting strategies to use in a multiperiod linear program to optimize industrial salmon production. The first strategy is to only harvest the most profitable fish, based upon their weight. The second strategy is to harvest and sell similar sized fish. He concludes that the first strategy is the more profitable alternative.

Guttormsen (2008) presents a dynamic programming model that builds upon the original rotation problem with the addition of some adjustments to aquaculture. He declares that the importance of production schedules is increasing as markets within aquaculture are becoming more prone to competition. Moreover, he claims that timing of harvests can determine whether the activities of a fish farming company in a time period are profitable or not. He includes relative price relationships and the limitations surrounding release time windows. Unlike earlier models, his growth function depends upon the temperature of the seawater. As a result, seasonal growth development is a central part of the model.

3.1.3 Modeling with uncertainty

Hæreid et al. (2013) present a multi-stage stochastic model that attempts to solve a tactical planning production problem of industrial salmon farming. Furthermore, they study different sources of uncertainty that can appear in salmon farming. Uncertainties that are included in their model are the development of biomass, mortality rates and prices.

Næss and Patricksson (2019) propose a model that allows the deployment of different smolt types, specifically gender-partioned smolt. They study whether the inclusion of the new smolt types increases the volume of harvested biomass. Furthermore, they do a comparison of deterministic and stochastic models, where the stochastic variable is the seawater temperature. Their results show that both the deterministic and stochastic models benefit with the inclusion of more smolt types, as male smolt have higher weight development. However, the stochastic model benefits less than the deterministic model.

Further, Aasen (2021) takes inspiration from the model presented in Næss and Patricksson (2019), with the addition of even more smolt types and the

uncertainty of when and how often it is necessary to have lice treatments. Unlike Næss and Patricksson (2019), Aasen maximizes biomass and revenue by including weight-dependent prices in his model. The inclusion of new smolt types increase the revenues and the amount of harvested biomass. However, the representation of the real world in Aasen (2021) and Næss and Patricksson (2019) is limited due to both models having a low number of scenarios.

3.2 Risk-averse production planning

Companies within a broad variety of industries use risk-averse optimization as a tool to hedge against uncertainty. The type of planning problem within other industries varies from the tactical planning problem of industrial salmon farming. However, the risk measures of CVaR and variance are popular across different industries. Therefore, in this section we present literature where CVaR and variance have been used to handle risk-averse attitudes.

Kawas et al. (2011) present a product allocation problem where companies must make decisions to minimize the risk of regulatory inspections failing, which in turn leads to loss in revenue. Furthermore, each inspection results in a Bernoulli distributed stochastic variable that depends upon the decisions regarding production. Their model maximizes the CVaR of the revenue. Moreover, for smaller instances they use a branch and bound algorithm to solve it to optimality. However, for larger instances they apply a stochastic constraint programming approach, since it is not possible to solve the problem to optimality. Kawas et al. (2011) shows how CVaR can be used as the objective function as well as how the size of a problem affects the solution method.

Vardanyan and Hesamzadeh (2015) propose a multi-objective model that optimizes coordinated production for a risk-averse hydropower producer. Furthermore, they have a weighted sum of the expected profit of production and the variance of profit as their objective function. They study three different markets, the real time, intraday and day ahead market. Moreover, their model is tested on a three-reservoir system. They explore how the number of locations affects risk. Lastly, their results suggest that it is profitable to coordinate planning in sequential planning.

Schütz and Westgaard (2018) present a multi-stage stochastic programming model that determines the optimal hedging decisions for a risk-averse salmon farmer. Their objective is to maximize the weighted sum of the CVaR of the revenue from the planning horizon and the expected revenues of sales in future contracts. Furthermore, they study three different CVaR percentiles and levels of risk-aversion. Their results indicate that salmon farmers should use future contracts for low levels of risk-aversion to hedge price risk.

Chapter 4

Problem description

In this chapter we present the problem description which forms the basis for the mathematical model in Chapter 6.

The production system of a salmon farming company consists of a set of locations where deployments of smolt take place. For each deployment the company must determine initial smolt weight and smolt type. However, not all smolt weights can be deployed throughout the year. The duration of the planning horizon is finite and it is divided into a set of time periods. Moreover, deployments must take place in a set of release time periods. We assume that all deployments and harvests that take place in the same time period happen at the same time.

Biomass requirements affect production at different locations. The MAB at the company and location-level limit employed biomass.

Operational restrictions limit production and contribute to making production sustainable. The amount of smolt deployed at a location in a time period is restricted. Moreover, the duration of the employment at sea of a cohort is limited. There is an activity requirement at all locations which means that there is a limit on how long a location can be empty.

Occasionally locations must be fallowed. Moreover, the amount of harvested biomass at a location and company-wide level is restricted. Cohorts cannot be harvested if the average weight of a salmon in the cohort is too low or high. In addition, all biomass employed at the end of a planning horizon must be

above a certain level to ensure continuous production.

The company is exposed to uncertainty through the percentage of gender maturation. The uncertainty concerning gender maturation gives rise to the risk of lost production value. Salmon that go through gender maturation experience a reduction in their value.

We represent the planning problem as a two-stage stochastic problem due to the uncertainty of gender maturation. Decisions that must be made before the beginning of the planning horizon make up the first stage of the problem. Furthermore, they include timing, size and location of deployments of smolt as well as the initial smolt weight and smolt type of the deployments. In the second stage, the company has entered the planning horizon and learns the actual gender maturation percentages. Decisions regarding location, size and timing of harvests of salmon make up the second stage. Also, as a part of the second stage the company must keep track of the biomass development for every cohort.

A company can either be risk-neutral or risk-averse. Therefore, it is of interest to develop two different objective functions. If the company is risk-neutral the objective is to maximize the expected value of the harvested salmon. However, if the company is risk-averse, it wants to maximize the CVaR of the value of harvests. This corresponds to the expected value of a percentage of the worst scenarios. Furthermore, the company can select different degrees of risk exposure by altering the percentage of scenarios that make up the CVaR.

Chapter 5

Modeling approaches

In this chapter we present the modeling approaches that are used when formulating the mathematical model presented in Chapter 6. Firstly, we present how we model biomass development. Then, we introduce the modeling of gender maturation.

5.1 Modeling biomass development

Biomass development is one of the most central parts of industrial fish farming since it determines the revenue of harvests. There are many ways to model the development of biomass with respective advantages and drawbacks. Factors like growth, mortality and harvests affect the total biomass of a salmon cohort.

We apply the thermal growth coefficient (TGC) for growth modeling as it is presented in Thorarensen and Farrell (2011). This way of modeling has the benefit of the TCG value being independent of the weight of the fish, making it easy to find the final weight of the fish (Jover and Estruch, 2017). Furthermore, our implementation follows Aasen (2021).

Equation (5.1.1) shows how TGC models growth development in a salmon cohort. w_t refers to the mean weight of an individual salmon in time period t, T_t is the average seawater temperature in Celsius during time period t and L_t is the duration of time period t in days. Lastly, TGC_t is a parameter that is proportional to the growth rate of a salmon and depends on the amount of time a salmon cohort has spent at sea.

$$w_{t+1} = (w_t^{\frac{1}{3}} + \frac{1}{1000} \cdot TGC_t \cdot T_t \cdot L_t)^3 \tag{5.1.1}$$

The mortality rate, μ_t, is the ratio between deaths and total individuals in time period t. Moreover, the survival percentage, s_t, is the percentage of a salmon cohort that is alive at time period t. Equation (5.1.2) shows the relationship between μ_t and s_t.

$$s_t = (1 - \mu_{t-1}) \cdot s_{t-1} \tag{5.1.2}$$

The product of s_t and ω_t is the expected amount of biomass employed at sea in time period t. We introduce parameter A_t, as the ratio between the total biomass in t and the total biomass at deployment as shown in equation (5.1.3).

$$A_t = \frac{s_t \cdot w_t}{w_1} \tag{5.1.3}$$

Moreover, we denote the total biomass of a deployed cohort and the total biomass at the start of t, as y and W_t respectively. The relationship between the two parameters is expressed in equation (5.1.4).

$$W_t = A_t \cdot y. \tag{5.1.4}$$

We let R_t be the monthly growth rate of a cohort. It measures the ratio between the total biomass at time period t, A_t, and the total biomass at time period $t-1$, A_{t-1}, given that no harvesting occurs. This can be seen in equation (5.1.5).

$$R_t = \frac{A_t}{A_{t-1}} \tag{5.1.5}$$

Unlike equation (5.1.4), equation (5.1.6) takes harvesting into consideration, by denoting H_t as the harvested amount of biomass at time t.

$$W_t = R_t(W_{t-1} - H_{t-1}) \tag{5.1.6}$$

Since the TGC_t parameter is incorporated into the parameters A_t and R_t, it does not appear in the mathematical model presented in Chapter 6.

5.2 Modeling of gender maturation

In Chapter 2, we discuss the uncertainty concerning gender maturation. Salmon within a cohort can go through gender maturation at different points in time. Moreover, the gender maturation percentage in a cohort can never decrease, since gender maturation is irreversible. When a salmon experiences gender maturation, the value of the fish decreases. However, we assume that gender maturation does not affect the growth of a salmon.

We assume that there are three factors that affect the gender maturation percentage. Firstly, the most important factor is the smolt type of the salmon cohort, due to male salmon having a higher probability of going through gender maturation. Secondly, the mean weight of a salmon in a cohort affects gender maturation. If the weight is below a certain level, gender maturation will not take place in the cohort. This is a reasonable assumption, since the number of fish that experience gender maturation below a certain weight level are negligible (Aquagen, 2021). Lastly, the gender maturation percentage is affected by how many gender maturation months the salmon have experienced at sea. A gender maturation month is a month where salmon can experience gender maturation. Moreover, gender maturation can only take place in late-summer and autumn. We use Eidsfjord Sjøfarm et al. (2017) and Aquagen (2021) as the basis for the gender maturation modeling.

We assume that the gender maturation percentage is 0 until the first gender maturation month $GM1$. For every gender maturation month, the gender maturation percentage increases with the same percentage. Hence, the growth of gender maturation percentage is linear in the gender maturation months. $D^s_{t'fglt}$ is the gender maturation percentage of a cohort at time t, deployed at time period t' in scenario s.

We denote ρ_g^s as the increase in the gender maturation percentage a cohort experiences in a gender maturation month in scenario s, when the smolt type is g. Moreover, we express $J_{t'fglt}^s$ as the number of gender maturation months a cohort has experienced at time t, deployed at time period t' in scenario s.

Equation (5.2.1) shows that the gender maturation percentage, $D_{t'fglt}^s$, equals the product of the monthly increase in the gender maturation percentage, ρ_g^s, and the number of gender maturation months the cohort has experienced, $J_{t'fglt}^s$. Furthermore, ρ_g^s and $J_{t'fglt}^s$ do not appear in the mathematical model presented in Chapter 6 since they are incorporated into the parameter $D_{t'fglt}^s$.

$$D_{t'fglt}^s = \rho_g^s J_{t'fglt}^s \tag{5.2.1}$$

An example of the development of the gender maturation percentage is illustrated in Figure 5.1. Here the monthly increase in the gender maturation percentage in gender maturation months, ρ_g^s, is 3 %. The cohort experiences four gender maturation months in total. Furthermore, the gender maturation percentage does not increase after month 11, since the cohort does not go through any more gender maturation months.

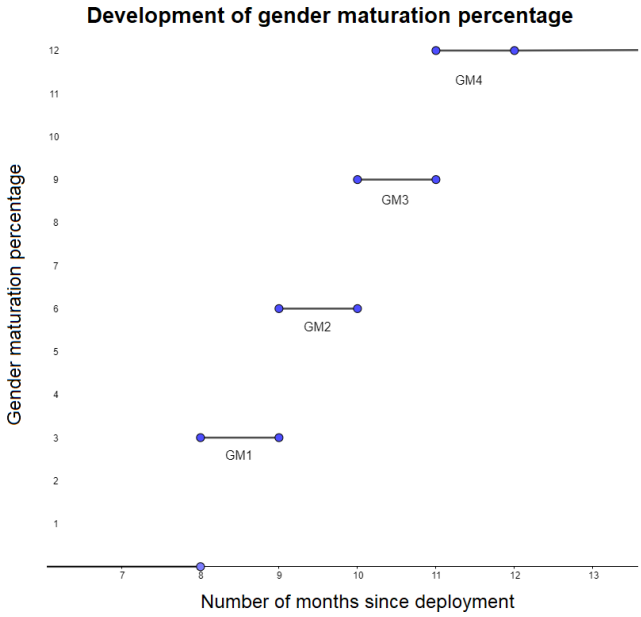

Figure 5.1: The development of the gender maturation percentage.

Chapter 6

Mathematical model

In the following chapter we introduce the mathematical model for the problem presented in Chapter 4. Firstly, we introduce the notation of the model. Thereafter, we present the two objective functions. Lastly, we describe the constraints that make up the problem. The model is inspired by Aasen (2021) and builds largely upon Lien (2021). A compacted version of the objective functions and constraints is presented in Appendix A.

6.1 Notation

In this section we present the sets and parameters that are used to formulate the objective function and constraints. Then, we introduce the decision variables that constitute the problem.

6.1.1 Sets

Symbol	Description
$\mathcal{L}$	The set of all locations.
$\mathcal{T}$	The set of all time periods that make up the planning horizon.
$\mathcal{T}^+$	The set of all time periods that make up the planning horizon with the addition of an extra dummy period representing the time period following the final time period in $\mathcal{T}$.
$\mathcal{T}^R$	The set of all time periods in the planning horizon where deployments of smolt are possible.
$\mathcal{T}_0^R$	The set of all time periods in the planning horizon, where deployments of smolt are possible, with the addition of an extra dummy time period preceding the first time period in $\mathcal{T}^R$.
$\mathcal{F}$	The set of all deployment weights for smolt.
$\mathcal{F}_t$	The set of all deployment weights for smolt that are available for deployment in time period t, $t \in \mathcal{T}_0^R$.
$\mathcal{G}$	The set of all smolt types.
$\mathcal{G}_t$	The set of all smolt types, where deployment is possible during the time period t, $t \in \mathcal{T}_0^R$.
$\mathcal{S}$	The set of all scenarios.
$\mathcal{T}_{fglt}^G$	The set of all time periods where a cohort is of a non-harvestable size, with a deployment weight f, smolt type g and deployed during time period t at location l, $t \in \mathcal{T}^+$, $f \in \mathcal{F}_t$, $g \in \mathcal{G}_t$ and $l \in \mathcal{L}$.
$\mathcal{T}_{fglt}^H$	The set of all time periods where a cohort is of a harvestable size, with a deployment weight of f, smolt type g and deployed during time period t at location l, $t \in \mathcal{T}^+$, $f \in \mathcal{F}_t$, $g \in \mathcal{G}_t$ and $l \in \mathcal{L}$.
$\mathcal{T}_{fglt}^{H+}$	Identical to $\mathcal{T}_{fglt}^H$, with an additional extra dummy time period for all situations when harvests can take place after the planning horizon, $t \in \mathcal{T}^+$, $f \in \mathcal{F}_t$, $g \in \mathcal{G}_t$ and $l \in \mathcal{L}$.

Symbol	Description
$\mathcal{T}^D_{fglt}$	The set of all time periods where a cohort can be deployed, with a deployment weight of f, smolt type g and harvested during time period t at location l, $t \in \mathcal{T}^R_0$, $f \in \mathcal{F}_t$, $g \in \mathcal{G}_t$ and $l \in \mathcal{L}$.
$\mathcal{T}^{\Lambda^-}_t$	The set of the Λ time periods preceding t, $t \in \mathcal{T}^R_0$.
$\mathcal{T}^{\Lambda^-_R}_t$	The set of all time periods where deployments can occur in time period t or during the $\Lambda - 1$ time periods preceding t, $t \in \mathcal{T}^R_0$.
$\mathcal{T}^{\Gamma-}_t$	The set of time periods consisting of t and $\Gamma - 1$ preceding time periods, $t \in \mathcal{T}$.
$\mathcal{T}^{\Gamma^{INIT}}_l$	The set of all time periods where deployments must occur during the first time periods of the planning horizon at location l, $l \in \mathcal{L}$.
$\mathcal{T}^E$	The set of all time periods taking place after the planning horizon, where salmon can experience growth.
$\mathcal{B}^G_{lt}$	The set of tuples containing (f,g,t'), $t' \in \mathcal{T}^R_0$, $f \in \mathcal{F}_{t'}$ and $g \in \mathcal{G}_{t'}$. When deployment occurs, the tuples represent deployments that could grow in time period t at location l in scenario s, $t \in \mathcal{T}^E$ and $l \in \mathcal{L}$.

6.1.2 Parameters

Symbol	Description
π_s	The probability of scenario s, $s \in \mathcal{S}$.
N_f	The number of smolt that make up one kilogram, with deployment weight f, $f \in \mathcal{F}$.
L_l^{LOC}	The lower bound of the number of smolt that can be deployed at location l simultaneously, $l \in \mathcal{L}$.
U_l^{LOC}	The upper bound of the number of smolt that can be deployed at location l simultaneously, $l \in \mathcal{L}$.
L_l^{TYPE}	The lower bound of the number of smolt that can be deployed at location l simultaneously of one smolt type, $l \in \mathcal{L}$.
U_l^{TYPE}	The upper bound of the number of smolt that can be deployed at location l simultaneously of one smolt type, $l \in \mathcal{L}$.
L_l^H	The lower bound of the biomass harvested during a time period at location l, $l \in \mathcal{L}$.
U_l^H	The upper bound of the biomass harvested during a time period at location l, $l \in \mathcal{L}$.
U_t^{COM}	The upper bound of biomass harvested on a company-wide level in time period t, $t \in \mathcal{T}$.
MAB_l	The maximum allowed biomass (MAB) at location l, $l \in \mathcal{L}$.
MAB^{COM}	The maximum allowed biomass for the company as a whole.
β_{l0}	A binary parameter that is set to the value of 1 if biomass is employed at location l before the beginning of the planning horizon, otherwise 0, $l \in \mathcal{L}$.
q_{0fgl0}	The initial amount of biomass employed in the first period of the planning horizon at location l with deployment weight f and smolt type g, $l \in \mathcal{L}$, $f \in \mathcal{F}_0$ and $g \in \mathcal{G}_0$.

Symbol	Description
y_{fgl0}	The initial amount of biomass employed in the first time period of the planning horizon at location l with deployment weight f and smolt type g, $l \in \mathcal{L}$, $f \in \mathcal{F}_0$ and $g \in \mathcal{G}_0$.
Γ	The maximum number of time periods that a location can be empty before the risk of the production license being withdrawn appears.
Δ	The maximum number of time periods that a cohort can be employed in the sea.
Λ	The minimum number of time periods that a location must be fallowed after harvest before deployment of new smolt can occur.
$A_{t'fglt}$	The ratio between biomass employed in time periods t and t', with deployment weight f, smolt type g and deployed during time period t' at location l, $t' \in \mathcal{T}_{\prime}^{\mathcal{R}}$, $l \in \mathcal{L}$, $f \in \mathcal{F}_{t'}$, $g \in \mathcal{G}_{t'}$ and $t \in \mathcal{T}^{+} \cup \mathcal{T}^{E}$.
$R_{t'fglt}$	The ratio between biomass employed in time periods t and $t-1$, with deployment weight f, smolt type g and deployed during time period t' at location l, $t' \in \mathcal{T}_0^R$, $l \in \mathcal{L}$, $f \in \mathcal{F}_{t'}$, $g \in \mathcal{G}_{t'}$ and $t \in \mathcal{T}^{+} \cup \mathcal{T}^{E}$.
$D^{s}_{t'fglt}$	The percentage of a salmon cohort that have experienced gender maturation, in scenario s, $t' \in \mathcal{T}_0^R$, $g \in \mathcal{G}$, $f \in \mathcal{F}$, $l \in \mathcal{L}$, $t \in \mathcal{T}$, $j \in \mathcal{J}$ and $s \in \mathcal{S}$.
P_{Low}	The relative value of salmon that have experienced gender maturation.
P_{High}	The relative value of salmon that have not gone through gender maturation.
α	The cut-off point of the distribution, where the breakpoint of VaR is set.

6.1.3 Decision variables

Decision variables that have an s indexation are second stage variables, while all other decision variables are first stage variables.

Symbol	Description
δ_{fglt}	Binary variable that is 1 if deployment occurs for a cohort, with deployment weight f and smolt type g during time period t at location l, otherwise 0. $t \in \mathcal{T}^R$, $l \in \mathcal{L}$, $f \in \mathcal{F}_t$ and $g \in \mathcal{G}_t$.
δ_{lt}	Binary variable that is 1 if deployment occurs for a cohort in time period t at location l, otherwise 0. $l \in L$ and $t \in \mathcal{T}^R$.
y_{fglt}	Amount of biomass within a cohort deployed, with deployment weight f and smolt type g during time period t at location l, $f \in \mathcal{F}_t$, $g \in \mathcal{G}_t$, $l \in \mathcal{L}$ and $t \in \mathcal{T}^R$.
ω^s_{lt}	Binary variable that is 1 if harvesting takes place in time period t at location l, in scenario s, otherwise 0. $s \in \mathcal{S}$, $t \in \mathcal{T}$ and $l \in \mathcal{L}$.
$\omega^s_{t'fglt}$	Amount of biomass harvested from time period t' to time period t at location l, with deployment weight f and smolt weight g in scenario s, $s \in \mathcal{S}$, $t' \in \mathcal{T}^R_0$, $f \in \mathcal{F}_{t'}$, $g \in \mathcal{G}_{t'}$, $l \in \mathcal{L}$ and $t \in \mathcal{T}^{H+^s}_{fglt'}$.
β^s_{lt}	Binary variable that is 1 if biomass is employed in time period t at location l in scenario s, otherwise 0. $s \in \mathcal{S}$, $t \in \mathcal{T}$ and $l \in \mathcal{L}$.
$q^s_{t'fglt}$	Amount of biomass that is employed in time period t that stems from a cohort with deployment weight f and smolt weight g and deployed during time period t' at location l in scenario s, $s \in \mathcal{S}$, $t \in \mathcal{T}^R_0$, $f \in \mathcal{F}_{f'}$, $g \in \mathcal{G}_{t'}$, $l \in \mathcal{L}$, $t \in \mathcal{T}^{Gs}_{fglt'} \cup \mathcal{T}^{H+^s}_{fglt'}$.
q^s_{lt}	The amount of biomass employed in time period t at location l in scenario s, $s \in \mathcal{S}$, $t \in \mathcal{T}$ and $l \in \mathcal{L}$.
x_s	The return shortfall beneath the VaR in scenario s, $x_s = [0, z - R_s]$ with R_s being the harvested value of scenario s, $s \in \mathcal{S}$. It is only relevant when the objective is to maximize the CVaR.
z	Variable that is set to the value of VaR at the optimal solution. It is only relevant when the objective is to maximize the CVaR.

6.2 Objective function

In this thesis there are two distinct objectives we wish to maximize, depending upon the risk preference of the decision maker. The decision maker can either use the expected value of harvests or the CVaR of the value of harvests. Through the use of a weighted sum, it is possible to include both objectives in the objective function.

Equation (6.2.1) presents the objective function that maximizes the expected value of harvests. For each scenario $s \in \mathcal{S}$, the value of the harvests consists of two parts. In the first part we find the value of the harvested salmon that have experienced gender maturation while we find the value of non-gender matured salmon in the second part. We find the value of gender matured salmon by multiplying the total weight of a cohort with the product of the relative price of gender matured salmon P_{Low} and the percentage of a cohort that have experienced gender maturation $D^s_{t'fglt}$. Moreover, to find the value of non-gender matured salmon we multiply the total weight of a cohort with the product of the relative price of non-matured salmon P_{High} and the percentage of salmon that have not experienced gender maturation $1 - D^s_{t'fglt}$. Lastly, we sum over the value of the harvests of a scenario multiplied with the probability of the scenario occurring.

$$\max \quad \sum_{s\in S} \pi_s \Big(\sum_{t'\in\mathcal{T}_0^R} \sum_{f\in\mathcal{F}_{t'}} \sum_{g\in\mathcal{G}_{t'}} \sum_{l\in\mathcal{L}} \sum_{t\in\mathcal{T}^{Hs}_{fglt'}} (P_{High}(1-D^s_{t'fglt}) + P_{Low}(D^s_{t'fglt}))\omega^s_{t'fglt} \Big) \tag{6.2.1}$$

We use Uryasev and Rockafellar (2001) as the basis for the linear representation of the CVaR. When maximizing the CVaR the inclusion of constraint (6.2.2) is necessary. The constraint determines the excess shortfalls x_s for every scenario s. The excess shortfall must be larger than the difference between the value that approaches VaR at optimal solution and the expected value of harvests. As a result of the aim being to maximize the CVaR, the excess shortfall x_s, will approach the right-hand side of the constraint.

$$x_s \geq z - \sum_{t' \in \mathcal{T}_0^R} \sum_{f \in \mathcal{F}_{t'}} \sum_{g \in \mathcal{G}_{t'}} \sum_{l \in \mathcal{L}} \sum_{t \in \mathcal{T}_{fglt'}^{Hs}} (P_{High}(1 - D^s_{t'fglt}) + P_{Low}(D^s_{t'fglt}))\omega^s_{t'fglt}$$

$$s \in \mathcal{S} \tag{6.2.2}$$

The objective function is expressed in equation (6.2.3). It maximizes the expected value of the value of harvests of the α % scenarios with the lowest objective value.

$$\max \quad z - \frac{1}{1-\alpha} \sum_{s \in \mathcal{S}} \pi_s x_s \tag{6.2.3}$$

For the remainder of the thesis, we will respectively denote the problem where we maximize the expected value and the CVaR as the $ExpectedRevenueProblem$ and $CVaRProbem$.

6.3 Constraints

In industrial salmon farming all companies must comply with regulatory and operational restrictions. This forms the basis for the constraints presented in this section. In all constraints we make the assumption that growth, mortality, gender maturation, deployments and harvests take place at the beginning of a time period. Moreover, if a cohort is harvested during a time period, it does not experience growth during this time period.

6.3.1 Smolt deployment constraints

To ensure that the size of an individual deployment of a cohort is within the bounds of L_l^{TYPE} and U_l^{TYPE} constraint (6.3.1) is in place. The number of smolt in a cohort is found by multiplying the amount of smolt that constitute a kilogram, N_f, with the deployment weight of the smolt, y_{fglt}. Furthermore, the constraint requires δ_{fglt} to be 1, when y_{fglt} is positive. The lower bound

ensures that cohorts with few smolt are not deployed. In addition, the upper bound is in place to ensure that y_{fglt} takes the value of zero, whenever δ_{fglt} does.

$$L_l^{TYPE}\delta_{fglt} \leq N_f y_{fglt} \leq U_l^{TYPE}\delta_{fglt} \quad t \in \mathcal{T}, f \in \mathcal{F}_t, g \in \mathcal{G}_t, l \in \mathcal{L} \tag{6.3.1}$$

Constraint (6.3.2) enforces that the number of smolt deployed at location l in time period t is less than U_l^{LOC} and more than L_l^{LOC}. U_l^{LOC} is in place to ensure that deployments are of a size below the capacity of a company, while L_l^{LOC} secures that the costs and resources of all deployments are justified.

$$L_l^{LOC}\delta_{lt} \leq \sum_{f\in\mathcal{F}_t}\sum_{g\in\mathcal{G}_t} N_f y_{fglt} \leq U_l^{LOC}\delta_{lt} \quad l \in \mathcal{L}, t \in \mathcal{T} \tag{6.3.2}$$

The model is tightened by including constraint (6.3.3), due to δ_{lt} being assigned to the value of 1, when a deployment of a cohort occurs in a specific time period. The right-hand side of the constraint (6.3.3) represents the maximum number of deployments that can occur at a location in a time period.

$$\sum_{f\in\mathcal{F}_t}\sum_{g\in\mathcal{G}_t} \delta_{fglt} \leq |F_t||G_t|\delta_{lt} \quad l \in \mathcal{L}, t \in \mathcal{T}^R \tag{6.3.3}$$

Constraint (6.3.4) is included in the model to ensure that cohorts are employed throughout their growth phase. As a result, cohorts cannot be harvested before they reach harvestable weights.

$$\sum_{f\in\mathcal{F}_t}\sum_{g\in\mathcal{G}_t} \delta_{fglt} \leq \beta_{l\tau}^s \quad s \in \mathcal{S}, l \in \mathcal{L}, t \in \mathcal{T}^R, f \in \mathcal{F}_t, g \in \mathcal{G}_t, l \in \mathcal{L}, \tau \in \mathcal{T}_{fglt}^G \tag{6.3.4}$$

6.3.2 Fallowing constraints

Constraint (6.3.5) is in place to make sure that the fallowing period between harvest and deployment has a duration of at least Λ time periods. Whenever

δ_{lt} is set to the value of 1, β^s_{lt} must take the value of zero for the Λ preceding time periods.

$$\Lambda\delta_{lt} + \sum_{\tau \in \mathcal{T}_t^{\Lambda^-}} \beta^s_{l\tau} \leq \Lambda \quad l \in \mathcal{L}, t \in \mathcal{T}^R \quad \setminus \quad (1, .., \Lambda) \tag{6.3.5}$$

6.3.3 Harvesting constraints

There is a need for restrictions regarding harvests due to limited capacities. The lower bound of the size of a harvest, L^H_l, is in place to avoid non-profitable decisions.

We must sum over all cohorts that can be in their harvest phase to find the biomass of all harvested salmon at a location. In addition, constraint (6.3.6) ensures that ω^s_{lt} is solely set to the value of 1 if harvesting takes place, given that the value of L^H_l is greater than zero.

$$L^H_l \omega^s_{lt} \leq \sum_{f \in \mathcal{F}'_t} \sum_{g \in \mathcal{G}'_t} \omega^s_{t'fglt} \leq U^H_l \omega^s_{lt} \quad s \in \mathcal{S}, l \in \mathcal{L}, t \in \mathcal{T} \tag{6.3.6}$$

By including constraint (6.3.7) we ensure that the total harvest for the company in a time period is less than U^{COM}_t. This restriction must be included, to ensure that the company does not break the company-wide MAB.

$$\sum_{t' \in \mathcal{T}^D_{fglt}} \sum_{f \in \mathcal{F}} \sum_{g \in \mathcal{G}} \sum_{l \in \mathcal{L}} \omega^s_{t'fglt} \leq U^{COM}_t \quad s \in \mathcal{S}, t \in \mathcal{T} \tag{6.3.7}$$

6.3.4 Activity constraints

Constraint (6.3.8) is in place to ensure that the company keeps its production licenses. The constraint enforces that a location has biomass present for Γ consecutive time periods. This is ensured by giving at least one of Γ consecutive time periods, β^s_{lt}, the value of 1.

$$\sum_{\tau \in \mathcal{T}_t^{\Gamma-}} \beta_{l\tau}^s \geq 1 \quad s \in \mathcal{S}, l \in \mathcal{L}, t \in \mathcal{T} \quad \setminus \quad (1, .., \Gamma - 1) \tag{6.3.8}$$

6.3.5 Biomass development and MAB constraints

An employed cohort at a location will either experience growth or be harvested in a time period. The biomass of a cohort is $q_{t'fglt}^s$ when the cohort experiences growth. The value of $q_{t'fglt}^s$ is the product of the growth ratio, $A_{t'fglt}$, and the initially deployed biomass, y_{fglt}. This equality is enforced in constraint (6.3.9). It applies to all time periods where the cohort can experience growth as well as the first time period where the cohort can be harvested. The latter is included to account for the growth the cohort experiences in the final time period of growth. A detailed introduction of the parameters $A_{t'fglt}$ and $R_{t'fgi(t+1)}$ with fewer subscripts is presented in Section 5.1.

$$q_{t'fglt}^s = A_{t'fglt} y_{fglt'}^s \quad s \in \mathcal{S}, t' \in \mathcal{T}_0^R, g \in \mathcal{G}_{t'}$$

$$s \in S, t' \in \mathcal{T}_0^R, g \in \mathcal{G}_{t'}, \quad s \in \mathcal{S}, l \in \mathcal{L}, t \in (\mathcal{T}_{fglt'}^G \cup \min \mathcal{T}_{fglt'}^H) \tag{6.3.9}$$

By including constraint (6.3.10) in the model, we ensure that the biomass employed in a time period equals the product of the monthly growth ratio, $R_{t'fgi(t+1)}$, and the difference between the amount of harvested biomass in the previous period, $\omega_{t'fglt}^s$, and the biomass employed in the previous period, $q_{t'fglt}^s$. We must use $t \in T_{fglt'}^{H+^s}$, since cohorts can experience growth in time periods following the planning horizon.

$$q_{t'fglt}^s = R_{t'fglt}(q_{t'fgi(t-1)}^s - \omega_{t'fgi(t-1)}^s)$$

$$s \in \mathcal{S}, t' \in \mathcal{T}_0^R, g \in \mathcal{G}_{t'}, l \in \mathcal{L}, t \in (\mathcal{T}_{fglt'}^{H+^s} \cup \min \mathcal{T}_{fglt'}^{H^s}) \tag{6.3.10}$$

Constraint (6.3.11) ensures that all deployed cohorts are harvested at a later point in time. This is achieved by setting the biomass of the harvested cohorts in the final time period at a location equal to the locations' remaining biomass. The final time period is an extra dummy time period and will therefore not be included in the objective function.

$$q^s_{t'fgi[max\mathcal{T}^{H+}_{fglt'}]} - \omega^s_{t'fgi[max\mathcal{T}^{H+}_{fglt'}]} = 0$$

$$s \in \mathcal{S}, t' \in \mathcal{T}^R_0, f \in \mathcal{F}_{t'}, g \in \mathcal{G}_{t'}, l \in \mathcal{L} \tag{6.3.11}$$

MAB regulations at locations form the basis of constraint (6.3.12). Constraints (6.3.12) and (6.3.4) enforce that β^s_{lt} may be set only to the value of 1, when there is biomass deployed at location l in time period t.

$$q^s_{lt} <= MAB_l \beta^s_{lt} \quad s \in \mathcal{S}, l \in \mathcal{L}, t \in \mathcal{T} \tag{6.3.12}$$

The decision variable q^s_{lt} is used to keep track of the amount of biomass at location l in time period t. Constraint (6.3.13) ensures this by iterating over the time period t and the $\Delta - 1$ preceding time periods.

$$q^s_{lt} = \sum_{t' \in \mathcal{T}^{\Delta^-_R}} \sum_{f \in \mathcal{F}_t} \sum_{g \in \mathcal{G}_{t'}} q^s_{t'fglt} \quad s \in \mathcal{S}, l \in \mathcal{L}, t \in \mathcal{T} \tag{6.3.13}$$

Finally, to ensure that the employed biomass is less than the company-wide MAB, MAB^{COMP}, constraint (6.3.14) is included.

$$\sum_{l \in \mathcal{L}} q^s_{lt} \leq MAB^{COMP} \quad s \in \mathcal{S}, t \in \mathcal{T} \tag{6.3.14}$$

6.3.6 Initial Conditions Constraints

We have an initial dummy time period due to the fact that salmon can be deployed before the beginning of the planning horizon. Cohorts that have been deployed before the planning horizon will first experience mortality and growth in the beginning of the second time period. We must also ensure that a cohort cannot be employed for more than Δ time periods. These cohorts are assigned to the same weight class f, since it does effect further growth.

Constraint (6.3.15) must be included in the model to ensure that fallowing takes place in at least one of the Γ first time periods of the planning horizon.

$$\beta_{lt}^{s} \leq 0 \quad s \in \mathcal{S}, l \in \mathcal{L}, t \in \mathcal{T}_{l}^{\Gamma^{INIT}} \tag{6.3.15}$$

Constraint (6.3.16) makes sure that the activity requirements are satisfied at the start of the planning horizon. The set of $\mathcal{T}_{l}^{\Gamma^{INIT}}$ contains all time periods for location l where there must be biomass present in at least one time period, to avoid the loss of a production license.

$$\sum_{t \in \mathcal{T}_{l}^{\Gamma^{INIT}}} \beta_{l\tau}^{s} \geq 1 \quad s \in \mathcal{S}, l \in \mathcal{L} \tag{6.3.16}$$

6.3.7 End of horizon constraints

Since most salmon farming companies operate for an unknown amount of time it is necessary to facilitate production after the planning horizon. Therefore, constraint (6.3.17) enforces that the company-wide biomass employed at the end of the planning horizon is greater than or equal to the amount of biomass employed at the beginning of the first time period of the planning horizon. Without this constraint present, the model would suggest that the company harvests all biomass before the end of the planning horizon.

In many cases this will be a fitting approach for modeling the end of the horizon. It allows the farming company to keep salmon at the locations it identifies as preferable. Furthermore, it functions well when the initial biomass lies close to the average amount of biomass employed.

$$\sum_{l \in \mathcal{L}} q_{l|T|}^{s} \geq \sum_{f \in \mathcal{F}} \sum_{g \in \mathcal{G}} \sum_{l \in \mathcal{L}} y_{fgl0} \quad s \in \mathcal{S} \tag{6.3.17}$$

Constraints (6.3.18) and (6.3.19) ensure that the level of biomass is respectively below locational and the company-wide MAB in the time periods following the planning horizon. This is necessary since the MAB is present and salmon keep growing after the planning horizon.

$$\sum_{(f,g,t') \in \mathcal{B}_{lt}^{G}} A_{t'fglt} y_{fglt'}^{s} \leq MAB_{l} \quad s \in \mathcal{S}, l \in \mathcal{L}, t \in \mathcal{T}^{E} \tag{6.3.18}$$

$$\sum_{l \in L} \sum_{(f,g,t') \in \mathcal{B}_{lt}^{G}} A_{t' f g l t} y_{f g l t'}^{s} \leq MAB^{COMP} \quad s \in \mathcal{S}, t \in \mathcal{T}^{E} \tag{6.3.19}$$

6.3.8 Requirements of decision variables

$$\delta_{f g l t} \in \{0,1\} \tag{6.3.20}$$

$$\delta_{l t} \in \{0,1\} \tag{6.3.21}$$

$$\beta_{l t} \in \{0,1\} \tag{6.3.22}$$

$$\omega_{l t}^{s} \in \{0,1\} \tag{6.3.23}$$

$$\omega_{t' f g l t}^{s} \geq 0 \tag{6.3.24}$$

$$q_{l t}^{s} \geq 0 \tag{6.3.25}$$

$$q_{t' f g l t}^{s} \geq 0 \tag{6.3.26}$$

$$x^{s} \geq 0 \tag{6.3.27}$$

$$z \quad free \tag{6.3.28}$$

Chapter 7

Solution method

In this chapter we present the solution method used to solve the mathematical model presented in Chapter 6. We begin by studying structures that appear in the problem. Then, we introduce the methods of Dantzig-Wolfe decomposition and column generation which we apply to the problem structure. Thereafter, we present the Dantzig-Wolfe reformulation of the model. Lastly, we explain branch and price as the solution method, to ensure that integrality conditions are satisfied.

7.1 Problem structure

In this section we identify two different structures in the problem. Then, we discuss how the structures can be exploited. Lastly, we select one of the structures to exploit for the remainder of the thesis.

7.1.1 Two-stage structure

The uncertainty in the model gives rise to a two-stage structure in the problem. The structure can be decomposed to a master problem representing the first-stage decisions and $|\mathcal{S}|$ problems representing the second stage decisions of individual scenarios. This decomposition is illustrated in Figure 7.1.

This problem structure can be exploited by using the L-shaped algorithm. A complete review of the algorithm is presented in Birge and Louveaux (2011). The main idea of this method is to approximate the recourse function of the objective function in the master problem. Furthermore, for every iteration of the algorithm, the solutions retrieved from the subproblems will be used to generate cuts that are added to the master problem as constraints. Moreover, two types of cuts can be generated in the subproblems, depending upon whether the subproblem is feasible. If the solution of the subproblem is feasible, optimality cuts are generated. However, if the solution of the subproblem is infeasible, feasibility cuts are generated. The addition of cuts in the master problem improves the approximation of the recourse function. By using the L-shaped algorithm, the aim is to solve larger problems and reduce the computational running time of the problem.

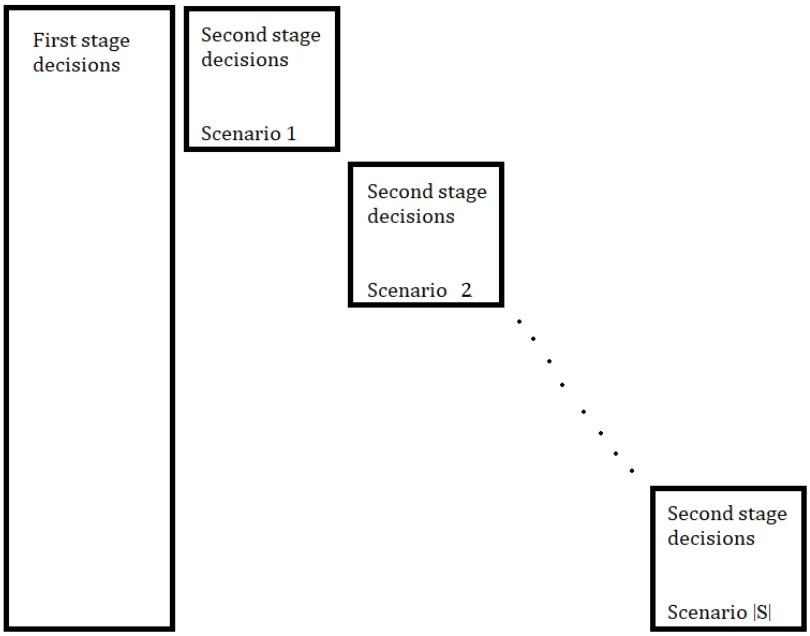

Figure 7.1: The two-stage structure of the problem.

7.1.2 Production system

Most of the constraints in the model can be isolated per location, except for the company-wide regulatory restrictions. The constraints that cannot be isolated per location make up the set of connecting constraints. By relaxing the constraints that link locations together, we get a production system structure. The structure is shown in Figure 7.2. This makes the problem separable per location and creates $|N|$ independent subproblems, with every non-connecting constraint linked to one location, and one master problem containing the connecting constraints. Each subproblem then represents a two-stage production planning problem at a single location. The structure can be exploited by using a Dantzig-Wolfe decomposition method, which in turn can decrease the running time of the problem (Lundgren et al., 2010).

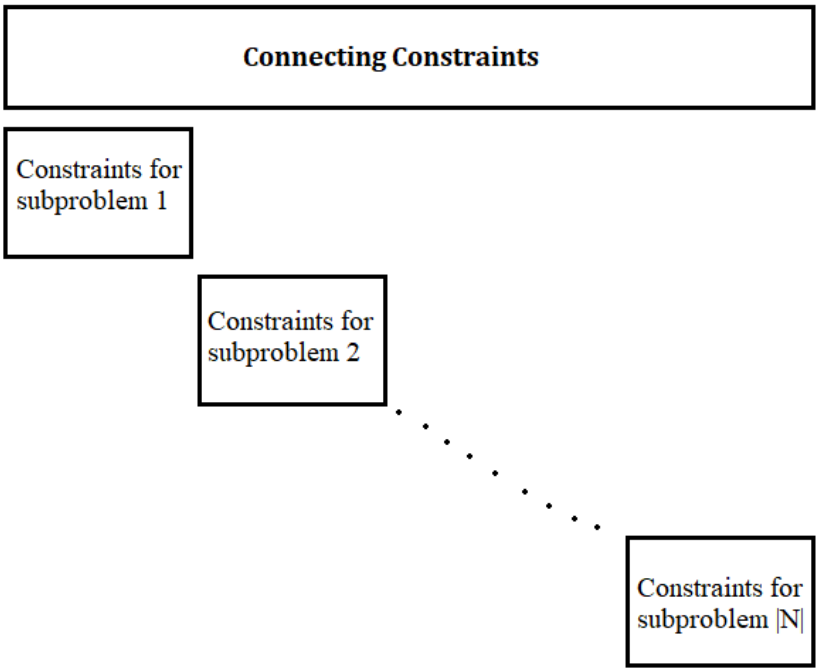

Figure 7.2: The production system structure of the problem.

For the remainder of the thesis, we choose to exploit the production system structure, since the interpretation of the subproblems and master problem is clear and practical. Moreover, Føsund and Strandkleiv (2021) reported

promising results when exploiting the production system structure in a deterministic land-based salmon production planning problem.

7.2 Dantzig-Wolfe decomposition

Decomposition is a method of solving a problem by dividing it into smaller problems and separately solving them (Boyd et al., 2003). By solving several smaller problems instead of one large problem, the complexity and running time can decrease. To exploit the structure of the problem, we will use Dantzig-Wolfe decomposition. It is a decomposition method closely tied to column generation, a tool used to solve large problems (Lundgren et al., 2010). The presentation of Dantzig-Wolfe decomposition is taken from Williams (2013).

We begin with the linear problem (P), presented in equations (7.2.1)–(7.2.4). (P) has the production system structure presented in Section 7.1.2, with constraint (7.2.2) and the set of constraints (7.2.3), respectively making up the connecting and non-connecting constraints of the problem. Furthermore, the set of the non-connecting constraints (7.2.3) can be isolated into N sets of separate constraints.

$$(P) \quad \max \quad \sum_{n}^{N} c^T x_n \tag{7.2.1}$$

$$s.t. \quad \sum_{n}^{N} A x_n \leq b \tag{7.2.2}$$

$$\begin{aligned} D_1 x_1 &\leq e_1 \\ &\ddots \\ &D_N x_N \leq e_N \end{aligned} \tag{7.2.3}$$

$$x_n \geq 0 \tag{7.2.4}$$

By isolating the set of constraints (7.2.3) we can divide (P) into N subproblems, expressed in equations (7.2.5)–(7.2.7). The connecting constraint (7.2.2) is not a part of the subproblems. Each subproblem n is subject to a set of separate constraints, $D_n x_n \leq e_n$. The optimal solution of the subproblem is a vertex in the solution space of the subproblem. Moreover, all solutions of a subproblem can be written as a linear combination of vertices of the solution space. A solution of a subproblem and its objective value is known as a column.

$$(SP_n) \quad \max \quad c_n x_n \quad n = 1...N \tag{7.2.5}$$

$$s.t. \quad D_n x_n \leq e_n \quad n = 1...N \tag{7.2.6}$$

$$x_n \geq 0 \quad n = 1...N \tag{7.2.7}$$

It is possible to write any solution of (P) as a convex linear combination of vertices of the subproblems. This is expressed in equation (7.2.8), where $x^{(kn)}$ is a vertex connected to column k and subproblem n. Moreover, λ_{kn} is the weighting variable associated with the vertex $x^{(kn)}$. The weighting variables must be non-negative and the sum of the weighting variables connected to a subproblem must be 1.

$$x_n = \sum_{k=1}^{K} \lambda_{kn} x^{(kn)}, \quad \sum_{k=1}^{K} \lambda_{kn} = 1 \wedge \lambda_{kn} \geq 0, \quad k = 1, ..., K, \quad n = 1, ..., N \tag{7.2.8}$$

We can use equation (7.2.8) to substitute the decision variables x in (P). This reformulates (P) into the master problem (MP), expressed in equations (7.2.9)–(7.2.12). In the (MP) the aim is to find the optimal mixture of vertices of each subproblem. However, there is no guarantee that the combination of the optimal columns of the different subproblems is feasible for (P). The reason for this is that the combination of the optimal columns might not comply with the connecting constraint.

The connecting constraints (7.2.2) of (P) appear in the (MP) as constraint (7.2.10). Furthermore, the non-connecting constraints (7.2.3) are expressed as a convex combination of vertices of each subproblem and do therefore not appear as a constraint in the (MP). Moreover, v is a dual value, linked to constraint (7.2.10). The reformulation from (P) to (MP) reduces the number of constraints and increases the number of decision variables.

$$(MP) \quad \max \sum_{k=1}^{K} \sum_{n=1}^{N} (c^T x^{(kn)}) \lambda_{kn} \tag{7.2.9}$$

$$s.t. \quad \sum_{k=1}^{K} \sum_{n=1}^{N} (Ax^{(kn)}) \lambda_{kn} \leq b \quad |v \tag{7.2.10}$$

$$\sum_{k=1}^{K} \lambda_{kn} = 1 \quad n = 1, ..., N \tag{7.2.11}$$

$$\lambda_{kn} \geq 0 \quad k = 1, ..., K \quad n = 1, ..., N \tag{7.2.12}$$

Before solving the (MP), it is necessary to have all possible columns from the subproblems. However, finding all columns can be as difficult as solving (P) (Tone and Fushimi, 1995). We resort to column generation to avoid this problem.

Column generation utilizes that most of the decision variables in large problems are non-basic, taking the value of zero, in the optimal solution (Lübbecke and Desrosiers, 2005). It exploits the idea that only a selection of the columns will ever enter the optimal solution. Therefore, there is no need to find all columns. The presentation of column generation is retrieved from Williams (2013).

In column generation we begin with a restricted master problem (RMP). The (RMP) has the same structure as the (MP), but it does not need to contain all columns. New columns, that improve the objective value of the (RMP), are added until the optimal solution of the (MP) is found.

The generation of new columns takes place in the subproblems. To ensure that new columns are generated, the objective function of the subproblem is updated to the reduced cost. The reduced cost incorporates the pricing of the shared resource, which is the connecting constraint of the (RMP) (7.2.10). This adjusts the amount new columns use of the shared resource. The updated objective function is presented in equation (7.2.13). A combination of columns from all subproblems make up a solution of the (RMP).

$$\max \quad (c_n^T - v^T A) x_n \tag{7.2.13}$$

In column generation information is exchanged between the subproblems and the (RMP), illustrated in Figure 7.3, to find the optimal solution of the

problem. The dual value v of the (RMP) is sent to the subproblems and becomes a part of the objective function. This ensures that new columns are generated that contribute to increasing the objective. Moreover, the values of the decision variables in the subproblems are sent and used as parameters in the (RMP). The exchange of dual values and columns between the (RMP) and subproblems continue until all newly generated columns in the subproblems already exist in the (RMP). Then, the optimal solution of the (RMP) is the same as the optimal solution of the (MP).

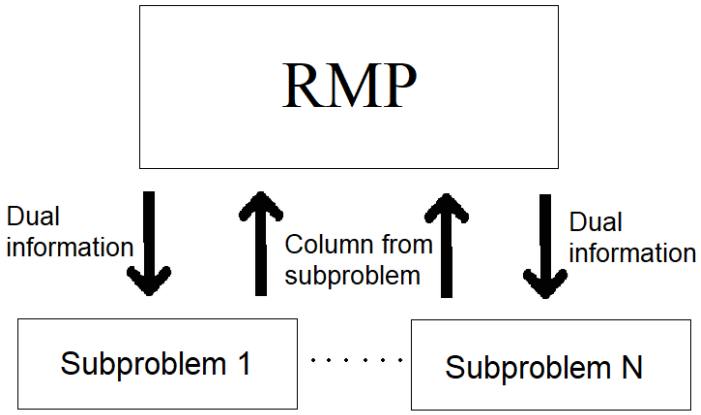

Figure 7.3: Information exchanged between the (RMP) and the subproblems.

If the original problem (P) is a mixed-integer or integer problem additional considerations are necessary. Binary and integer restrictions do not generate dual values. Since dual values are an essential part of the column generation algorithm, we remove binary and integer restrictions in the (RMP). Hence, the column generation algorithm solves the linear relaxation of the problem. Therefore, the optimal solution obtained from the column generation algorithm is not guaranteed to comply with the binary or integer restrictions. In such cases an additional algorithm, like branch and price, is required to ensure that the solution complies with the binary and integer restrictions.

7.3 Dantzig-Wolfe reformulation

In this section we use Dantzig-Wolfe decomposition on the mathematical problem presented in Chapter 6. We begin by presenting the subproblems of the *ExpectedRevenueProblem*, which generate the production plan for a location, by using dual information retrieved from the (RMP). Thereafter, we introduce the (RMP) of the *ExpectedRevenueProblem*, which combines the production plans from the subproblems into a company-wide production plan, while complying with the connecting constraints and maximizing the value of harvests. Lastly, we discuss how reformulating the $CVaRProblem$ demands additional considerations.

7.3.1 Subproblems

Each subproblem corresponds to the two-stage production planning problem at a single location l. Moreover, for every iteration of the column generation algorithm each subproblem generates a column that corresponds to the production plan of a location.

By relaxing the constraints that connect locations together, we can isolate the subproblems for each location. We let u^H_{ts}, u^M_{ts}, u^F_s and u^E_{ts} be dual values connected to the company-wide regulatory constraints (6.3.7), (6.3.14), (6.3.17) and (6.3.18) respectively. The objective of the subproblems is to maximize the reduced cost, shown in equation (7.3.1).

$$\begin{aligned}\max \sum_{s\in\mathcal{S}} \pi^s \Big(& \sum_{t'\in\mathcal{T}^{R_0}} \sum_{f\in\mathcal{F}_{t'}} \sum_{g\in\mathcal{G}_{t'}} \sum_{t\in\mathcal{T}^{H^s}_{fglt'}} (P_{High}(1-D^s_{t'fglt}) + P_{Low}(D^s_{t'fglt}))\omega^s_{t'fglt}) \\ & - \sum_{s\in\mathcal{S}}\sum_{t\in\mathcal{T}} \Big(\sum_{t'\in\mathcal{T}^D_{fglt}} \sum_{f\in\mathcal{F}} \sum_{g\in\mathcal{G}} \omega^s_{t'fglt}\Big) u^H_{ts} - \sum_{s\in\mathcal{S}}\sum_{t\in\mathcal{T}} (q^s_{lt}) u^M_{ts} - \\ & + \sum_{s\in\mathcal{S}} (q^s_{l|T|}) u^F_s - \sum_{s\in\mathcal{S}} \sum_{t\in\mathcal{T}^{Es}} \Big(\sum_{(f,g,t')\in\mathcal{B}^{Gs}_{lt}} A^s_{t'fglt} y^s_{fglt'}\Big) u^E_{ts} \end{aligned} \tag{7.3.1}$$

The constraints of the subproblems (7.3.2)–(7.3.23) are nearly identical to the ones used in the original problem formulation in Chapter 6, with the exception being that the scope decreases from the set of locations to a single location.

Deployment constraints

$$L_l^{TYPE}\delta_{fglt} \leq_f y_{fglt} \leq U_l^{TYPE}\delta_{fglt} \quad t \in \mathcal{T}, f \in \mathcal{F}_t, g \in \mathcal{G}_t \tag{7.3.2}$$

$$L_l^L\delta_{lt} \leq \sum_{f\in\mathcal{F}_t}\sum_{g\in\mathcal{G}_t} N_f y_{fglt} \leq U_l^L\delta_{lt} \quad t \in \mathcal{T} \tag{7.3.3}$$

$$\sum_{f\in\mathcal{F}_t}\sum_{g\in\mathcal{G}_t} \delta_{fglt} \leq |F_t||G_t|\delta_{lt} \quad t \in \mathcal{T}^{\mathcal{R}} \tag{7.3.4}$$

$$\sum_{f\in\mathcal{F}_t}\sum_{g\in\mathcal{G}_t} \delta_{fglt} \leq \beta_{l\tau}^s \quad s \in \mathcal{S}, l \in \mathcal{L}, t \in \mathcal{T}^R, f \in \mathcal{F}_t, g \in \mathcal{G}_t, \tau \in \mathcal{T}_{fglt}^G \tag{7.3.5}$$

Harvesting and fallowing constraints

$$\Lambda\delta_{lt} + \sum_{\tau\in\mathcal{T}_t^{\Lambda-}} \beta_{l\tau}^s \leq \Lambda \quad t \in \mathcal{T}^{\mathcal{R}} \quad \setminus \quad (1,..,\Lambda) \tag{7.3.6}$$

$$L_l^H\omega_{lt}^s \leq \sum_{f\in\mathcal{F}_t'}\sum_{g\in\mathcal{G}_t'} \omega_{t'fglt}^s \leq U_l^H\omega_{lt}^s \quad s \in \mathcal{S}, t \in \mathcal{T} \tag{7.3.7}$$

Activity constraints

$$\sum_{\tau\in\mathcal{T}_t^{\Gamma-}} \beta_{l\tau}^s \geq 1 \quad s \in \mathcal{S}, t \in \mathcal{T} \quad \setminus \quad (1,..,\Gamma-1) \tag{7.3.8}$$

Biomass development and MAB constraints

$$q_{t'fglt}^s = A_{t'fglt}$$

$$s \in S, t' \in \mathcal{T}^{\mathcal{R}}{}_0, g \in \mathcal{G}_{t'}, \quad t \in (\mathcal{T}_{fglt'}^G \cup \min\mathcal{T}_{fglt'}^H) \tag{7.3.9}$$

$$q_{t'fglt}^s = R_{t'fglt}(q_{t'fgi(t-1)}^s - \omega_{t'fgi(t-1)}^s)$$

$$s \in \mathcal{S}, t' \in \mathcal{T}_0^R, g \in \mathcal{G}_{t'}, t \in (\mathcal{T}_{fglt'}^{H+s} \cup \min\mathcal{T}_{fglt'}^{Hs}) \tag{7.3.10}$$

$$q^s_{t'fgi[max\mathcal{T}^{H+}_{fglt'}]} - \omega^s_{t'fgi[max\mathcal{T}^{H+}_{fglt'}]} = 0$$

$$s \in \mathcal{S}, t' \in \mathcal{T}^{\mathcal{R}}{}_0, f \in \mathcal{F}_{t'}, g \in \mathcal{G}_{t'} \tag{7.3.11}$$

$$q^s_{lt} \leq MAB_l \beta^s_{lt} \quad s \in \mathcal{S}, t \in \mathcal{T} \tag{7.3.12}$$

$$q^s_{lt} = \sum_{t' \in \mathcal{T}^{\Delta^-_R}} \sum_{f \in \mathcal{F}_t} \sum_{g \in \mathcal{G}_{t'}} q^s_{t'fglt} \quad s \in \mathcal{S}, t \in \mathcal{T} \tag{7.3.13}$$

Initial conditions constraints

$$\beta^s_{lt} \leq 0 \quad s \in \mathcal{S}, t \in \mathcal{T}^{\Lambda^{INIT}_l} \tag{7.3.14}$$

$$\sum_{t \in \mathcal{T}^{\Gamma INIT}_l} \beta^s_{l\tau} \geq 1 \quad s \in \mathcal{S} \tag{7.3.15}$$

End of horizon constraints

$$\sum_{(f,g,t') \in \mathcal{B}^G_{lt}} A_{t'fglt} y^s_{fglt'} \leq MAB_l \quad s \in \mathcal{S}, t \in \mathcal{T}^E \tag{7.3.16}$$

Binary and non negativity constraints

$$\delta_{fglt} \in \{0, 1\} \tag{7.3.17}$$

$$\delta_{lt} \in \{0, 1\} \tag{7.3.18}$$

$$\beta_{lt} \in \{0, 1\} \tag{7.3.19}$$

$$\omega^s_{lt} \in \{0, 1\} \tag{7.3.20}$$

$$\omega^s_{t'fglt} \geq 0 \tag{7.3.21}$$

$$q^s_{lt} \geq 0 \tag{7.3.22}$$

$$q^s_{t'fglt} \geq 0 \tag{7.3.23}$$

7.3.2 Restricted master problem

The restricted master problem corresponds to the company-wide production planning problem. It generates a company-wide production plan.

Each location l has a set of available columns K_l. Let $x^{(kl)}$ be the column found in the subproblem representing location l during iteration k of the column generation algorithm. In cases where a subproblem generates a new column, we extend the (RMP) with $x^{(kl)}$. The column consists of the following parameters, $[\delta^k_{fglt}, \delta^k_{lt}, y^k_{fglt}, \beta^{sk}_{lt}, \omega^{sk}_{lt}, \omega^{sk}_{t'fglt}, q^{sk}_{lt}, q^{sk}_{t'fglt}]$ and its objective value. We combine columns from all subproblems in the (RMP). The decision variable in the (RMP) is the weighing variable, λ_{lk}, connected to location l and iteration k of the column generation algorithm.

The objective function of the (RMP) for the *ExpectedRevenueProblem* is presented in equation (7.3.24).

$$\max \sum_{s\in\mathcal{S}} \pi^s \Big(\sum_{t'\in\mathcal{T}^{R_0}} \sum_{f\in\mathcal{F}_{t'}} \sum_{g\in\mathcal{G}_{t'}} \sum_{l\in\mathcal{L}} \sum_{t\in\mathcal{T}^{H^s}_{fglt'}} \sum_{k\in K_l} \lambda_{lk} \big(P_{High}(1 - D^s_{t'fglt}) \quad + \\ P_{Low}(D^s_{t'fglt}) \big) \omega^{sk}_{t'fglt} \Big) \tag{7.3.24}$$

The constraints from the original formulation that we cannot isolate per location are included in the (RMP). These are the company-wide harvesting limit, MAB during the planning horizon, minimum final biomass and MAB after the planning horizon, respectively expressed in constraints (6.3.7), (6.3.14), (6.3.17) and (6.3.19). They are reformulated as constraints (7.3.25)–(7.3.28) and are included in the (RMP). Furthermore, the connecting constraints are respectively linked to the dual values u^H_{ts}, u^M_{ts}, u^F_s and u^E_{ts}.

$$\sum_{f\in\mathcal{F}} \sum_{g\in\mathcal{G}} \sum_{l\in\mathcal{L}} \sum_{t\in\mathcal{T}^D_{fglt}} \sum_{k\in K_l} \omega^{sk}_{t'fglt} \lambda_{lk} \le U^{COM}_t \quad s\in\mathcal{S}, t\in\mathcal{T} \quad | \quad u^H_{ts} \tag{7.3.25}$$

$$\sum_{l\in\mathcal{L}} \sum_{k\in K_l} q^{sk}_{lt} \lambda_{lk} \le MAB^{COMP} \quad s\in\mathcal{S}, t\in\mathcal{T} \quad | \quad u^M_{ts} \tag{7.3.26}$$

$$\sum_{l\in\mathcal{L}} \sum_{k\in K_l} \lambda_{lk} q^s_{l|T|} \ge \sum_{f\in\mathcal{F}} \sum_{g\in\mathcal{G}} \sum_{l\in\mathcal{L}} y_{fgl0} \quad s\in\mathcal{S} \quad | \quad u^F_s \tag{7.3.27}$$

$$\sum_{l\in\mathcal{L}}\sum_{(f,g,t')\in\mathcal{B}_{lt}^{Gs}}\sum_{k\in K_l} A_{t'fglt}y_{fglt'}^{k}\lambda_{lk} \leq MAB^{COMP} \quad s\in\mathcal{S}, t\in\mathcal{T}^{E^s} \quad | \quad u_{ts}^{E} \tag{7.3.28}$$

Constraint (7.3.29) is in place to ensure that there is a convex combination of all of the weighting variables. In constraint (7.3.30) we require that the decision variables λ_{lk} are non-negative.

$$\sum_{l\in K_l}\lambda_{lk} = 1 \quad l\in\mathcal{L} \tag{7.3.29}$$

$$\lambda_{lk} \geq 0, \quad l\in\mathcal{L}, k\in K_l \tag{7.3.30}$$

Since the production plan for a location is represented as a column, the convex combination of the decision variables belonging to different columns equal the original decision variables, expressed in constraints (7.3.31)–(7.3.38).

$$\sum_{k\in K_{kl}}\lambda_{lk}\delta_{fglt}^{k} = \delta_{fglt} \quad l\in\mathcal{L}, t\in\mathcal{T}^{R}, g\in\mathcal{G}_t, f\in\mathcal{F}_t \tag{7.3.31}$$

$$\sum_{k\in K_{kl}}\lambda_{lk}\delta_{lt}^{k} = \delta_{lt} \quad l\in\mathcal{L}, t\in\mathcal{T}^{R} \tag{7.3.32}$$

$$\sum_{k\in K_{kl}}\lambda_{lk}\omega^{sk}{}_{lt} = \omega_{lt}^{s} \quad l\in\mathcal{L}, t\in\mathcal{T}^{R} \tag{7.3.33}$$

$$\sum_{k\in K_{kl}}\lambda_{lk}\beta^{sk}{}_{lt} = \beta_{lt}^{s} \quad l\in\mathcal{L}, t\in\mathcal{T}^{R} \tag{7.3.34}$$

$$\sum_{k\in K_{kl}}\lambda_{lk}y_{fglt}^{k} = y_{fglt} \quad l\in\mathcal{L}, s\in\mathcal{S}, l\in\mathcal{L}, t\in\mathcal{T}^{\mathcal{R}} \tag{7.3.35}$$

$$\sum_{k\in K_{kl}}\lambda_{lk}\omega_{t'fglt}^{sk} = \omega_{t'fglt}^{s} \quad l\in\mathcal{L}, s\in\mathcal{S}, l\in\mathcal{L}, t\in\mathcal{T}^{\mathcal{R}} \tag{7.3.36}$$

$$\sum_{k\in K_{kl}}\lambda_{lk}q_{t'fglt}^{sk} = q_{t'fglt}^{s} \quad s\in\mathcal{S}, t\in\mathcal{T}^{\mathcal{R}}{}_0, f\in\mathcal{F}_{f'}, g\in\mathcal{G}_{t'}, l\in\mathcal{L},$$

$$t\in\mathcal{T}_{fglt'}^{Gs}\cup\mathcal{T}_{fglt'}^{H+^s} \tag{7.3.37}$$

$$\sum_{k \in K_{kl}} \lambda_{lk} q_{lt}^{sk} = q_{lt}^{s} \quad s \in \mathcal{S}, t \in \mathcal{T}, l \in \mathcal{L} \tag{7.3.38}$$

7.3.3 Decomposition with CVaR objective

In this section we present the Dantzig-Wolfe reformulation of the $CVaRProblem$. We introduce and discuss the (RMP) and subproblems.

Restricted master problem

We use the standard CVaR formulation according to Rockafellar and Uryasev (2000) and Kaut and Wallace (2007) as a starting point when formulating the (RMP) of the $CVaRProblem$. The reason for this is that the formulation is the same as the (RMP) for the $ExpectedRevenueProblem$, presented in Section 7.3.2, with the inclusion of two additional constraints.

The (RMP) of the $ExpectedRevenueProblem$ with the additional constraints is shown in equations (7.3.39)–(7.3.41). Constraints (7.3.25)–(7.3.30) are also a part of the (RMP). The CVaR constraint (6.2.2) is included in the (RMP) as constraint (7.3.41) since it links locations together. The dual value u_s^C is linked with this constraint. Constraint (7.3.40) ensures that the CVaR is above the minimal allowable CVaR, θ. By including this constraint, we can use the expected value, instead of the CVaR, as the objective function of the (RMP).

$$\max \sum_{s \in S} \pi_s \Big(\sum_{t' \in \mathcal{T}^{\mathcal{R}}{}_0} \sum_{f \in \mathcal{F}_{t'}} \sum_{g \in \mathcal{G}_{t'}} \sum_{l \in \mathcal{L}} \sum_{t \in \mathcal{T}^{Hs}_{fglt'}} \sum_{k \in K_l} \big(P_{High}(1 - D^s_{t'fglt}) + P_{Low}(D^s_{t'fglt}) \big) \omega^{sk}_{t'fglt} \lambda_{lk} \Big) \tag{7.3.39}$$

$$s.t. \quad z - \frac{1}{1-\alpha} \sum_{s \in \mathcal{S}} \pi_s x_s \geq \theta \tag{7.3.40}$$

$$x_s \geq z - \sum_{t' \in \mathcal{T}^{\mathcal{R}}{}_0} \sum_{f \in \mathcal{F}_{t'}} \sum_{g \in \mathcal{G}_{t'}} \sum_{l \in \mathcal{L}} \sum_{t \in \mathcal{T}^{Hs}_{fglt'}} \sum_{k \in K_l} \big(P_{High}(1 - D^s_{t'fglt}) + P_{Low}(D^s_{t'fglt}) \big) \omega^{s}_{t'fglt} \lambda_{lk}$$

$$| u_s^C \quad s \in \mathcal{S} \tag{7.3.41}$$

The drawback of including constraint (7.3.40) is that we must assign a value to θ. On one hand, setting it too high, will make the problem infeasible. On the other hand, setting it too low, will make the problem not incorporate the element of risk sufficiently. To deal with the issues of assigning a value to θ, we change the objective function of the (RMP) to the left-hand side of constraint (7.3.40). Hence, we maximize the CVaR in the (RMP). This reformulates the $ExpectedRevenueProblem$ to the $CVaRProblem$. As a result, we can remove constraint (7.3.40) from the (RMP). The final (RMP) of the $CVaRProblem$ is then shown in equations (7.3.42)–(7.3.43) and (7.3.25)–(7.3.30).

$$\max \quad z - \frac{1}{1-\alpha} \sum_{s \in \mathcal{S}} \pi_s x_s \tag{7.3.42}$$

$$x_s \geq z - \sum_{t' \in \mathcal{T}^{\mathcal{R}}{}_0} \sum_{f \in \mathcal{F}_{t'}} \sum_{g \in \mathcal{G}_{t'}} \sum_{l \in \mathcal{L}} \sum_{t \in \mathcal{T}^{Hs}_{fglt'}} \sum_{k \in K_l} (P_{High}(1 - D^s_{t'fglt}) + P_{Low}(D^s_{t'fglt}))\omega^{sk}_{t'fglt}\lambda_{lk}$$

$$|u^C_s \quad s \in \mathcal{S} \tag{7.3.43}$$

Subproblems

For the subproblems of the $CVaRProblem$ we use the subproblems from the $ExpectedRevenueProblem$, presented in Section 7.3.1, as the starting point.

The objective function of the subproblem is presented in equation (7.3.44). Furthermore, the objective function of the subproblems of the $CVaRProblem$ differs only from the subproblems of the $ExpectedRevenueProblem$, with the inclusion of the additional dual variable u^C_s, linked with the the extra connecting constraint. The constraints of the subproblems (7.3.2)–(7.3.23) are the same as in the subproblems of the $ExpectedRevenueProblem$.

$$\max \sum_{s \in S} \pi^s \Big(\sum_{t' \in T^{R_0}} \sum_{f \in F_{t'}} \sum_{g \in G_{t'}} \sum_{t \in T^{Hs}_{fglt'}} (P_{High}(1 - D^s_{t'fglt}) + P_{Low}(D^s_{t'fglt}))\omega^s_{t'fglt} \Big)$$

$$- \sum_{s \in \mathcal{S}} \sum_{t \in \mathcal{T}} \Big(\sum_{t' \in \mathcal{T}^D_{fglt}} \sum_{f \in \mathcal{F}} \sum_{g \in \mathcal{G}} \omega^s_{t'fglt} \Big) u^H_{ts} - \sum_{s \in S} \sum_{t \in T} (q^s_{lt}) u^M_{ts} -$$

$$+ \sum_{s \in \mathcal{S}} (q^s_{l|T|}) u^F_s - \sum_{s \in S} \sum_{t \in T^{Es}} \Big(\sum_{(f,g,t') \in B^{Gs}_{lt}} A^s_{t'fglt} y^s_{fglt'} \Big) u^E_{ts}$$

$$+\sum_{s\in\mathcal{S}}\Big(\sum_{t'\in\mathcal{T}^{\mathcal{R}}_0}\sum_{f\in\mathcal{F}_{t'}}\sum_{g\in\mathcal{G}_{t'}}\sum_{t\in\mathcal{T}^{H^s}_{fglt'}}\sum_{j\in\mathcal{J}} P_j D^s_{t'fgitj}\omega^s_{t'fglt}\Big)u^C_s - v^*_l \tag{7.3.44}$$

7.4 Branch and price algorithm

In this section we describe the branch and price algorithm. Next, we explain algorithmic configurations, like the branching and search strategy. Lastly, we present algorithmic extensions to reduce the running time of the algorithm.

7.4.1 Overview of the algorithm

The branch and price algorithm can be used as the solution method to solve a Dantzig-Wolfe decomposed mixed-integer problem as it ensures that the integrality conditions are satisfied. A detailed description of the branch and price algorithm can be found in Barnhart et al. (1970).

The branch and price algorithm builds upon the branch and bound algorithm. The column generation algorithm, expressed in Algorithm 1, is applied to every node in the branch and bound tree. The root node is the first node that is solved using the column generation algorithm. Moreover, after having performed the column generation algorithm on a node, no more profitable columns can be found and the solution to the (MP) is found. However, since the column generation algorithm finds the linear relaxation of the problem, there is no guarantee that the solution is integer feasible. Hence, branching occurs on the original decision variables and creates two new nodes. This will continue, until a feasible solution from the column generation algorithm is generated from a node that fulfills the stopping criterion of the algorithm. Throughout the algorithm, the incumbent IP keeps track of the objective value of the best feasible solution. A visual overview of the branch and price algorithm is shown in Figure 7.4.

Algorithm 1 Pseudocode for the implementation of column generation algorithm. Retrieved from Føsund and Strandkleiv (2021).

Set up initial columns;
Optimize the (RMP) and extract dual values from the (RMP);
Optimize subproblems based on dual values from RMP;
while Subproblems generate new columns **do**
    Add new solutions as columns to (RMP) and re-optimize the (RMP);
    Extract new dual values from (RMP)
    and re-optimize subproblems with new values;
end while
Results λ_{kl} variables are the optimal weighting of columns.

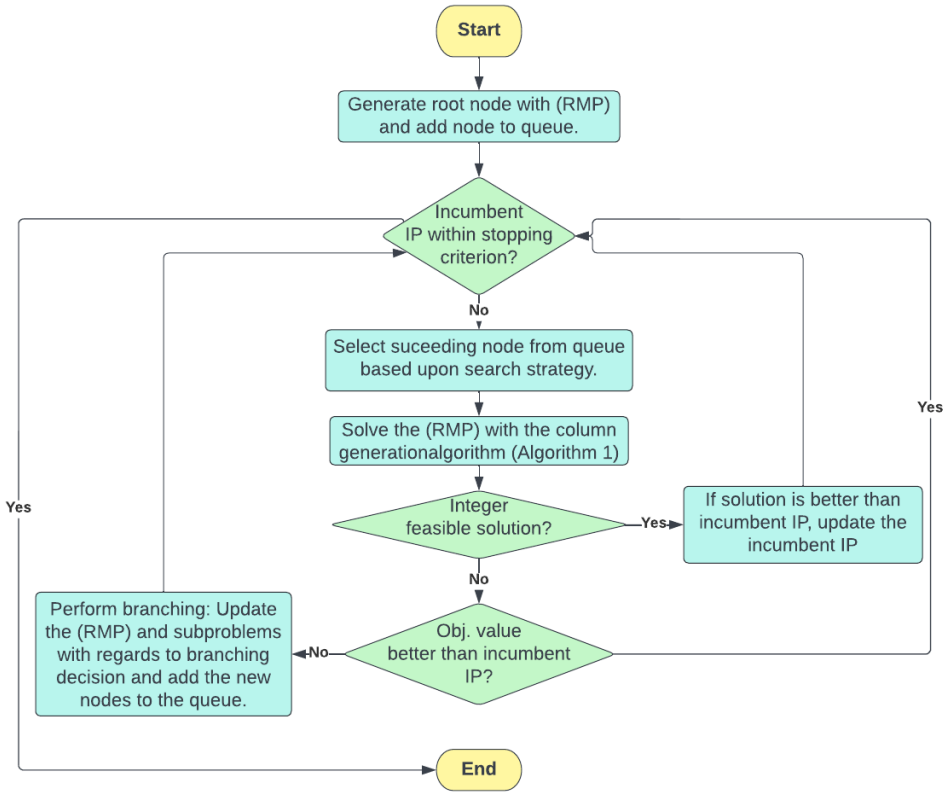

Figure 7.4: Overview of the branch and price algorithm.

7.4.2 Algorithmic configurations

Morrison et al. (2016) state that the performance of the branch and price algorithm depends greatly on which strategies and configurations are in place. In this section we present the algorithmic configurations used for the problem. We explain how we generate the initial columns in the root node and the stopping criterion for both the column generation and branch and price algorithm. Lastly, we describe the search and branching strategy.

Initial columns generation

We generate two sets of initial columns for the root node of the branch and price tree. In the first column the value of all variables is set to zero, while the second column contains a feasible set of solutions retrieved from the initial column matheuristic presented in Section 7.4.3. By combining a column containing a feasible solution and a column where all variables are set to zero, the objective value of the (RMP) increases quickly in the beginning of the column generation algorithm.

Stopping criterion of branch and price algorithm

The algorithm stops running when the total running time of the algorithm has exceeded two days or when the optimality gap, defined in equation (7.4.1), is below 5 %. Such an optimality gap is acceptable due to the complexity and size of the problem. The upper bound is the highest upper bound of a leaf node in the branch and price tree. Furthermore, the lower bound is the best integer feasible solution.

$$\text{Optimality Gap} = \frac{\text{Upper Bound} - \text{Lower Bound}}{\text{Lower Bound}} \tag{7.4.1}$$

Stopping criterion of column generation algorithm

In Section 7.2 we mention that the column generation algorithm is complete when all newly generated columns of an iteration already exist. When using

this stopping criterion the runtime of the column generation algorithm can be very high. The reason for this is that both binary and continuous variables are a part of the subproblems. This can lead to the subproblems generating several columns with the same values assigned to the binary variables and almost identical values assigned to the continuous variables. As a result, the objective value of the (RMP) can increase minimally with the inclusion of new columns.

It is of great interest to reduce the running time of the column generation algorithm, since it will increase the number of nodes the branch and price algorithm can solve. We replace the stopping criterion to reduce the running time of the column generation algorithm. We stop the algorithm when all newly generated columns are less than 0.1 % different from existing columns. This will prevent columns from having the same value assigned to binary variables and very similar values assigned to the continuous variables.

When using the new stopping criterion there is no guarantee that the optimal solution of the (RMP) corresponds to the optimal solution of the (MP). This is not a problem as long as the solution found in the (RMP) is better than optimal solution of the original mixed-integer problem (P). Therefore, we only consider the new stopping criterion valid as long as the best-feasible solution is worse than the solution of the (RMP)

Even though the optimal objective value of the (RMP) can be lower than the optimal objective value of the (MP), we consider using the stopping criterion as beneficial as it drastically reduces the running time of the column generation algorithm.

Search strategy

Morrison et al. (2016) highlights the benefits of picking the right search strategy in the branch and price algorithm as it may reduce computation time and memory requirements. Savelsbergh (1997) argues that a combination of a best first search and primal heuristic is effective. The reason for this being that the branch and price tree focuses on finding the best dual bound. It generates many different columns for the primal heuristic, by exploring the branch and price tree in a scattered manner. Therefore, we use the best first search strategy in the implementation. The node that has the highest objective

value is chosen from the queue as the next node. To find an estimate of the objective value for unexplored nodes, we use the parent nodes objective value.

Branching strategy

Branching leads to the creation of two new nodes, with the binary variable being set to zero or one. Moreover, branching is performed when the final solution of the (RMP) does not meet the binary requirements. We do not branch on the weighting variables since they are continuous. Instead, we branch on the binary variables of the original problem.

We give the different sets of binary variables branching priorities. This determines which set of binary variables we branch on first. Within a set of binary variables, we always branch upon the variable with the fractional value closest to 0.5.

The binary variables in the subproblem are deployment at a location δ_{lt}, deployment of a cohort δ_{fglt}, harvesting ω^s_{lt} and biomass present β^s_{lt}. We firstly branch upon δ_{lt} and δ_{fglt}. This is due to both sets of variables being first stage variables. We expect that first stage variables add a much stricter guidance than second stage variables and will therefore lead to the optimal solution faster. The binary variable δ_{lt} is given the highest branching priority followed by δ_{fglt}. This is due to the value of δ_{lt} being more general than δ_{fglt}. When δ_{lt} is set to 0, it forces all δ_{fglt} at location l during time period t to 0. Moreover, ω^s_{lt} is given a higher branching priority than β^s_{lt}, since harvest implies that the location has biomass present in a several preceding time periods.

7.4.3 Extensions to the branch and price algorithm

We have implemented algorithmic extensions to the branch and price algorithm, to reduce the amount of time needed to find a solution within the optimality gap. Firstly, we parallelize the process of solving the subproblems to optimality. Next, we generate additional columns in each subproblem every iteration. Lastly, we include two matheuristics to improve the algorithm.

Parallelization of subproblems

Since there are $|\mathcal{L}|$ subproblems, it is possible to exploit the structure of the problem, by solving the subproblems in parallel. For every iteration, we supply each subproblem with its relevant dual information from the (RMP). Then, we solve the subproblems in parallel. After all subproblems have been solved, the value given to the decision variables is sent as parameters to the (RMP).

Generating multiple columns

For every iteration of the column generation algorithm, presented in Algorithm 1, up to five columns from each subproblem are sent to the (RMP). The five best feasible solutions are collected, when an individual subproblem is solved. Furthermore, if the columns do not already exist in the (RMP), they are added as columns. We include this extension, since there is a chance that the optimal column of the subproblem is not a part of optimal solution of the (RMP). However, non-optimal solutions can be. Therefore, by adding multiple columns during the same iteration, the chance of a column being a part of the optimal solution of the (RMP) increases.

Initial column matheuristic

Before running the column generation algorithm, we generate a feasible solution for the problem, which is used as one of the sets of initial columns. This gives a head-start in the column generation algorithm, as the first iteration of the (RMP) results in a higher objective value. As a result, we are able ignore the addition of columns that would be added during the first iterations of the column generation algorithm. The branch and price algorithm with this matheuristic is illustrated in Figure 7.5.

To find the initial feasible solution, we solve the deterministic problem with a time limit of 2000 seconds. Then, we take the first-stage decisions of the deterministic problem and fix them, before evaluating the first-stage solution on the stochastic problem, with a time limit of 2000 seconds. This results in a feasible solution. Furthermore, when the problem is the $ExpectedRevenueProblem$ we set the gender maturation percentages to the mean gender maturation percentages over all scenarios. However, when the

problem is the $CVaRProblem$, we select the scenario with the highest gender maturation percentages, since this solution will to a larger extent be tuned for scenarios with lower gender maturation percentages.

If no solution has been found within the time limit of a problem, we choose the first feasible solution found after.

Primal bound matheuristic

To speed up the process of finding primal bounds, we implement a matheuristic. Figure 7.5 depicts the branch and price algorithm with this matheuristic. After the column generation algorithm stops, we solve the (RMP) as a mixed-integer problem to find a feasible solution to the original problem. Moreover, here a feasible solution refers to a weighted combination of columns from the (RMP). The binary requirements of the original problem are included here. We set the time limit to 3600 seconds.

To reduce the time needed to find a good primal bound within the time limit, we force all deployment variables, δ_{lt}, that have a weighted sum, $\sum_{k \in K_{kl}} \lambda_{lk} \delta^k_{lt}$, above 0.85 to 1. If we obtain a solution from this matheuristic and it is better than the incumbent IP, it is updated. However, if this is not the case the branch and price algorithm continues.

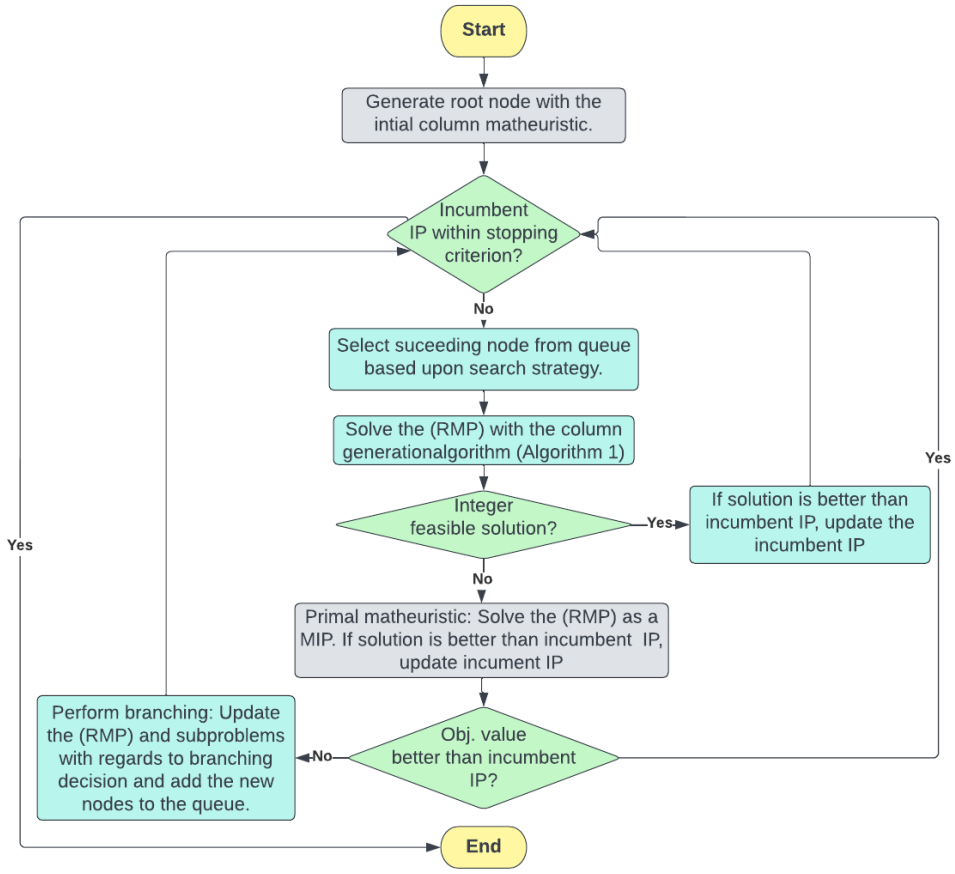

Figure 7.5: Overview of the branch and price algorithm with matheuristics.

Chapter 8

Case Study

In this chapter we present the input data for the case study of the production planning problem representing Eidsfjord Sjøfarm. We introduce the production system of Eidsfjord Sjøfarm and the planning horizon. Then, we present the deployment weights, parameters that depend upon smolt type and seawater temperatures. Next, we present gender maturation parameters and describe how we generate scenarios. Lastly, we present all other parameters.

8.1 Production system and planning horizon

In this section we present the production system of Eidsfjord Sjøfarm and the planning horizon used in the case study.

8.1.1 Production system

Eidsfjord Sjøfarm is a Norwegian salmon farming company of medium size. Their production facilities are located in northern Norway. The company produces approximately 15 000 tonnes of head-gutted (HG) salmon annually. HG salmon have their head and viscera removed. The production facilities are located in Vesterålen, Senja and Inner-Troms, with respectively 11, three and three facilities in each production zone. Vesterålen, Senja and Inner-

Troms are located in three different production zones. Moreover, Eidsfjord Sjøfarm has gained permission to have an inter-regional MAB between all its production zones. The inter-regional MAB is 14 528 tonnes. Details regarding its production facilities can be found in Table 8.1. The geographic location of the production facilities is presented in Figure 8.1.

Location	**MAB (tonnes)**	**Initial mean weight of salmon (g)**	**Total initial biomass (kg)**	**Months at sea**
Holand	3120	0	0	0
Innerbroksløysa	3120	0	0	0
Reinsnes	3120	1464	1007000	5
Bremnes	3900	2207	1864000	10
Toftenes	3120	0	0	0
Sandan Sø	2340	0	0	0
Kuneset	3120	2641	999000	5
Trolløya	3120	0	0	0
Langholmen	3120	3273	2316000	13
Daljorda	3120	0	0	0
Flesen	3120	5261	1033000	17
Lavika	2700	689	571000	2
Kvenbukta	2700	317	225000	2
Stretarneset	2700	0	0	0
Haukøya	3600	0	0	0
Hagebergan	3600	6000	1497000	17
Russelva	3500	1591	1298000	5

Table 8.1: Overview of the locations Eidsfjord Sjøfarm operates.

Figure 8.1: The geographical locations of the facilities of Eidsfjord Sjøfarm.

8.1.2 Planning horizon

We use a planning horizon with a duration of five years and a monthly time resolution. As a result, we have a total of 60 time periods. January 2021 marks the beginning of the first time period, while the last time period is December 2025. Deployments can take place in all months except for February, March, October and November.

8.2 Deployment weights and smolt types

In this section we present deployment weights and parameters that are dependent upon the smolt type of the salmon.

8.2.1 Deployment weights

Eidsfjord Sjøfarm has the choice of deploying 100, 150 or 250 g smolt. However, they do not deploy all weights throughout the year. There are fewer smolt weights available during the months the seawater temperatures are lower. This

is due to the growth of the salmon depending upon the seawater temperature. In January and December, deployed smolt must weigh 250 g. Moreover, in April, May and June the weight of deployed smolt cannot be 100 g. During the remaining months all smolt weights are permitted.

8.2.2 Characteristics of smolt types

Aquagen AS study and sell a number of different smolt types. In this case study, three of these smolt types are included, being regular, male and female smolt. We include these three smolt types since there have been extensive studies performed on them by Aquagen AS. The smolt types differ when it comes to mortality, TGC and gender maturation rates. The TGC rate is proportional to the growth rate of salmon. The data regarding TGC rates and mortality rates is taken from Aasen (2021).

Even though the smolt types have different biomass development characteristics, all can be deployed in all release months. The development of the TGC for the different smolt types is presented in Figure 8.2. Generally, the TGC rates are slightly higher for male smolt, which corresponds to higher growth rates.

The mortality rate is presented in Figure 8.3 and is dependent upon the smolt type and the number of months a cohort has been employed in the sea. When comparing the smolt types, we observe that the rates are generally lower for female.

Figure 8.4 shows the survival percentage of the different smolt types. At the end of a rearing cycle, female salmon have the highest survival percentage.

The biomass development of a salmon cohort is affected by the growth and mortality rates. The expected weight development for the three different smolt types deployed in the month of January with an initial weight of 250 g can be seen in Figure 8.5. Moreover, the expected weight development for regular cohorts is higher than the average weight development of female and male cohorts, since regular cohorts have higher mortality rates.

The month of deployment affects the mean seawater temperature for a cohort, which in turn affects the weight development of a cohort. Cohorts deployed in January have the lowest weight development of all cohorts.

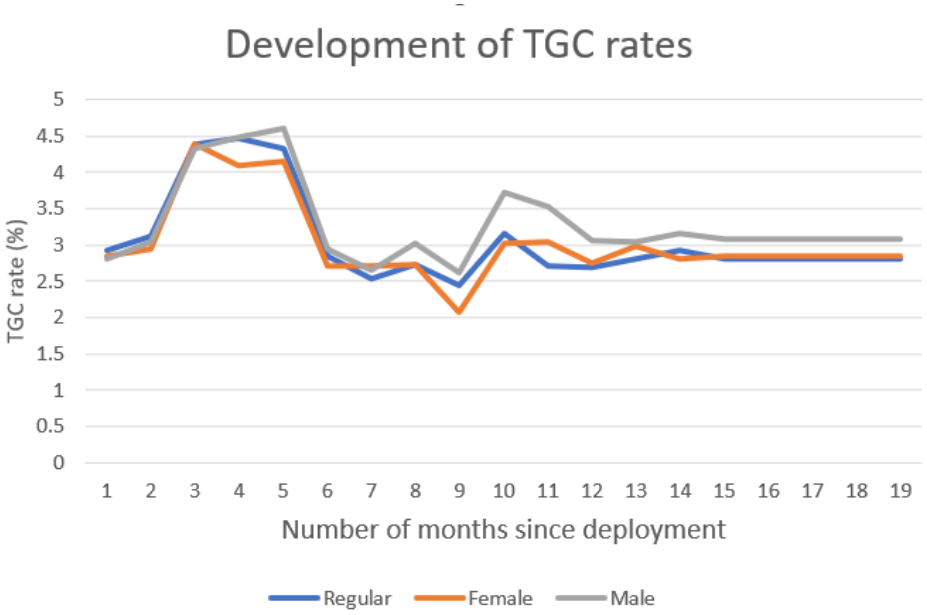

Figure 8.2: The development of the TGC for all smolt types.

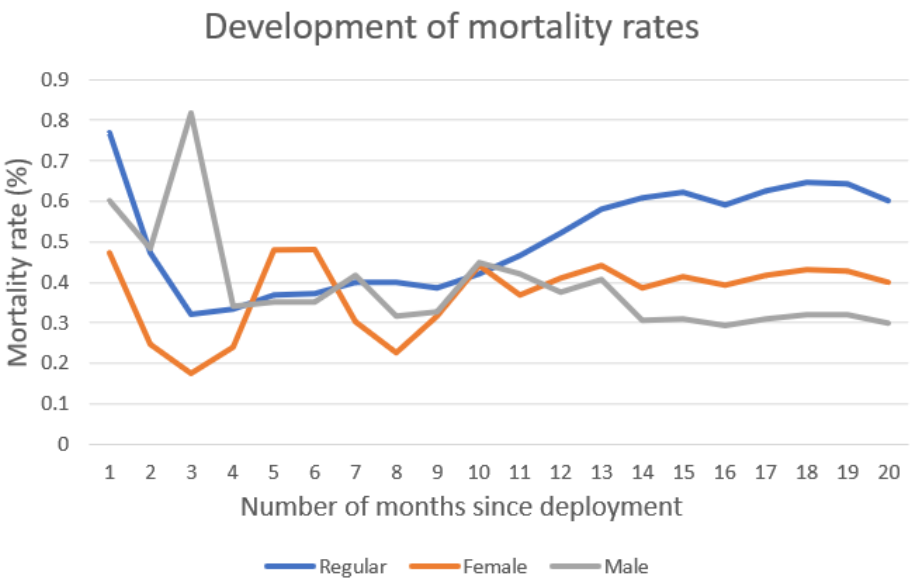

Figure 8.3: The development of the mortality rates for all smolt types.

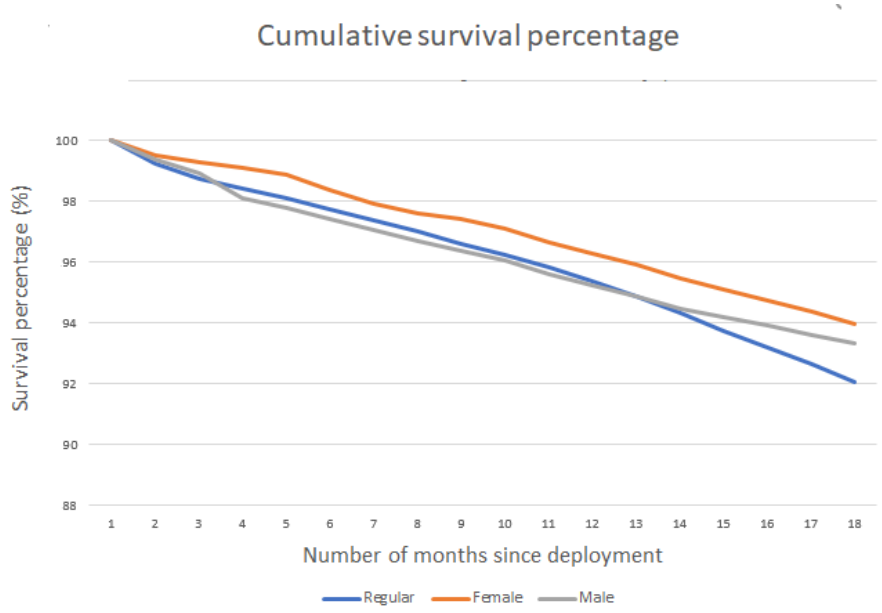

Figure 8.4: The development of the survival percentages for all smolt types.

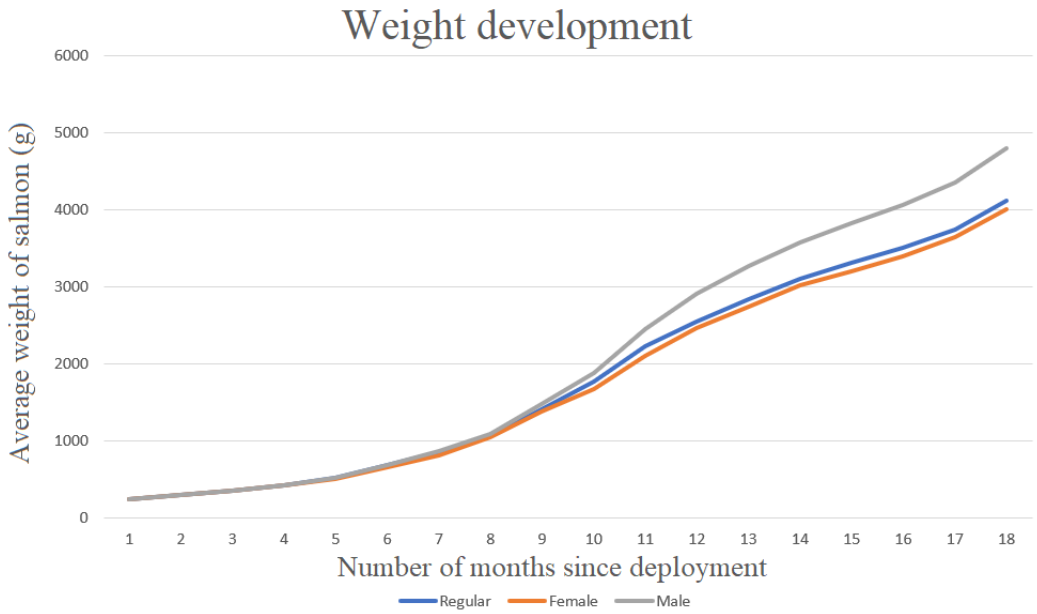

Figure 8.5: The expected biomass development for the different smolt types when the month of deployment is January.

8.3 Seawater temperatures

The most important factor of the TGC rate is the seawater temperature. We use the historical monthly seawater temperature at the different locations, retrieved from Barentswatch (2021a), to calculate the mean historic monthly temperature. We assume that seawater temperatures are repeated yearly. An overview of the temperatures at different locations is illustrated in Figure 8.6.

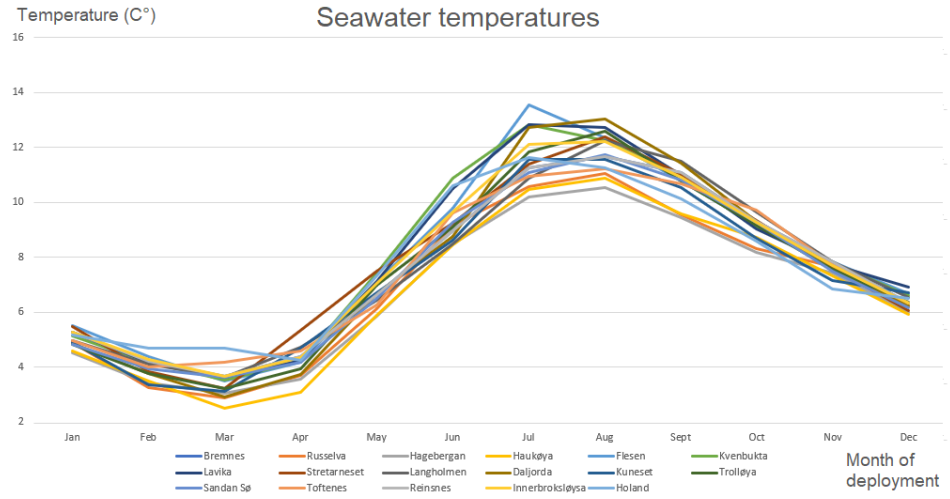

Figure 8.6: An overview of the temperatures in Celsius at all locations.

8.4 Gender maturation and scenario generation

In this section we specify the value of the several gender maturation parameters. Next, we explain and discuss how we perform scenario generation to get the gender maturation percentages, $D^s_{t'fglt}$.

8.4.1 Gender maturation

The source of uncertainty in the model is the percentage of a salmon cohort that have experienced gender maturation at harvest, $D^s_{t'fglt}$. From Section 5.2

we know that the gender maturation percentage is dependent upon the mean weight of a salmon in a cohort, smolt type and number of gender maturation months the salmon have been at sea.

We set the lower limit of when a salmon can experience gender maturation to 2.5 kilograms, since smaller salmon rarely go through gender maturation (Aquagen, 2021). Furthermore, the months where gender maturation can occur, known as the gender maturation months, are August, September, October and November (Aquagen, 2021). A cohort never experiences gender maturation months in two different years. For this to happen a salmon would have to be employed at sea one year after reaching 2.5 kilograms. However, all salmon are harvested before this occurs. Hence, the maximum number of gender maturation months a cohort can go through, J_{max}, is four.

Salmon that go through gender maturation experience a reduction in their value. Furthermore, in this thesis, gender maturation is the only factor that causes such a reduction. We set the relative value of salmon that have not experienced gender maturation, P_{High}, to 1. However, setting the relative value of the gender matured salmon, P_{Low}, is challenging since it depends upon the market. The reduction can vary between 5 and 95 % (Aquagen, 2021). To capture risk-averse attitudes of farmers we decide to set P_{Low} to 30 %.

8.4.2 Scenario generation

Aquagen AS have supplied data of the gender maturation percentage at harvest for the different smolt types. The data is presented as histograms in Figure 8.7, 8.8 and 8.9. The collection of data points for all smolt types is presented in Figure 8.10.

We denote B_g^s as the gender maturation percentage at harvest for salmon belonging to smolt type g in scenario s. Moreover, we generate a lognormal distribution of the data points of the gender maturation percentages at harvest received from Aquagen AS. By sampling from the lognormal distribution we can find B_g^s in different scenarios. Using the lognormal distribution prevents sampling of negative values. To generate the lognormal distribution we need the mean of the logarithmic values, μ, and standard deviation of logarithmic values, σ, of the data points provided by Aquagen AS. μ and σ for the different smolt types are presented in Table 8.2. The lognormal distributions are fitted

to the data provided by Aquagen AS in Figure 8.8, 8.9, 8.7 and 8.10.

	Female	Male	Regular
μ	-0.3251	2.5385	1.8149
σ	1.2753	0.6122	0.7343

Table 8.2: The μ and σ for the different smolt types.

In Figure 8.10, we observe that the gender maturation percentage at harvest, B_g^s, is much higher for male and regular cohorts than female cohorts. We use a lognormal distribution, to sample B_g^s for regular and male salmon. We do not use a lognormal distribution to sample B_g^s for female smolt since the data points are very close to zero, with the mean being 0.13 %. Instead, we set B_g^s for female salmon to the constant value of 0. This is an acceptable approach since it will have minimal effect on the outcome of the model due to the data points for female salmon being much lower than the data points for other smolt types.

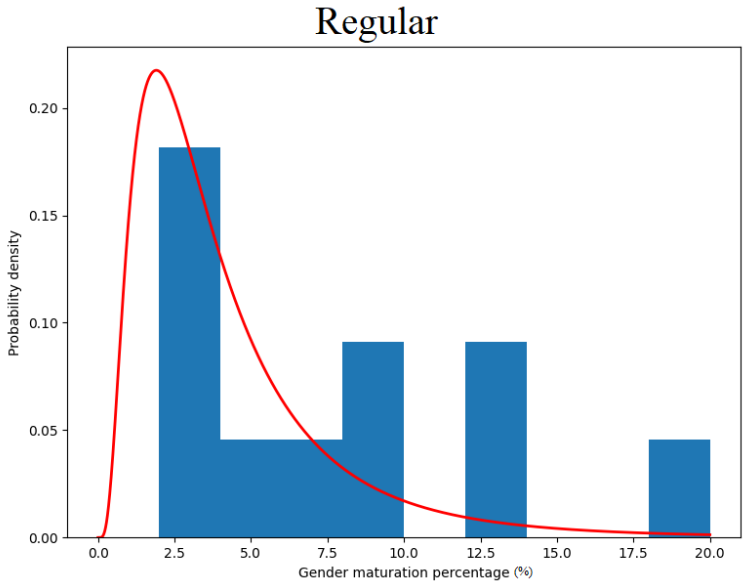

Figure 8.7: Lognormal distributions fitted to data of the gender maturation percentages at harvest of regular salmon. Provided by Aquagen AS.

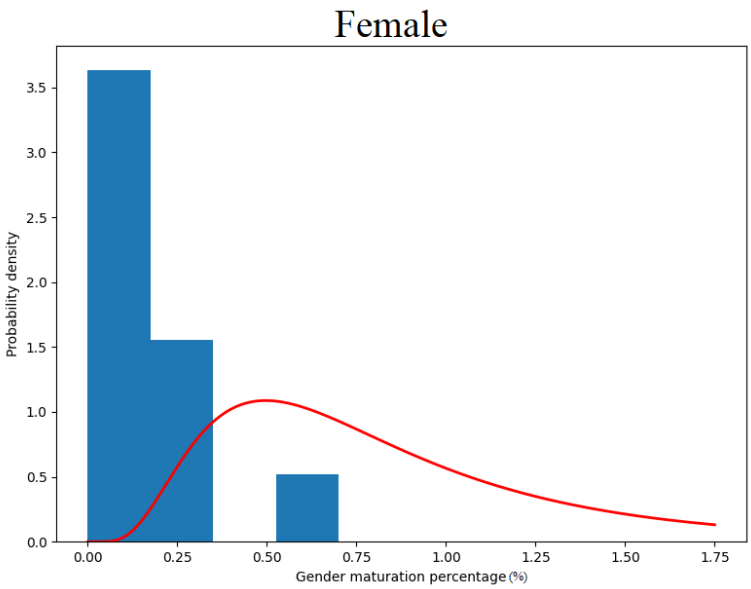

Figure 8.8: Lognormal distributions fitted to data of the gender maturation percentages at harvest of female salmon. Provided by Aquagen AS.

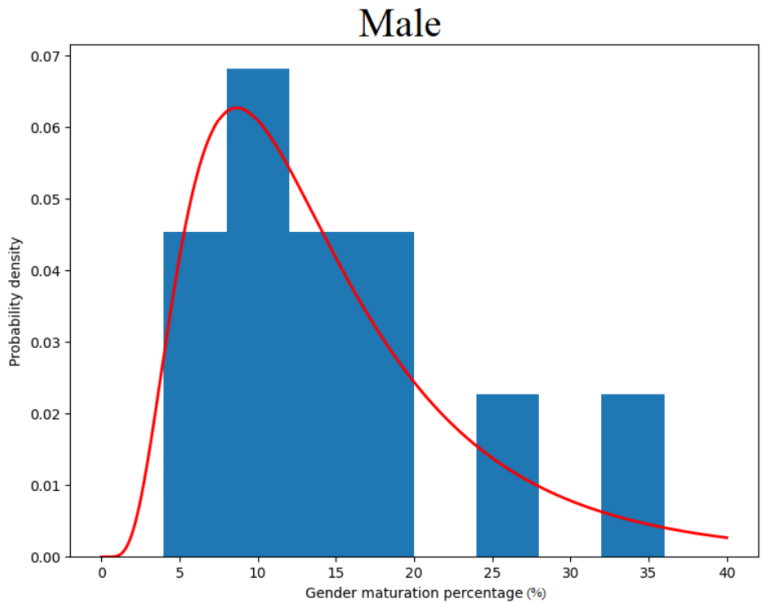

Figure 8.9: Lognormal distributions fitted to data of the gender maturation percentages at harvest of male salmon. Provided by Aquagen AS.

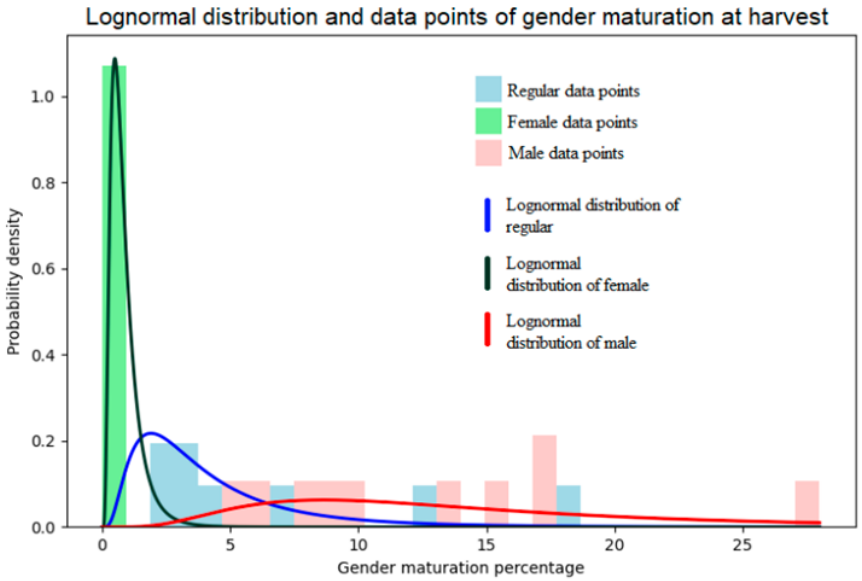

Figure 8.10: Lognormal distributions fitted to data of the gender maturation percentages at harvest for all smolt types. Provided by Aquagen AS.

To be able to incorporate gender maturation into the model, we must assign values to the gender maturation percentage, $D^s_{t'fglt}$, for the cohort respectfully deployed and harvested in time period t' and t in scenario s. From Section 5.2, we know that equation (8.4.1) applies. $J^s_{t'fglt}$ is the number of gender maturation months a cohort has experienced in time period t, deployed in t', while ρ^s_g is the monthly increase in the gender maturation percentage.

$$D^s_{t'fglt} = \rho^s_g J^s_{t'fglt} \tag{8.4.1}$$

Finding a relationship between B^s_g and ρ^s_g is necessary to model gender maturation. However, it is difficult since B^s_g measures the gender maturation at harvest, while ρ^s_g the monthly increase in the gender maturation percentage. Therefore, to set up a relationship between B^s_g and ρ^s_g we need to make assumptions concerning the number of gender maturation months the cohorts Aquagen AS studied have experienced and the development of the gender maturation percentage.

We assume that all the cohorts from Aquagen AS studies have experienced

J_{max} gender maturation months at harvest. The reason for this is that many salmon go through J_{max} gender maturation months in the year following their year of deployment (Eidsfjord, 2021). Hence, B_g^s is the gender maturation percentage at harvest for salmon that have experienced J_{max} gender maturation months, where g is the smolt type and s is the scenario. This assumption lets us express the relationship between B_g^s and ρ_g^s in equation (8.4.2). ρ_g^s is the gender maturation percentage at harvest, B_g^s, divided by the maximum number of gender maturation months a cohort can experience J_{max}. We have now found a way to incorporate the data points from Aquagen AS into $D_{t'fglt}^s$.

$$\rho_g^s = \frac{B_g^s}{J_{max}} \tag{8.4.2}$$

8.5 Other parameters

In this section we present the value of the remaining parameters. Aquagen AS have provided the data that has been used to estimate the HG yield of salmon. The market demand for salmon is dependent upon their weight. Moreover, the demand is the highest when the HG weight is between 3.5 and 6.5 kilograms. To find the harvest thresholds we divide the limit of the preferable HG weights by the HG yield. Table 8.3 presents the HG yields and the harvest thresholds of salmon. We assume that all smolt types have the same HG yield. Salmon that have a weight that lies in this interval are in their harvest periods and can be harvested. However, salmon that weigh less than the lower limit are in their growth periods and cannot be harvested. All salmon must be harvested before they reach their upper weight limits.

HG yield (%)	**Lower harvest limit (kg)**	**Upper harvest limit (kg)**
0.8124	4.31	8.00

Table 8.3: The HG yield and harvest weight limits of salmon.

Due to Norwegian law requiring that fallowing periods must be two months or more, we set Λ to two. Also, the maximum time duration a cohort can

be employed at sea, Δ, is set to 18 months. At that point cohorts approach the upper harvestable weight limit. Lastly, the maximum number of months a company can leave a location empty Γ is 24, to avoid risking withdrawal of production licenses.

Restrictions regarding deployment are necessary to avoid cost inefficient operations and stay within capacities of the company. The number of smolt that can be deployed at a location is limited by how many would fit in four and 12 net pens. As a result, we respectively set L_l^{LOC} and U_l^{LOC} to 480 000 and 1 440 000. In addition, we set L_l^{TYPE} to 240 000, to ensure that the deployed cohort at least fills two net pens. The upper limit for the size of a deployed cohort corresponds to the limit for the location. Hence U_l^{TYPE} is set to U_l^{LOC}.

The monthly harvesting goal of Eidsfjord Sjøfarm forms the basis for their harvesting restrictions. Their aim is to harvest two full net pens every month. The restrictions regarding deployments of smolt represent the amount of smolt. Furthermore, the harvesting bounds represent the biomass in kilograms. The company-wide limit for maximum biomass that can be harvested, U_t^{COM}, is set to 3 800 000, which corresponds to twice the monthly harvest goal. The upper harvesting bound is set to the minimum of the company-wide upper bound and the MAB of the location, $U_l^H = \min(MAB_l, 3\ 800\ 000)$. The lower harvesting limit, L_l^H, is set to 425 000, since it is slightly less than a full net pen. It ensures that cost inefficient harvests do not take place.

The percentage of scenarios that make up the CVaR, α, is set to 10 %.

8.6 Problem instances

In this thesis we primarily study five instances to get a better understanding of how the risk of gender maturation affects production planning within salmon farming. The instances are shown in Table 8.4. They differ by the use of objective function, available smolt types and number of scenarios. The name of the problem instance consists of three parts: the objective function, number of scenarios and available smolt types.

*EV*1*All* corresponds to the expected value problem where the gender maturation percentage is the mean of the gender maturation percentage over all scenarios. All instances with the same number of scenarios contain the

same scenarios.

Problem instance	**Objective function**	**Number of scenarios**	**Available smolt types**
$EV1All$	Expected value	1	All
$EV10All$	Expected value	10	All
$CVaR10All$	CVaR	10	All
$EV10Reg$	Expected value	10	Regular
$CVaR10Reg$	CVaR	10	Regular

Table 8.4: Overview of the main instances used in this thesis.

Chapter 9

Computational Study

In this chapter we present and analyze the results retrieved from solving the problem instances of the production planning problem. Firstly, we present the technical analysis, where we study the results and benefits of using the branch and price algorithm as the solution method. Thereafter, we discuss and compare the production planning problem of the different instances.

9.1 Technical analysis

The branch and price algorithm is implemented with Python version 3.9.6 as the programming language. Moreover, we use Gurobi version 9.5 to solve all linear and mixed-integer problems. To solve the problem instances, we use a computer with a 2x 2.4GHz Intel Xeon Gold 5115 CPU – 10 core CPU, linux-64 operating system and 96 GB of RAM.

In this section, we discuss and analyze technical aspects that appear when using the branch and price algorithm as solution method. We begin by comparing the results of solving $EV10All$ and $CVaR10All$ with Gurobi's MIP solver and the branch and price algorithm. Next, we study the performance and areas of improvement for the branch and price algorithm.

9.1.1 Comparison of solution methods

In Table 9.1, we present the lower bound (LB), upper bound (UB) and optimality gap (Gap) associated with the problem instance $EV10All$ and $CVaR10All$ when varying the solution method.

Problem instance	**Solution method**	**Runtime (s)**	**LB (10^6)**	**UB (10^6)**	**Gap (%)**
$EV10All$	MIP solver	172 800	123.74	140.05	13.18
$CVaR10All$	MIP solver	172 800	119.50	137.80	15.31
$EV10All$	Branch and price	172 800	123.93	132.43	7.04
$CVaR10All$	Branch and price	172 800	122.07	131.30	7.56

Table 9.1: Overview of results for $EV10All$ and $CVaR10All$ when varying the solution method.

The optimality gap of $EV10All$ and $CVaR10All$ respectively decreases with 6.14 and 7.75 percentage points as the solution method is changed from the MIP solver to the branch and price algorithm. The reduction in the optimality gap is due to improvement in both the lower and upper bounds, but primarily the latter. The lower bound improves with 0.15 % and 2.15 % respectively for $EV10All$ and $CVaR10All$. The increase in the lower bound is due to the matheuristics of the branch and price algorithm finding better feasible solutions than the MIP solver. Furthermore, the upper bound respectively improves with 5.44 % and 4.35 % for $EV10All$ and $CVaR10All$. The substantial decrease of the upper bounds when the solution method is the branch and price algorithm indicates that the algorithm describes the convex hull of the mixed-integer problem well.

Independent of the solution method the optimality gap is higher for $CVaR10All$ compared to $EV10All$. One possible reason for this is that $CVaR10All$ maximizes the objective value of the scenario with the lowest objective value while $EV10All$ maximizes the expected value of all scenarios. Furthermore, the improvement of finding the lower bound when using the branch and price algorithm compared to the MIP solver is higher for $CVaR10All$ compared to $EV10All$ since the matheuristics of the branch and price algorithm are able to find better feasible solutions.

Figure 9.1 and 9.2 show the respective development of the bounds for $EV10All$ and $CVaR10All$ when the solution method varies.

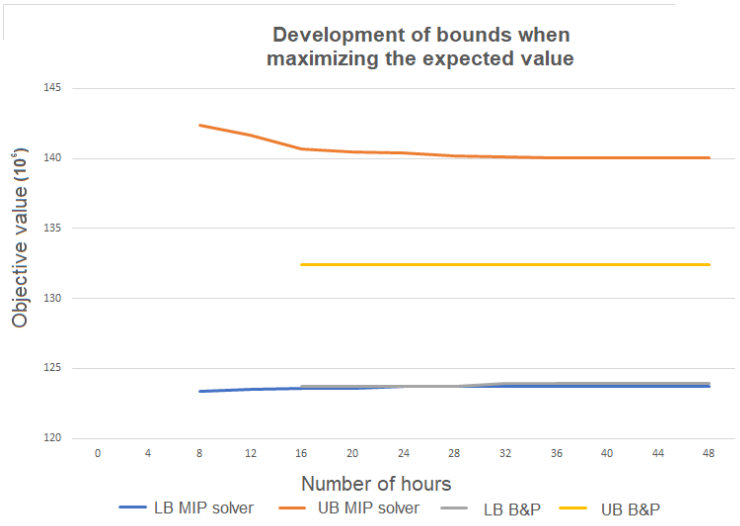

Figure 9.1: Development of bounds when maximizing the expected value.

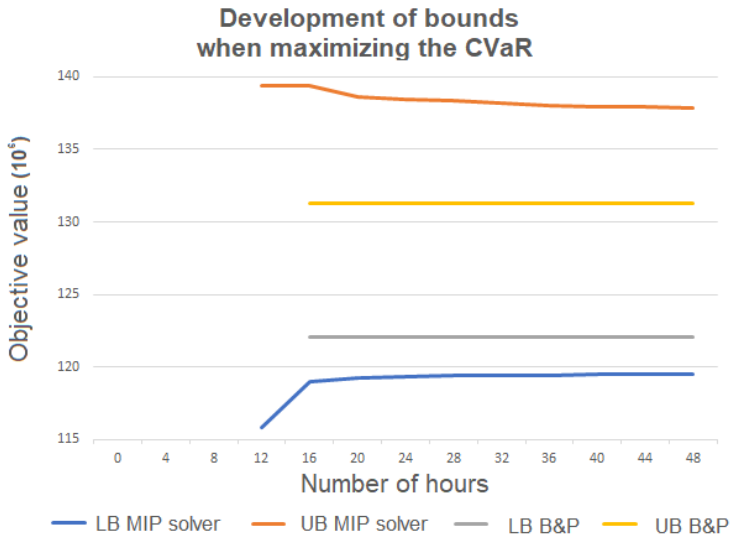

Figure 9.2: Development of bounds when maximizing the CVaR.

When the solution method is the MIP solver the bounds are improved continually, with the improvements becoming smaller as the running time increases. Moreover, the upper bound experiences improvement throughout the running time of the algorithm, while the lower bound stagnates towards the end of the running time of the algorithm. One possible explanation is that the lower bound cannot be greatly improved, but it can also be due to it being difficult to find better feasible solutions. It takes a longer time to find the first bounds of $CVaR10All$ compared to $EV10All$ when the solution method is the MIP solver. This is due to $CVaR10All$ being more difficult to solve than $EV10All$.

When the solution method is the branch and price algorithm the bounds rarely improve after having found the first bounds. It takes approximately 16 hours before a lower and upper bound are found when the solution method is the branch and price algorithm. This shows that the branch and price algorithm is better at finding good upper and lower bound than the MIP solver early in the runtime of the algorithm. However, having a higher runtime leads to little improvement in the lower and upper bounds.

9.1.2 Technical aspects of branch and price

In this section, we study the performance and areas of improvement of the branch and price algorithm. We present the number of solved nodes in the branch and price tree (# Nodes), the total number of iterations from the column generation algorithm (# Iterations), the number of solved subproblems (# Solved SP) and the percentage of time the program uses to solve the subproblems. Time not spent in the subproblems primarily involves matheuristics and solving of the (RMP).

Problem instance	**Runtime (s)**	**# Nodes**	**# Iterations**	**# Solved SP**	**Time in SP (%)**
$EV10All$	172 800	3	396	20196	78.5
$CVaR10All$	172 800	3	411	20961	79.2

Table 9.2: Technical aspects regarding the branch and price algorithm.

Both instances stop running due to the runtime having reached maximum runtime rather than the optimality gap becoming less than 5 %. Branching occurs in both instances, but the time limit prevents the program from solving more than three nodes in each instance. The bounds can only improve when the branch and price algorithm has completed a node. Furthermore, the low number of nodes explain why there is little improvement in the bounds after the first bounds have been found. Even though the branch and price algorithm performs better than the MIP solver, it is of interest to increase the number of solvable nodes. More binary variables will be fixed, which can lead to the branch and price algorithm improving the lower and upper bounds further.

Solving the (RMP) takes substantially less time than solving the subproblems. The main reason for this is that the (RMP) is a linear problem while the subproblems are mixed-integer problems. The (RMP) is solved to optimality. Moreover, proving that the optimal solution of the subproblems is found make the subproblems difficult to solve. Therefore, we set a time limit of 25 seconds for the subproblems. This reduces the time spent in the subproblems. This means that there is no guarantee that the best columns are sent to the (RMP) every iteration. However, we consider the inclusion of a time limit in the subproblems acceptable as all subproblems are either solved to optimality or produce solutions with low optimality gaps.

Since the subproblems are the bottleneck of the program reducing the time spent solving subproblems is of interest since it can lead to an increased number of nodes being solved in the branch and price algorithm. This can be achieved by solving fewer subproblems or decreasing the runtime of an individual subproblem.

A method of decreasing the number of subproblems in future work is to reuse columns in the different nodes in the branch and price tree. All columns of a parent node can be used in one of its two children nodes. By reusing columns in a child node, the number of columns that must be generated in the child node can be reduced. Hence, the amount of time spent solving an individual subproblem remains the same, but the number of subproblems that need to be solved is reduced. Moreover, it will not change the number of subproblems that need to be solved in the root node, but it decreases the number of subproblems that need to be solved in the children nodes.

Even though, the branch and price algorithm only solves three nodes in the branch and price tree, it performs better than the MIP solver. However, to

improve and study how well the algorithm can perform, it is necessary to increase the number of solvable nodes. This can be achieved by reducing the time spent in the subproblems of column generation algorithm, which can be done by reusing columns.

9.2 Analysis of the production planning problem

Traditionally companies have been using regular smolt in industrial salmon farming. However, studies have found that each gender has different characteristics. This makes it beneficial to separate female and male salmon (Aquagen, 2021). Both the results of Lien (2021) and Aasen (2021) indicate that male salmon is preferable for risk-neutral decision makers, due to higher growth rates. Nevertheless, is this still the case when the decision makers are risk-averse and the salmon experience a substantial drop in their relative value when experiencing gender maturation?

In this section we begin by presenting how we evaluate the solution over an increased number of scenarios to make the production plans represent the real world better. Then, we present an overview of the expected value and CVaR of harvests of different evaluations. Thereafter, we study the overview of deployments for the different instances. We continue by comparing key performance indicators of the instances. Lastly, we do a sensitivity analysis, where we vary the relative value of salmon that have experienced gender maturation P_{Low}.

The results retrieved in the different runs correspond to the five-year production plan for a salmon farming company. Moreover, the initial value of P_{Low} is set to 30 %.

9.2.1 Evaluating the solution on more scenarios

When optimizing the production planning problem, it is of interest to use a substantial number of scenarios to represent the real world. This applies in particular when maximizing the CVaR of the value of harvests, since only 10 % of the scenarios determine the production plan. However, increasing the

number of scenarios increase the complexity of the problem. When setting the number of scenarios to 20, the branch and price algorithm is unable to find a solution in two days.

Rather than solving an increased number of scenarios, we evaluate the first stage solution from the instances with 10 scenarios, on a problem with 200 sampled scenarios. We use 200 scenarios since it represents a number of scenarios that is a trade-off between representing the real world sufficiently and having a reasonable runtime. This approach prevents the setting of an upper bound to the problem. Hence, we are not able to estimate the optimality gap. Nonetheless, for the decision maker it is more important to find a feasible solution, as it corresponds to a production plan. Further in this section we use branch and price with this approach on all instances with the same set of sampled scenarios.

9.2.2 Overview of expected value and CVaR

We analyze the production planning problems of six different evaluations. Table 9.3 presents the problem instance used for finding the first-stage solution, the objective function for the evaluation, the expected value and the CVaR of the value of harvests for all evaluations. If the problem instance for the first-stage solution is the same, the first-stage solutions are the same. To be able to compare all evaluations, the expected value and CVaR of the value of harvests are included independent of the objective function.

Problem instance for the first-stage solution	**Objective function for evaluation**	**Expected value of harvests (10^6)**	**CVaR of the value of harvests (10^6)**
EV1All	Expected value	123.90	121.60
EV1All	CVaR	122.50	121.60
EV10Reg	Expected value	117.06	110.62
CVaR10Reg	CVaR	113.41	110.79
EV10All	Expected value	123.93	121.72
CVaR10All	CVaR	122.46	122.04

Table 9.3: Overview of the expected value and CVaR of the different evaluations.

The inclusion of gender-partioned smolt types respectively increase the expected value of harvests by 5.87 % and the CVaR of the value of harvests by 10.15 %. The increase of the expected value is mainly due to deployments of male smolt while the increase of the CVaR is primarily due to deployments of female smolt. This shows that both male and female deployments are better than regular deployments.

The difference between the expected value and the CVaR is smaller when maximizing the CVaR compared to when maximizing the expected value. The reason for this is that maximizing the CVaR improves the objective value of the worst scenarios and worsens the objective value of the best scenarios. When varying the objective function for the evaluation of $EV1All$ there is no gain in the CVaR when maximizing the CVaR compared to maximizing the expected value. Hence, it is better to maximize the expected value since it will lead to a 1.14 % higher expected value of harvests. However, when evaluating $EV10All$ and $CVaR10All$ there is a 0.34 % increase in the CVaR when maximizing the CVaR. Here it is can be beneficial to maximize the CVaR if the decision maker is sufficiently risk-averse.

9.2.3 Overview of deployments

We do not present complete production plans that specify when biomass is present and when harvesting occurs, since it can vary in different scenarios. Instead, we present an overview of the deployments since they are a part of the first-stage decisions and remain the same in all scenarios. The overview of deployments for $EV1All$, $EV10Reg$, $CVaR10Reg$, $EV10All$ and $CVaR10All$ are respectively presented in Figure 9.3, 9.4, 9.5, 9.6 and 9.7. Initial deployments are deployments that take place before the planning horizon and consist of regular salmon. Moreover, if a box contains several colors it means that different types of deployments take place in different nets at a location.

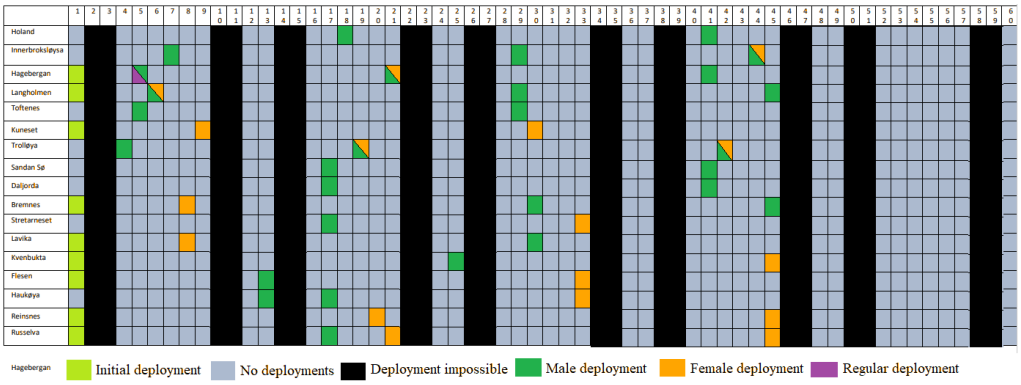

Figure 9.3: Overview of deployments for $EV1All$.

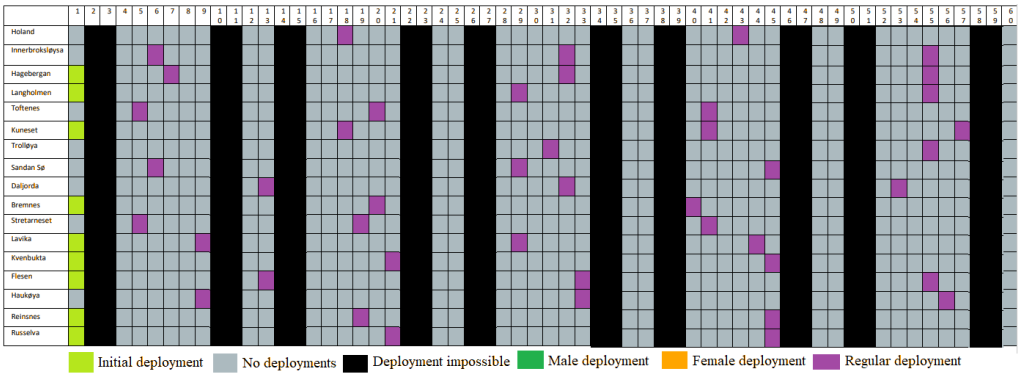

Figure 9.4: Overview of deployments for $EV10Reg$.

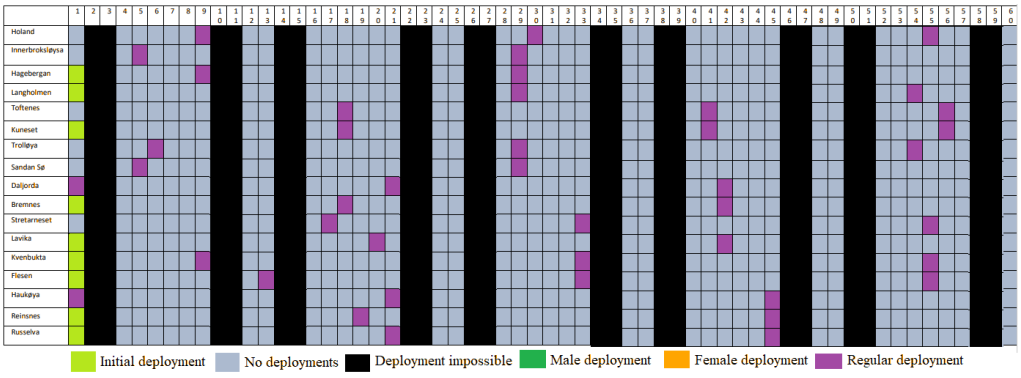

Figure 9.5: Overview of deployments for $CVaR10Reg$.

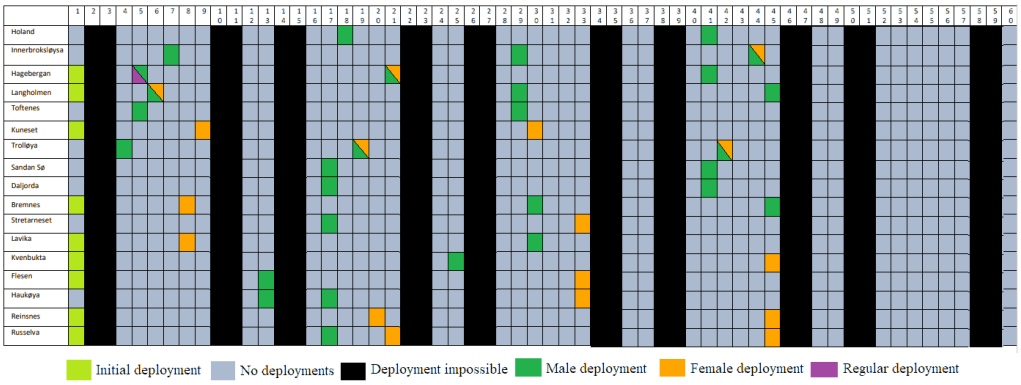

Figure 9.6: Overview of deployments for $EV10All$.

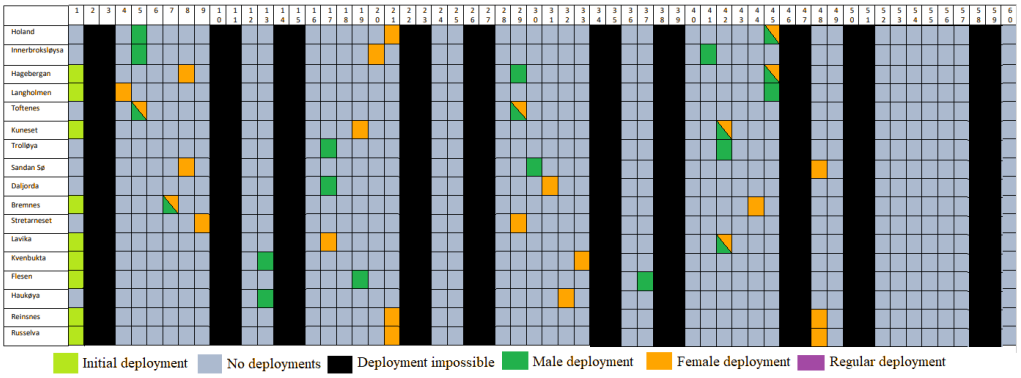

Figure 9.7: Overview of deployments for $CVaR10All$.

Figure 9.8 shows which smolt type is used for deployments in the different problem instances. Initial deployments are not included in this distribution as they take place in all instances. Moreover, almost all deployments in the problem instances use the highest deployment weight of 250 g, since they grow to harvestable weights the fastest. When other deployment weights are chosen, it is to comply with MAB restrictions.

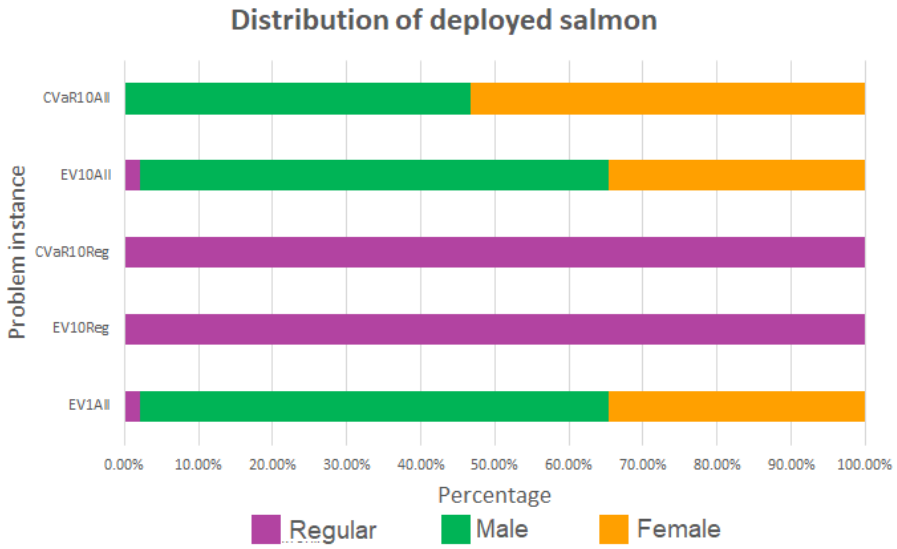

Figure 9.8: The distribution of smolt types of deployments of the different problem instances.

When all smolt types are available both female and male deployments take place. However, the most deployed smolt type depends largely upon the choice of the objective function. Even though male smolt have the highest gender maturation percentages, they are the most appealing smolt type when the objective is to maximize the expected value. The reason for this is that male smolt have the highest growth rates. When the objective is to maximize the CVaR female smolt is slightly more preferable than male smolt. The reason for this is that they do not experience gender maturation. This means that there is no risk of lost production value when deploying female smolt. Regular smolt is the least appealing smolt type since they only have slightly higher growth rates and significantly higher gender maturation percentages than female smolt while having considerably lower growth rates than male smolt.

It is of interest to study whether some deployment months are more popular for the different smolt types. There are potentially two main reasons that contribute to making a month attractive for deployment. Firstly, for all smolt types May, June, July and August are attractive deployment months since cohorts deployed in these months experience a higher mean seawater temperature during their rearing period compared to smolt deployed in other

months. As a result, these deployments have higher growth rates. Secondly, male smolt deployed in May, June, July and August have the highest gender maturation percentages at harvest. The reason for this is that they experience four gender maturation months. To avoid high gender maturation percentages these smolt types should be deployed in other months. By studying the overview of deployments, we clearly see that this is not the case. Male deployments largely occur in these months. Moreover, in all instances where all smolt types are available, over 30 % of all deployments take place in May. Hence, higher growth rates outweigh lower gender maturation percentages.

Independent of the objective function and available smolt types, we observe that few deployments take place in January and February. The reason for this is that cohorts deployed in these months experience lower mean seawater temperatures during their rearing period compared to all other deployments. As a result, they have the lowest weight development of all cohorts.

In $EV1All$, $EV10All$ and $CVaR10All$ no deployment takes place after time period 48, while deployments take place throughout the planning horizon for $EV10Reg$ and $CVaR10Reg$. This indicates that there is a weakness in the end of horizon modeling. The end of horizon modeling we have implemented ensures that a certain amount of biomass is employed at the end of the planning horizon, this is not harvested and does not contribute to the objective value. However, it does not specify how big the remaining salmon must be, which make deployments at the end of the planning horizon unnecessary. The lack of deployments at the end of the planning horizon can create issues in the time following the planning horizon. Nonetheless, this is not a problem since we do not compare any of the results with the actual results of Eidsfjord Sjøfarm and the same end of horizon constraints apply to all instances. Moreover, the final deployments in all instances do not contribute to the objective value, which makes the results of the different instances comparable.

9.2.4 Key performance indicators

We examine different key performance indicators to study how salmon farming is affected by available smolt types and the objective function. The value of harvests, MAB utilization rate (MAB), mean length of a rearing period (Length), mean weight of a harvested salmon (Weight) and mean gender maturation percentage of harvests (Gender maturation) of the instances are

presented in Table 9.4. The MAB utilization rate is the average amount of company-wide biomass divided by the company-wide MAB. It is included to examine which instances utilize the company-wide MAB constraint the best.

Problem instance for first-stage solution	**Objective function for evaluation**	**MAB (%)**	**Length (Months)**	**Weight (kg)**	**Gender maturation (%)**
$EV1All$	Expected value	89.3	14.76	6313	3.16
$EV1All$	CVaR	88.2	14.71	6155	3.07
$EV10Reg$	Expected value	87.7	15.19	6161	5.17
$CVaR10Reg$	CVaR	84.5	15.46	5989	5.16
$EV10All$	Expected value	89.4	14.70	6081	3.48
$CVaR10All$	CVaR	88.2	14.79	6071	2.73

Table 9.4: Overview of key performance indicators for all instances.

The MAB utilization rate is higher, the length of a rearing period is lower and the mean weight of salmon is often higher when all smolt types are available. The main reason for this is the inclusion of male smolt. Male smolt have higher growth rates that allow earlier harvests and more deployments compared to other smolt types. Also, we observe that when the objective is to maximize the CVaR rather than the expected value the mean gender maturation percentage at harvest is lower. The reason for this is that female salmon make up a larger part of the harvests. Moreover, the difference between the gender maturation percentage in the evaluation of $EV10All$ and $CVaR10All$ is higher than the evaluation of $EV10Reg$ and $CVaR10Reg$. The reason for this is that when all smolt types are available it is possible to lower the gender maturation percentage when the objective function changes by deploying female smolt. This is not possible when regular smolt is the only available smolt. Hence, the inclusion of male and female smolt increases the flexibility of the model.

In Table 9.5 we present the percentage of harvests that belong to the different smolt types for the evaluation of $EV1All$, $EV10All$ and $CVaR10All$. The

percentage of harvests that belong to the different smolt types can vary from the percentage of deployments that belong to different smolt types due to varying lengths of rearing periods and differences in the biomass development for different smolt types. Most of the regular harvests are due to the initial deployments. Harvests consist mainly of male salmon when the objective is to maximize the expected value, since they have the highest growth rates. However, when maximizing the CVaR harvests primarily consist of female salmon as they are a less risky alternative since they do not experience gender maturation.

Problem instance for first-stage solution	**Objective function for evaluation**	**Regular harvests (%)**	**Female harvests (%)**	**Male harvests (%)**
$EV1All$	Expected value	21.59	29.13	49.28
$EV1All$	CVaR	21.55	29.43	49.02
$EV10All$	Expected value	20.74	29.26	50.00
$CVaR10All$	CVaR	20.33	44.51	35.16

Table 9.5: Overview of the harvested amount of the different smolt types for all instances.

It is of great interest to compare the evaluation of $EV1All$ when varying the objective function of the evaluation since they have the same first-stage solution. This means that the deployments are the same. The length of a rearing period, the mean weight of a salmon and the gender maturation percentage is slightly higher in the evaluation that maximizes the expected value compared to the evaluation that maximizes the CVaR. The reason for this is that salmon are harvested earlier and at lower weights to decrease the gender maturation percentage. Moreover, the percentage of female harvests slightly increase while the percentage of male harvests slightly decrease. The percentage of female harvests would be even larger for the evaluation that maximizes the CVaR if the first-stage solutions were not fixed.

9.2.5 Sensitivity analysis

To highlight how the value assigned to the relative value of gender matured salmon P_{Low} affects the solution of the production planning problem, we perform a sensitivity analysis where we vary P_{Low}. Firstly, we study how the expected value and CVaR of the value of harvests is affected. Thereafter, we examine how the choice of smolt type differs.

We respectively use $EV10All$ and $CVaR10All$ for fixing the first-stage solution when maximizing the expected value and the CVaR of the value of harvests, before evaluating it on the 200 scenarios. Moreover, for each objective function we perform four runs where P_{Low} is set to 10 %, 30 %, 50 % and 70 %. The default case where P_{Low} is set to 30 % is discussed in detail above.

Table 9.6 shows the expected value and CVaR of the value of harvests when varying P_{Low}. The expected value and CVaR of the value of harvests decrease when P_{Low} decreases. The reason for this is that gender maturation takes place in all runs and all gender matured salmon experience a price drop. Moreover, as the relative value of gender matured salmon decrease the optimal production plan does not fully avoid gender maturation, it rather reduces the number of salmon that experience gender maturation.

P Low (%)	**Maximizing expected value**		**Maximizing CVaR**	
	Expected value of harvests (10^6)	**CVaR of harvests (10^6)**	**Expected value of harvests (10^6)**	**CVaR of harvests (10^6)**
10	122.99	121.01	122.04	121.43
30	123.70	121.72	122.46	122.04
50	124.52	122.05	123.43	123.01
70	126.19	123.86	124.12	123.73

Table 9.6: The expected value and CVaR of the value of harvests when varying the relative value of gender matured salmon.

When maximizing the CVaR the expected value is on average 1.09 % lower than what it would have been if the objective was to maximize the expected value. However, when maximizing the expected value, the CVaR is on average 0.32 % lower than it would have been if the objective was to maximize the

CVaR. This shows that there is only a small gain in the CVaR for risk-averse salmon farmers compared to risk-neutral salmon farmers, when α is 10 %.

Figure 9.9 shows the percentage of deployed salmon that belong to the different smolt types. In all evaluations female and male deployments occur, while regular deployments rarely occur. However, the preferable smolt type for deployment is largely dependent upon P_{Low}. Generally, female deployments become more appealing while male deployments become less appealing as P_{Low} decreases. Moreover, regular deployments largely remain unattractive for the same reasons as mentioned in Section 9.2.3.

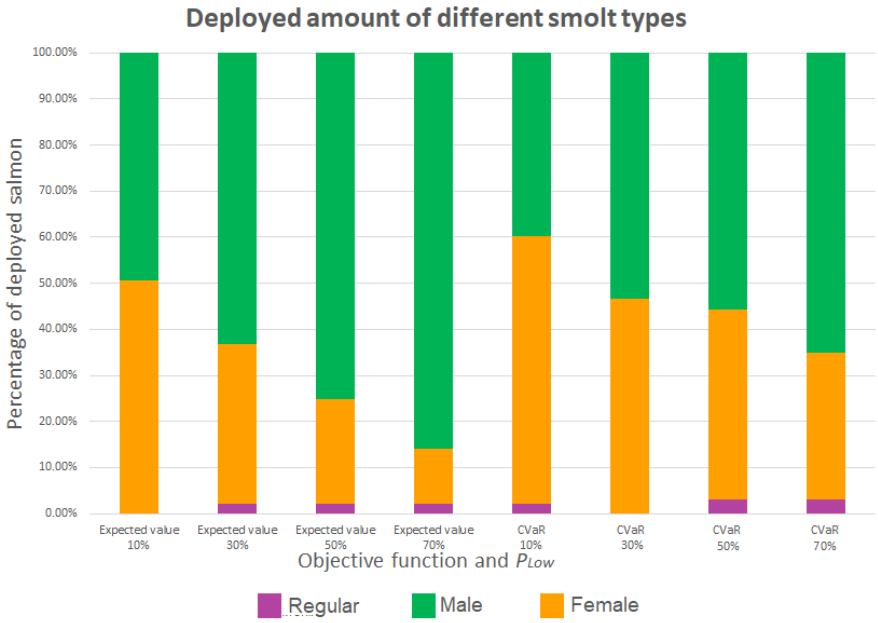

Figure 9.9: Percentage of deployed salmon that belong to different smolt types.

Another important factor when it comes to the choice of smolt type is the objective function. Female deployments are more attractive when maximizing the CVaR of the value of harvests. Moreover, the amount of deployed female smolt is between 7.62 and 19.71 percentage points higher for a specific value of P_{Low} when maximizing the CVaR compared to when maximizing the expected value. When maximizing the expected value of harvests male salmon is usually the most preferable choice for deployment. When P_{Low} is set to 10 %, slightly more female smolt are deployed than male smolt. When the objective is to

maximize the CVaR and P_{Low} is set to 10 % or 30 %, female smolt is the most deployed smolt type.

The inclusion of male and female smolt improve the solution independent of the choice of objective function and relative value of gender matured salmon P_{Low}. Regular smolt is the least attractive smolt type for deployment, since it does not have the highest growth rates or the lowest gender maturation percentages. Generally, regular smolt should not be deployed. The number of female deployments increase when the decision maker is risk-averse and P_{Low} is low. However, the number of male deployments increase when the decision maker is risk-neutral and P_{Low} is high. The difference between the CVaR is higher than the difference between the expected value when maximizing the expected value and CVaR. As a result, only sufficiently risk-averse salmon farmers should maximize the CVaR. When P_{Low} is above 50 % male smolt should make up most of the deployments independent of the risk-attitudes of the decision maker. However, when P_{Low} is less than 30 % and the decision maker is sufficiently risk-averse, female smolt should make up most of the deployments.

Chapter 10

Further research

In this chapter we outline suggestions for further research. Even though, the complexity of this model has increased compared to models presented in earlier projects, it is beneficial to increase the number of scenarios the program can solve further. One way of doing this is by reducing the time spent solving subproblems, the bottleneck of the problem. This will speed up the column generation algorithm, which will enable the inclusion of additional scenarios. Furthermore, this can be achieved by reusing columns in different nodes in the branch and price tree. This can reduce the number of generated columns and time spent solving subproblems.

It can be of great interest to study how the inclusion of production costs in the model impacts the production planning problem. In particular, feeding costs and the cost of purchasing smolt can be incorporated into the model. By capturing currently overlooked aspects, the model can to a greater extent represent an actual salmon farming production system.

Another aspect for further study is to include additional sources of uncertainties since gender maturation is currently the only included source of uncertainty in the model. Moreover, examining how the combination of gender maturation and other sources of uncertainty affect industrial salmon production can lead to a more realistic and reliable production plan. It is of particular interest to include sources of uncertainty that depend upon the smolt type, since it can to a greater extent clarify which smolt types should be used within salmon farming.

Chapter 11

Concluding remarks

In this thesis, we model the tactical production planning problem of industrial salmon farming as a two-stage stochastic mixed-integer problem. The model determines where, when, how much smolt and which smolt type to deploy and harvest. The uncertainty of gender maturation gives rise to the risk of lost production value. Therefore, we develop two objective functions, the expected value and CVaR of the value of harvests, to incorporate risk-neutral and risk-averse attitudes in the model. We apply a Dantzig-Wolfe reformulation and column generation to exploit the structure of the production system of the problem. Moreover, to ensure that the solution complies with integrality conditions we use a branch and price algorithm with several extensions.

We solve the problem with Gurobi's MIP solver and the branch and price algorithm. The branch and price algorithm performs better than the MIP solver by having a notably smaller optimality gap, mostly due to an improvement of the upper bound. To improve the results of the branch and price algorithm further, the algorithm must solve an increased number of nodes. This can be achieved by reducing the time spent solving subproblems.

The inclusion of additional smolt types leads to a respective improvement of 5.87 % and 10.15 % in the expected value and CVaR of the value of harvests. There is no superior smolt type. Regular smolt is the least attractive smolt type, while the appeal of male and female smolt depends upon the objective function and relative value of gender matured salmon. Generally, maximizing the CVaR and decreasing the relative value of gender matured salmon increase the use of female smolt, while maximizing the expected value and increasing the relative value of gender matured salmon increase the use of male smolt.

Bibliography

R. M. Aasen. Tactical procution planning for atlantic salmon farming under uncertainty of salmon lice. 2021. Master's thesis, Norwegian University of Science and Technology.

P. Adamko, E. Spuchľáková, and K. Valášková. The history and ideas behind VaR. *Procedia Economics and Finance*, 24:18–24, 2015. ISSN 2212-5671. doi: https://doi.org/10.1016/S2212-5671(15)00607-3. URL https://www.sciencedirect.com/science/article/pii/S2212567115006073. International Conference on Applied Economics (ICOAE) 2015, 2-4 July 2015, Kazan, Russia.

R. N. Anthony. *Planning and control systems; a framework for analysis*. Division of Research, Graduate School of Business Administration, Harvard University, Boston, 1965.

Aquagen. Meeting with Aquagen on the 10th of September, 2021.

Aquagen. Selective breeding progress, 2022. URL https://aquagen.no/en/2013/06/12/selective-breeding-progress/. Last accessed: 2022-02-02.

R. Arnason. Optimal feeding schedules and harvesting time in aquaculture. *Marine Resource Economics*, 7(1):15–35, 1992. doi: 10.1086/mre.7.1.42629021. URL https://doi.org/10.1086/mre.7.1.42629021.

P. Artzner, F. Delbaen, J.-M. Eber, and D. Heath. Coherent measures of risk. *Mathematical Finance*, 9(3):203–228, 1999. doi: https://doi.org/10.1111/1467-9965.00068. URL https://onlinelibrary.wiley.com/doi/abs/10.1111/1467-9965.00068.

A. Aunsmo, R. Krontveit, P. S. Valle, and J. Bohlin. Field validation of growth models used in atlantic salmon farming. *Aquaculture*, 428-429:249–

257, 2014. ISSN 0044-8486. doi: https://doi.org/10.1016/j.aquaculture.2014.03.007. URL https://www.sciencedirect.com/science/article/pii/S0044848614001100.

B. Bang Jensen, L. Qviller, and N. Toft. Spatio-temporal variations in mortality during the seawater production phase of atlantic salmon (salmo salar) in norway. *Journal of Fish Diseases*, 43(4):445–457, 2020. doi: https://doi.org/10.1111/jfd.13142. URL https://onlinelibrary.wiley.com/doi/abs/10.1111/jfd.13142.

Barentswatch. Fiskehelse, 2021a. URL https://www.barentswatch.no/fiskehelse/. Last accessed: 2022-06-06.

Barentswatch. Salmon lice, 2021b. URL https://www.barentswatch.no/en/articles/Salmon-lice/. Last accessed: 2022-06-06.

C. Barnhart, E. Johnson, G. Nemhauser, M. Savelsbergh, and P. Vance. Branch-and-price: Column generation for solving huge integer programs. *Operations Research*, 46, 02 1970. doi: 10.1287/opre.46.3.316.

O. Bergfjord. Risk perception and risk management in Norwegian aquaculture. *Journal of Risk Research*, 12:91–104, 01 2009. doi: 10.1080/13669870802488941.

J. Birge and F. Louveaux. Introduction to stochastic programming (2nd edition), Springer Verlag, New York, 2011.

T. Bjørndal. The Norwegian aquaculture industry: Industrial structure and cost of production. *Marine Policy*, 12:122–142, 1988.

S. Boyd, L. Xiao, and A. Mutapcic. Notes on decomposition methods. 2003.

P. Cirillo. About the coherence of variance and standard deviation as measures of risk. 2022. URL https://courses.edx.org/c4x/DelftX/TW3421x/asset/coherence.pdf.

J. Danielsson, B. Jorgensen, M. Sarma, G. Samorodnitsky, and C. Vries. Subadditivity re–examined: the case for value-at-risk. 01 2005.

A. Deependra. Fillet quality and yield of farmed atlantic salmon: variation between families, gender differences and the importance of maturation. 2011.

DNV. Marine aquaculture forecast to 2050. 2021. URL https://www.dnv.com/Publications/marine-aquaculture-forecast-to-2050-202391. Last accessed: 2022-06-06.

Eidsfjord. Meeting with Eidsfjord on the 19th of October, 2021.

Eidsfjord Sjøfarm, Sisomar, Aquagen, and NTNU. Produksjonsoptimalisering i verdikjede havbruk gjennom moderne avlsteknologi. 2017.

M. Faustmann. Calculation of the value which forest land and immature stands possess for forestry. *Allgemeine Forst und Jagdzeitung*, 15:441–55, 1849.

J. D. Fisher and J. D'Alessandro. Portfolio upside and downside risk—both matter! *The Journal of Portfolio Management*, 47(10):158–171, jun 2021. doi: 10.3905/jpm.2021.1.263. URL https://doi.org/10.3905%2Fjpm.2021.1.263.

Fiskeridirektoratet. Biomasse, 2022. URL https://www.fiskeridir.no/Akvakultur/Drift-og-tilsyn/Biomasse. Last accessed: 2022-06-06.

P. G. Fjelldal, T. J. Hansen, A. Wargelius, F. Ayllon, K. A. Glover, R. W. Schulz, and T. W. K. Fraser. Development of supermale and all-male Atlantic salmon to research the vgll3 allele - puberty link. *BMC Genetics*, 21(1):123, Nov 2020. ISSN 1471-2156. doi: 10.1186/s12863-020-00927-2. URL https://doi.org/10.1186/s12863-020-00927-2.

O. I. Forsberg. Optimal stocking and harvesting of size-structured farmed fish: A multi-period linear programming approach. *Mathematics and Computers in Simulation*, 42(2):299–305, 1996. ISSN 0378-4754. doi: https://doi.org/10.1016/0378-4754(95)00132-8. URL https://www.sciencedirect.com/science/article/pii/0378475495001328.

O. I. Forsberg. Optimal harvesting of farmed atlantic salmon at two cohort management strategies and different harvest operation restrictions. *Aquaculture Economics & Management*, 3(2):143–158, 1999. doi: 10.1080/13657309909380241. URL https://www.tandfonline.com/doi/abs/10.1080/13657309909380241.

M. Føre, M. Alver, J. A. Alfredsen, G. Marafioti, G. Senneset, J. Birkevold, F. V. Willumsen, G. Lange, Åsa Espmark, and B. F. Terjesen. Modelling growth performance and feeding behaviour of atlantic salmon (salmo salar

l.) in commercial-size aquaculture net pens: Model details and validation through full-scale experiments. *Aquaculture*, 464:268–278, 2016. ISSN 0044-8486. doi: https://doi.org/10.1016/j.aquaculture.2016.06.045. URL https://www.sciencedirect.com/science/article/pii/S0044848616303490.

J. Føsund and E. Strandkleiv. Using branch and price to optimize land-based salmon production. 2021. Master's thesis, Norwegian University of Science and Technology.

Global Farming Initiative. About salmon farming, 2022. URL https://globalsalmoninitiative.org/en/about-salmon-farming/. Last accessed: 2022-06-06.

E. Grefsrud, T. Svåsand, and K. Glover. Risikorapport norsk fiskeoppdrett 2019, 2019. URL https://www.hi.no/hi/nettrapporter/fisken-og-havet-2019-5. Last accessed: 2022-06-06.

H. Grootveld and W. Hallerbach. Variance vs downside risk: Is there really that much difference? *European Journal of Operational Research*, 114(2):304–319, 1999. ISSN 0377-2217. doi: https://doi.org/10.1016/S0377-2217(98)00258-6. URL https://www.sciencedirect.com/science/article/pii/S0377221798002586.

A. Guttormsen. Faustmann in the sea: Optimal rotation in aquaculture. *Marine Resource Economics*, 23(4):401–410, 2008. ISSN 07381360, 23345985. URL http://www.jstor.org/stable/42629671.

A. Hayes. Variance, 2021. URL https://www.investopedia.com/terms/v/variance.asp. Last accessed: 2022-06-06.

R. Hean. An optimal management model for intensive aquaculture — an application in atlantic salmon*. *Australian Journal of Agricultural and Resource Economics*, 38:31–47, 1994.

T. Heaps. Density dependent growth and the culling of farmed fish. *Marine Resource Economics*, 10(3):285–298, 1995. ISSN 07381360, 23345985. URL http://www.jstor.org/stable/42629592.

M. Hæreid, P. Schütz, and A. Tomasgard. *A Stochastic Programming Model for Optimizing the Production of Farmed Atlantic Salmon*, pages 289–311. 01 2013. ISBN 9789814407502. doi: 10.1142/9789814407519_0011.

M. Iversen, A. I. Myhr, and A. Wargelius. Approaches for delaying sexual maturation in salmon and their possible ecological and ethical implications. *Journal of Applied Aquaculture*, 28(4):330–369, 2016. doi: 10.1080/10454438.2016.1212756. URL https://doi.org/10.1080/10454438.2016.1212756.

A. Jakobsen. Oppdrettslaks klarer seg fint uten fôr i opptil fire uker, 2020. URL https://www.hi.no/hi/nyheter/2020/november/oppdrettslaks-klarer-seg-fint-uten-for-i-opptil-fire-uker. Last accessed: 2022-06-06.

M. Jover and V. Estruch. The quantile regression mixed growth model can help to improve the productivity in gilthead sea bream (sparus aurata) and european sea bass (dicentrarchus labrax) growing in marine farms. *Journal of aquaculture and marine biology*, 2017. URL http://medcraveonline.com/JAMB/JAMB-06-00161.pdf.

L. Karp, A. Sadeh, and W. L. Griffin. Cycles in agricultural production: The case of aquaculture. *American Journal of Agricultural Economics*, 68(3): 553–561, 1986. ISSN 00029092, 14678276. URL http://www.jstor.org/stable/1241540.

M. Kaut and S. W. Wallace. Evaluation of scenario-generation methods for stochastic programming. 2007.

B. Kawas, M. Laumanns, E. Pratsini, and S. Prestwich. Risk-averse production planning. In R. I. Brafman, F. S. Roberts, and A. Tsoukiàs, editors, *Algorithmic Decision Theory*, pages 108–120, Berlin, Heidelberg, 2011. Springer Berlin Heidelberg.

A. Lien. Tactical production planning for salmon farming with the risk of gender maturation. 2021. Project thesis, Norwegian University of Science and Technology.

J. Lundgren, M. Rønnkvist, and P. Værbrand. Optimization. 2010.

M. E. Lübbecke and J. Desrosiers. Selected topics in column generation. *Operations Research*, 53(6):1007–1023, 2005. doi: 10.1287/opre.1050.0234. URL https://doi.org/10.1287/opre.1050.0234.

Marine Institute. Salmon life cycle, 2020. URL https://www.marine.ie/Home/site-area/areas-activity/fisheries-ecosystems/salmon-life-cycle. Last accessed: 2022-06-06.

B. Misund. Fiskeoppdrett, 2021. URL https://snl.no/fiskeoppdrett. Last accessed: 2022-06-06.

D. R. Morrison, S. H. Jacobson, J. J. Sauppe, and E. C. Sewell. Branch-and-bound algorithms: A survey of recent advances in searching, branching, and pruning. *Discrete Optimization*, 19:79–102, 2016. ISSN 1572-5286. doi: https://doi.org/10.1016/j.disopt.2016.01.005. URL https://www.sciencedirect.com/science/article/pii/S1572528616000062.

Mowi. Salmon industry handbook 2021, 2021. URL https://corpsite.azureedge.net/corpsite/wp-content/uploads/2021/05/Salmon-Industry-Handbook-2021.pdf. Last accessed: 2022-06-06.

H. Munang'andu, N. Santi, B. Fredriksen, K.-E. Løkling, and Evensen. A systematic approach towards optimizing a cohabitation challenge model for infectious pancreatic necrosis virus in atlantic salmon (salmo salar l.). *PLOS ONE*, 11:e0148467, 02 2016. doi: 10.1371/journal.pone.0148467.

National Park Service. The salmon life cycle, 2019. URL https://www.nps.gov/olym/learn/nature/the-salmon-life-cycle.htm. Last accessed: 2022-06-06.

E. Nodland. En lusegrense på 0,2 lus skal erstatte våravlusningen, 2016. URL https://ilaks.no/en-lusegrense-pa-02-lus-skal-erstatte-varavlusningen/. Last accessed: 2022-06-06.

Nofima. Avl og genetikk, 2022. URL https://nofima.no/forskning/ravarer-fra-havbruk-fiskeri-og-landbruk/avl-og-genetikk/. Last accessed: 2022-06-06.

Norwegian Seafood Council. How do farmed salmon affect CO2 emmisions?, 2016a. URL https://salmonfacts.com/salmon-and-environment/how-does-farmed-salmon-affect-co2-emissions/. Last accessed: 2022-06-06.

Norwegian Seafood Council. Slaughter of farmed salmon, 2016b. URL https://salmonfacts.com/fish-farming-in-norway/slaughter-of-farmed-salmon/.

Norwegian Seafood Council. Salmon life cycle, 2022. URL https://salmon.fromnorway.com/sustainable-aquaculture/the-salmon-lifecycle/.

M. Næss and F. Patricksson. Production planning for atlantic salmon under uncertainty with impact of extensive site management. 2019. Master's thesis, Norwegian University of Science and Technology.

OECD. *OECD Review of Fisheries 2020*. 2020. doi: https://doi.org/https://doi.org/10.1787/7946bc8a-en. URL https://www.oecd-ilibrary.org/content/publication/7946bc8a-en.

S. Pascoe, P. Wattage, and D. Naik. Optimal harvesting strategies: Practice versus theory. *Aquaculture Economics Management*, 6:295–308, 01 2002. doi: 10.1080/13657300209380320. URL https://www.researchgate.net/publication/233346764_Optimal_harvesting_strategies_Practice_versus_theory.

E. Pino Martinez, P. Balseiro, C. Pedrosa, T. S. Haugen, M. S. Fleming, and S. O. Handeland. The effect of photoperiod manipulation on atlantic salmon growth, smoltification and sexual maturation: A case study of a commercial ras. *Aquaculture Research*, 52(6):2593–2608, 2021. doi: https://doi.org/10.1111/are.15107. URL https://onlinelibrary.wiley.com/doi/abs/10.1111/are.15107.

H. Ritchie and M. Roser. Seafood production, 2019. URL https://ourworldindata.org/seafood-production. Last accessed: 2022-06-06.

R. Rockafellar and S. Uryasev. Optimization of Conditional Value-At-Risk. *Journal of risk*, 2:21–42, 01 2000. URL https://www.ise.ufl.edu/uryasev/files/2011/11/CVaR1_JOR.pdf.

D. Roman, K. Darby-Dowman, and G. Mitra. Mean-risk models using two risk measures: a multi-objective approach. *Quantitative Finance*, 7(4):443–458, 2007. doi: 10.1080/14697680701448456. URL https://doi.org/10.1080/14697680701448456.

A. Ruszczyński and A. Shapiro. *6. Risk Averse Optimization*, pages 253–332. 2009. doi: 10.1137/1.9780898718751.ch6. URL https://epubs.siam.org/doi/abs/10.1137/1.9780898718751.ch6.

Salmar. Abc of salmon farming, 2022. URL https://www.salmar.no/en/abc-of-salmon-farming/. Last accessed: 2022-06-06.

M. Savelsbergh. A branch-and-price algorithm for the generalized assignment problem. *Operations Research*, 45:831–841, 12 1997. doi: 10.1287/opre.45.6.831. URL https://www.researchgate.net/publication/200622126_A_Branch-and-Price_Algorithm_for_the_Generalized_Assignment_Problem.

P. Schütz and S. Westgaard. Optimal hedging strategies for salmon producers. *Journal of Commodity Markets*, 12:60–70, 2018. ISSN 2405-8513. doi: https://doi.org/10.1016/j.jcomm.2017.12.009. URL https://www.sciencedirect.com/science/article/pii/S2405851317302234. Seafood: A Global Commodity.

T. Segal. Common methods of measurement for investment risk management, 2022. URL https://www.investopedia.com/ask/answers/041415/what-are-some-common-measures-risk-used-risk-management.asp. Last accessed: 2022-06-06.

S. Stefansson, G. Bæverfjord, S. Handeland, T. Hansen, S. Nygård, O. Rosseland, T. Rosten, H. Tofoten, and B. Havardsson. Fiskevelferdsmessig vurdering av produksjon av 0-års smolt. 2005.

D. Tasche. Expected shortfall and beyond. In Y. Dodge, editor, *Statistical Data Analysis Based on the L1-Norm and Related Methods*, pages 109–123, Basel, 2002. Birkhäuser Basel. URL https://www.researchgate.net/publication/222692244_Expected_Shortfall_and_Beyond.

The Fish Site. Why invest in offshore aquaculture production, 2022. URL https://thefishsite.com/articles/why-invest-in-offshore-aquaculture-production. Last accessed: 2022-06-06.

H. Thorarensen and A. P. Farrell. The biological requirements for post-smolt atlantic salmon in closed-containment systems. *Aquaculture*, 312(1):1–14, 2011. ISSN 0044-8486. doi: https://doi.org/10.1016/j.aquaculture.2010.

11.043. URL https://www.sciencedirect.com/science/article/pii/S0044848610008161.

K. Tone and M. Fushimi. *Apors: Development In Diversity And Hearmony - Proceedings Of The Third Conference*. World Scientific Publishing Company, 1995. ISBN 9789814549608. URL https://books.google.gr/books?id=3NBKDwAAQBAJ.

A. Tsanakas. Risk measure: Beyond coherence? https://www.actuaries.org.uk/system/files/documents/pdf/risk-measures-beyond-coherence.pdf, 2004. Last accessed: 2022–05-02.

United Nations. World population projected to reach 9.8 billion in 2050, and 11.2 billion in 2100, 2017. URL https://www.un.org/en/desa/world-population-projected-reach-98-billion-2050. Last accessed: 2022-06-06.

S. Uryasev and R. T. Rockafellar. *Conditional Value-at-Risk: Optimization Approach*, pages 411–435. Springer US, Boston, MA, 2001. ISBN 978-1-4757-6594-6. doi: 10.1007/978-1-4757-6594-6_17. URL https://doi.org/10.1007/978-1-4757-6594-6_17.

Y. Vardanyan and M. R. Hesamzadeh. Coordinated production planning of risk-averse hydropower producer in sequential markets. *International Transactions on Electrical Energy Systems*, 26:n/a–n/a, 09 2015. doi: 10.1002/etep.2131. URL https://onlinelibrary.wiley.com/doi/abs/10.1002/etep.2131.

H. P. Williams. *Model Building in Mathematical Programming*. 2013.

Appendix A

Compact model

A.1 Objective function

$$\sum_{s\in S}\pi_s(\sum_{t'\in\mathcal{T}_0^R}\sum_{f\in\mathcal{F}_{t'}}\sum_{g\in\mathcal{G}_{t'}}\sum_{l\in\mathcal{L}}\sum_{t\in\mathcal{T}_{fglt'}^{Hs}}(P_{High}(1-L^s_{t'fglt})+P_{Low}(L^s_{t'fglt}))\omega^s_{t'fglt}) \tag{A.1.1}$$

$$z-\frac{1}{1-\alpha}\sum_{s\in\mathcal{S}}\pi_s x_s \tag{A.1.2}$$

A.2 Constraints

$$L_l^{TYPE}\delta_{fglt}\leq_f y_{fglt}\leq U_l^{TYPE}\delta_{fglt}\quad t\in\mathcal{T},f\in\mathcal{F}_t,g\in\mathcal{G}_t,l\in\mathcal{L} \tag{A.2.1}$$

$$L_l^L\delta_{lt}\leq\sum_{f\in\mathcal{F}_t}\sum_{g\in\mathcal{G}_t}N_f y_{fglt}\leq U_l^L\delta_{lt}\quad l\in\mathcal{L},t\in\mathcal{T} \tag{A.2.2}$$

$$\sum_{f\in\mathcal{F}_t}\sum_{g\in\mathcal{G}_t}\delta_{fglt}\leq|F_t||G_t|\delta_{lt}\quad l\in\mathcal{L},t\in\mathcal{T}^{\mathcal{R}} \tag{A.2.3}$$

$$\sum_{f\in\mathcal{F}_t}\sum_{g\in\mathcal{G}_t}\delta_{fglt}\leq\beta^s_{l\tau}\quad s\in\mathcal{S},l\in\mathcal{L},t\in\mathcal{T}^R,f\in\mathcal{F}_t,g\in\mathcal{G}_t,l\in\mathcal{L},\tau\in\mathcal{T}^G_{fglt} \tag{A.2.4}$$

$$\Lambda\delta_{lt} + \sum_{\tau \in \mathcal{T}_t^{\Lambda^-}} \beta_{l\tau}^s \leq \Lambda \quad l \in \mathcal{L}, t \in \mathcal{T}^{\mathcal{R}} \quad \setminus \quad (1, .., \Lambda) \tag{A.2.5}$$

$$L_l^H \omega_{lt}^s \leq \sum_{f \in \mathcal{F}_t'} \sum_{g \in \mathcal{G}_t'} \omega_{t' fglt}^s \leq U_l^H \omega_{lt}^s \quad s \in \mathcal{S}, l \in \mathcal{L}, t \in \mathcal{T} \tag{A.2.6}$$

$$\sum_{t \in \mathcal{T}_{fglt}^D} \sum_{f \in \mathcal{F}} \sum_{g \in \mathcal{G}} \sum_{l \in \mathcal{L}} \omega_{t' fglt}^s \leq U_t^{COM} \quad s \in \mathcal{S}, t \in \mathcal{T} \tag{A.2.7}$$

$$\sum_{\tau \in \mathcal{T}_t^{\Gamma-}} \beta_{l\tau}^s \geq 1 \quad s \in \mathcal{S}, l \in \mathcal{L}, t \in \mathcal{T} \quad \setminus \quad (1, .., \Gamma - 1) \tag{A.2.8}$$

$$q_{t' fglt}^s = A_{t' fglt} y_{fglt'}^s \quad s \in \mathcal{S}, t' \in \mathcal{T}^{\mathcal{R}}{}_0, g \in \mathcal{G}_{t'}$$

$$s \in S, t' \in \mathcal{T}^{\mathcal{R}}{}_0, g \in \mathcal{G}_{t'}, \quad s \in \mathcal{S}, l \in \mathcal{L}, t \in (\mathcal{T}_{fglt'}^G \cup \min \mathcal{T}_{fglt'}^H) \tag{A.2.9}$$

$$q_{t' fglt}^s = R_{t' fglt}(q_{t' fgi(t-1)}^s - \omega_{t' fgi(t-1)}^s)$$

$$s \in \mathcal{S}, t' \in \mathcal{T}_0^R, g \in \mathcal{G}_{t'}, l \in \mathcal{L}, t \in (\mathcal{T}_{fglt'}^{H+^s} \cup \min \mathcal{T}_{fglt'}^{H^s}) \tag{A.2.10}$$

$$q_{t' fgi[max \mathcal{T}_{fglt'}^{H+}]}^s - \omega_{t' fgi[max \mathcal{T}_{fglt'}^{H+}]}^s = 0$$

$$s \in \mathcal{S}, t' \in \mathcal{T}^{\mathcal{R}}{}_0, f \in \mathcal{F}_{t'}, g \in \mathcal{G}_{t'}, s \in \mathcal{S}, l \in \mathcal{L} \tag{A.2.11}$$

$$q_{lt}^s <= MAB_l \beta_{lt}^s \quad s \in \mathcal{S}, l \in \mathcal{L}, t \in \mathcal{T} \tag{A.2.12}$$

$$q_{lt}^s = \sum_{t' \in \mathcal{T}^{\Delta_R^-}} \sum_{f \in \mathcal{F}_t} \sum_{g \in \mathcal{G}_{t'}} q_{t' fglt}^s \quad s \in \mathcal{S}, l \in \mathcal{L}, t \in \mathcal{T} \tag{A.2.13}$$

$$\sum_{l \in \mathcal{L}} q_{lt}^s \leq MAB^{COMP} \quad s \in \mathcal{S}, t \in \mathcal{T} \tag{A.2.14}$$

$$\beta_{lt}^s \leq 0 \quad s \in \mathcal{S}, l \in \mathcal{L}, t \in \mathcal{T}^{\Lambda_l^{INIT}} \tag{A.2.15}$$

$$\sum_{t \in \mathcal{T}_l^{\Gamma^{INIT}}} \beta_{l\tau}^s \geq 1 \quad s \in \mathcal{S}, l \in \mathcal{L} \tag{A.2.16}$$

$$\sum_{l\in\mathcal{L}} q^s_{l|T|} \geq \sum_{f\in\mathcal{F}}\sum_{g\in\mathcal{G}}\sum_{l\in\mathcal{L}} y_{fgl0} \tag{A.2.17}$$

$$\sum_{(f,g,t')\in\mathcal{B}^G_{lt}} A_{t'fglt} y^s_{fglt'} \leq MAB_l \quad s\in\mathcal{S}, l\in\mathcal{L}, t\in\mathcal{T}^E \tag{A.2.18}$$

$$\sum_{l\in L}\sum_{(f,g,t')\in\mathcal{B}^G_{lt}} A_{t'fglt} y^s_{fglt'} \leq MAB^{COMP} \quad s\in\mathcal{S}, t\in\mathcal{T}^E \tag{A.2.19}$$

$$x_s \geq z - \sum_{t'\in\mathcal{T}^R_0}\sum_{f\in\mathcal{F}_{t'}}\sum_{g\in\mathcal{G}_{t'}}\sum_{l\in\mathcal{L}}\sum_{t\in\mathcal{T}^{Hs}_{fglt'}} (P_{High}(1-L^s_{t'fglt})+P_{Low}(L^s_{t'fglt}))\omega^s_{t'fglt} \quad s\in\mathcal{S} \tag{A.2.20}$$

$$\delta_{fglt} \in \{0,1\} \tag{A.2.21}$$

$$\delta_{lt} \in \{0,1\} \tag{A.2.22}$$

$$\beta_{lt} \in \{0,1\} \tag{A.2.23}$$

$$\omega^s_{lt} \in \{0,1\} \tag{A.2.24}$$

$$\omega^s_{t'fglt} \geq 0 \tag{A.2.25}$$

$$q^s_{lt} \geq 0 \tag{A.2.26}$$

$$q^s_{t'fglt} \geq 0 \tag{A.2.27}$$

$$x^s \geq 0 \tag{A.2.28}$$

$$z \quad free \tag{A.2.29}$$

Andreas Lien

Using Branch and Price to Optimize the Production of Salmon Under the Risk of Gender Maturation

NTNU
Kunnskap for en bedre verden